AN LCAO LOCAL DENSITY FUNCTIONAL APPROACH TO SURFACE ELECTRONIC STRUCTURE CALCULATIONS

BY

JOHN WALLACE MINTMIRE

A DISSERTATION PRESENTED TO THE GRADUATE COUNCIL
OF THE UNIVERSITY OF FLORIDA
IN PARTIAL FULFILLMENT OF THE REQUIREMENTS FOR THE
DEGREE OF DOCTOR OF PHILOSOPHY

UNIVERSITY OF FLORIDA

1980

This dissertation is dedicated to those members of my family who wondered when I would ever graduate.

ACKNOWLEDGMENTS

I express my deepest appreciation to Prof. J. R. Sabin for the support and guidance which has made this dissertation possible. I would also like to express my gratitude to all the members of the Quantum Theory Project for the camaraderie which has made my period of graduate study a pleasant and productive one, with a special recognition of Prof. P.-O. Löwdin for the assistance he has provided in the development of my professional background. I am deeply indebted to Prof. S. B. Trickey, Dr. B. I. Dunlap, and Dr. J. P. Worth for their invaluable advice and help in the course of my research. The editorial assistance of Ms. Cynthia Kinney is most sincerely appreciated.

The financial support of the Northeast Regional Data Center and the National Science Foundation is gratefully acknowledged. I also acknowledge the use of computational facilities provided by the Department of Highway Safety and Motor Vehicles of the State of Florida.

TABLE OF CONTENTS

Abstract of Dissertation Presented to the Graduate Council
of the University of Florida in Partial Fulfillment of the
Requirements for the Degree of Doctor of Philosophy

AN LCAO LOCAL DENSITY FUNCTIONAL APPROACH TO SURFACE ELECTRONIC STRUCTURE CALCULATIONS

By

JOHN WALLACE MINTMIRE

DECEMBER 1980

Chairman: John R. Sabin

Major Department: Physics

A new method for calculating the electronic structure of thin films is presented using the local density functional formalism in the linear combination of atomic orbitals (LCAO) approximation. The self-consistent solution of the resulting secular equations is made tractable through the use of fitting procedures for approximating the charge density (for the Coulomb potential) and the cube root of the charge density (for the exchange potential) as linear combinations of fitting functions, allowing the construction of a more efficient (in terms of computational effort) procedure than would otherwise be possible. Hermite-Gaussian functions comprise the basis sets, with different sets of Hermite-Gaussian functions used for the orbital basis set, for the charge density fitting functions, and for the functions used to fit the cube root of the charge density. Results are presented for two systems, the atomic hydrogen monolayer and the atomic beryllium monolayer, which demonstrate the feasibility and

applicability of this approach. Techniques are discussed for improvement of the computational procedure in order to enable calculations to be made on larger and more complex systems than those presented in this dissertation.

CHAPTER I
INTRODUCTION

I-1. General Remarks

The study of the electronic properties of solid surfaces is becoming increasingly more important as techniques dependent on surface properties (such as catalysis techniques and ultra-thin-film devices) occupy more extensive roles in modern technology. Experimental interest in these systems has expanded greatly in recent years, in large measure due to improved vacuum techniques over the past two decades. The theoretical study of the electronic properties of surfaces thus faces a challenge to develop new methods for understanding the behavior of these systems.

Many experimental methods for studying surfaces have been developed or improved in the last decade using a multitude of probe techniques. Electron beams impinging upon the surface of interest are used in Auger Electron Spectroscopy (AES), Low Energy Electron Diffraction (LEED), and the Scanning Electron Microscope (SEM) to yield information about the electronic structure and nuclear geometry of the surface, while Electron Spectroscopy for Chemical Analysis (ESCA or XPS) and Ultraviolet Photon Spectroscopy (UPS) use photons (X-ray and UV respectively) as a probe to provide additional information about the electronic structure of surfaces (for a historical review of these methods, see Lee, 1977).

In this work we propose a new computational approach to calculate the approximate electronic two-dimensional band structure and total energy

of a slab having finite thickness in one direction and two-dimensional periodicity in the plane normal to the direction of finite thickness. The slab system will thus possess both a surface and the periodicity in directions parallel to the surface characteristic of the bulk solid. Thus by increasing the thickness of the slab, the properties of the semi-infinite solid may be approached as a limit.

Methods will be described in this work for solving the secular equation resulting from a Linear Combination of Atomic Orbitals (LCAO) tight-binding approach to the Xα formalism (for a review see Connolly, 1976). The computational difficulties arising from the evaluation of matrix elements involving $\rho^{1/3}(\underline{r})$ (where ρ is the electronic charge density) are treated by fitting $\rho^{1/3}$ to a linear combination of two-dimensionally periodic fitting functions in a manner equivalent to that of Dunlap (Dunlap, Connolly, and Sabin, 1979a and 1979b) for molecular systems. In order to reduce the number of computationally expensive integrals which must be evaluated, the electronic charge density ρ is also fit to a linear combination of a different set of two-dimensionally periodic fitting functions. A mathematical formalism is derived for fitting ρ based on the procedure introduced by Dunlap (Dunlap, Connolly, and Sabin, 1979a) and Mintmire (1979) for molecular systems which finds the variational extremum of an approximate electron repulsion energy functional of the fit to ρ. This approximate electron repulsion energy functional is bounded by the electron repulsion energy of ρ with itself and is equal to the electron repulsion energy of ρ with itself to second order in the difference between the exact density ρ and the fitted density. The formalism derived by Dunlap and Mintmire in the above mentioned references for the molecular case unfortunately cannot be used directly

for extended systems due to the long range nature of the Coulomb interaction resulting in certain integrals tending toward infinity in the limit as a finite molecular system increases in size to approach the two-dimensionally periodic slab. Thus changes were introduced into the original formalism to yield a scheme equivalent to the original molecular density scheme (Dunlap, Connolly, and Sabin, 1979a), but with proper limiting behavior.

This new computational scheme is tested on two systems: the atomic hydrogen monolayer and the atomic beryllium monolayer. The results for the hydrogen monolayer demonstrate the feasibility of the method and illustrate some of the effects of changes in basis sets and in the number of points considered in the surface Brillouin zone. The atomic beryllium results further demonstrate the feasibility of the method and selected results are compared with experimentally determined results such as the work function and Auger spectra of the beryllium surface.

1-2. Historical Background

Early calculations of the electronic structure of surfaces (excluding cluster calculation approaches) normally fell into one or two categories:

1) treating the system as an electron gas and neglecting the electron-nuclear lattice interactions (by assuming a homogeneous positive charge density), such as the results by Lang (1973) using a jellium model with a step potential to simulate the potential at the surface; or
2) band structure calculations taking into account the interactions between electrons and the nuclear lattice, although these

calculations almost universally were not self-consistent and frequently were semi-empirical methods using experimental data or bulk band structure data.

We wish to review briefly the history of calculations using the band structure approach (with self-consistent procedures) over the last several years in order to see how our proposed method compares with previous work. One of the earliest calculations to report self-consistent calculations for the electronic structure of a thin film system was by Alldredge and Kleinman (1972). These two workers calculated the band structure of a 13 atom thick layer lithium system, taking into account the effects of the nuclear lattice, using a non-self-consistent plane wave solution which was later extended to a self-consistent scheme for calculations on the same lithium system (Alldredge and Kleinman, 1974). The lack of translational symmetry in the direction normal to the surface was treated by forcing all orbitals to vanish at planes located some large distance from the surface (Alldredge and Kleinman used planes located three times the layer separation away from the exterior nuclear site.), equivalent to invoking an impenetrable barrier for electrons away from the surface. Core states were not treated directly in this method, but core effects were included in a pseudopotential model.

Applebaum and Hamann (1972) introduced a model of the semi-infinite surface by requiring all orbitals to match the bulk orbitals as boundary conditions on one side of a thin film system. Model potentials including core effects were used to generate orbitals in the Laue representation (von Laue, 1931), where a Fourier expansion in the parallel coordinates is combined with the coordinate representation in the normal direction, using a numerical grid for the coordinate representation component of

all evaluated functions. This approach was used primarily to study relaxation effects on the (111) surface (Appelbaum and Hamann, 1973) and the (100) surface (Appelbaum, Baraff, and Hamann, 1975a and 1975b) of silicon.

Cooper (1973) reported calculations on the copper (100) monolayer using a muffin-tin version of the KKR method adapted to two-dimensionally periodic systems. The lack of translational symmetry in the surface normal direction was treated with an impenetrable barrier in a similar manner to that of Alldredge and Kleinman (1972). Various refinements to this basic approach were introduced by Kohn (1975) and Kar and Soven (1975) who simultaneously reported muffin-tin KKR approaches that did not require the use of an impenetrable barrier located away from the surface. Krakauer and Cooper (1977) further adapted this approach into a local combination of muffin-tin orbitals (LCMTO) approach incorporating non-muffin-tin corrections to the potential.

Gay, Smith, and Arlinghaus (1977) introduced a self-consistent band structure method in an LCAO approach using Gaussian basis functions. Their approach utilized an effective potential constructed from two terms:

1) the initial potential generated by overlapping atomic potentials; and
2) differences between the effective potential at each iteration in the self-consistent process and the initial potential calculated as a Fourier expansion.

This approach has been very successful in describing the band structure of transition metals, leading to computed results for a nine layer model of the copper (100) surface (Smith, Gay, and Arlinghaus, 1980) and a nine layer model of the nickel (100) surface (Arlinghaus, Gay and Smith,

1980). This method unfortunately appears not to admit a straightforward method for evaluating the total energy of the system due to the nature of the Fourier transform techniques.

Wang and Freeman (1978) introduced another LCAO approach for thin films based on the Discrete Variation Method (DVM) of Ellis and Painter (1971) where the orbitals are expressed in a numerical basis set. The charge density used for generating the secular matrix of each iteration in this self-consistent procedure is constructed by fitting the current true charge density to a charge density resulting from superimposed overlapping spherically symmetric atomic charge densities. This method has been used to calculate the band structure of one, three, and five layer models of the nickel (001) surface (Wang and Freeman, 1979) and a nine layer model of the nickel (001) surface (Wang and Freeman, 1980). No total energies have been reported using this method, although no inherent difficulties appear to prevent this approach from yielding total energies in a straightforward fashion.

In addition to the method introduced by them mentioned previously, an alternative self-consistent LCAO procedure using Gaussian basis functions has been introduced by Appelbaum and Hamann (1978), with calculated results for the copper (100) monolayer. Their approach is similar to that derived in this work in the use of fitting techniques for the charge density ρ and for $\rho^{1/3}$. Appelbaum and Hamann fit the charge density with a least-squares fitting procedure to a periodic sum of spherically symmetric Gaussians using "floating" Gaussians at sites other than the nuclear centers in order to describe asymetric components of the charge density. Using the same basis of spherically symmetric Gaussians as used for fitting the charge density, Appelbaum and Hamann then fit the sum of the

local density functional exchange potential and the total Coulomb potential minus a screened nuclear attraction term, which is treated outside the fitting procedure. This approach has been used to calculate the band structure of the eleven layer model of the titanium (0001) surface (Feibelman, Appelbaum, and Hamann, 1979) and the same titanium system with a chemisorbed hydrogen monolayer (Feibelman and Hamann, 1980) and with a chemisorbed nitrogen monolayer (Feibelman and Himpsel, 1980). Recent calculations (Feibelman, Hamann, and Himpsel, 1980) report cohesive energy curves for the eleven layer model of the titanium (0001) surface with a chemisorbed hydrogen monolayer at various distances from the exterior layer of titanium. Unfortunately complete details as to how the total energy terms were evaluated in this formalism have not been published at this time.

The formalism described in this work is similar to the techniques discussed by Feibelman, Appelbaum, and Hamann (1979); the primary differences arise from the fitting techniques utilized. In our approach a basis set of Gaussian functions (not restricted to spherically symmetric Gaussians) is used to fit the $\rho^{1/3}$ portion of the local density functional exchange potential by using least-squares fitting methods. The charge density is then fitted using the variational methods mentioned in Section 1-1, which results in the evaluated Coulombic energy portion of the total energy agreeing with the Coulombic energy resulting from the non-fitted density to second order in the error in the charge density introduced by the fitting procedure. We feel this is a more rational scheme than a least-squares fitting method for fitting the charge density when the fitted charge density will be used to construct the Coulombic potential due to the electron charge and to evaluate the Coulombic contribution to the total energy.

I-3. Organization of Dissertation

There are two fundamental topics to cover in this dissertation. The first topic is a basic description of the electronic band structure approach. The mathematical formalism of our approach is presented in Chapter II, followed by a brief description of the computational techniques used to implement the formalism given in Chapter III. The results are the second fundamental topic to be discussed. Computational results for the atomic hydrogen monolayer and the atomic beryllium are presented and discussed in Chapter IV, with a summary of our method and results in Chapter V.

The appendices at the end of this dissertation discuss in extended detail several topics relating to the computational procedure. Appendix A defines the Hermite-Gaussian functions used in the work and integrals involving these functions are reduced to forms which may be evaluated using algorithms described in this appendix and later appendices. The multipole expansion techniques used in evaluating Coulomb integrals are discussed in Appendix B, while equations necessary for the evaluation of integrals using reciprocal lattice expansions are derived in Appendix C. Finally, Appendix D describes the three-dimensional grid used for the numerical integration algorithms which are part of the computational fitting procedure.

CHAPTER II
MATHEMATICAL FORMALISM AND THEORY

2-1. Symmetry Properties of Thin Films

As mentioned in Chapter I, the physical systems of actual interest were studied using an ideal periodic thin film model. Given an ideal three-dimensional periodic lattice of nuclei, the thin film may be visualized as that portion of the three-dimensional lattice enclosed between two parallel planes of finite separation as illustrated in Figure 2-1. A more formal definition of the systems under consideration is expressed by the following two conditions on the positions of the nuclei in the nuclear lattice:

1) There exist two independent vectors $\underline{R}_1$ and $\underline{R}_2$ such that a translation of coordinates by $\underline{R} = m\underline{R}_1 + n\underline{R}_2$, where m and n are integers, results in an equivalent lattice;
2) and there exist two planar surfaces, parallel to the plane of periodicity containing $\underline{R}_1$ and $\underline{R}_2$, with finite separation such that all of the nuclear sites are contained within the region enclosed by the two parallel planes.

The first condition requires two-dimensional periodicity while the second condition requires that the thin film indeed has finite thickness.

The set of all possible translations $\underline{R}$,

$$\underline{R} = m\underline{R}_1 + n\underline{R}_2 \ , \quad (m \text{ and } n \text{ integers}) \tag{2-1}$$

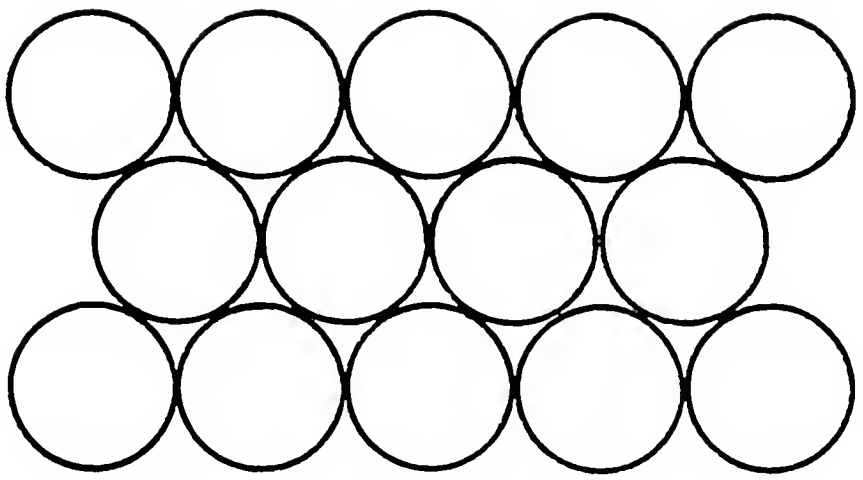

Figure 2-1. Schematic representation of a side view of a two-dimensionally periodic slab with three layers.

defines a two-dimensional geometric lattice of points, the planar Bravais lattice. There are five possible types of planar Bravais lattices, which have different point group symmetries associated with them in addition to the translational symmetry, as illustrated in Figure 2-2. An elementary treatment of these systems is given in Blakemore (1974).

Once a planar Bravais lattice is chosen, the treatment of symmetry is similar to that of the three-dimensional crystalline lattice as described by Tinkham (1964) or by Slater (1972a). A unit cell may be constructed as shown in Figure 2-3 in a manner analogous to that of the three-dimensional unit cell. Since the thin film is actually a three-dimensional system while the planar Bravais lattice is only a two-dimensional geometrical construct, the thin film unit cell is a parallelopiped which is finite in directions parallel to the plane of periodicity but infinite in extent in the directions normal to the plane of periodicity. The arrangement of nuclear centers inside each unit cell is unrestricted except for the previous constraint that the thin film have finite thickness. Therefore the complete arrangement of nuclei need not have the full point group symmetry of the Bravais lattice.

Thus the symmetry group of the total system (or rather the plane group, since we are currently considering the set of two-dimensional symmorphic symmetry operations) is a subgroup of the plane group of the Bravais lattice. Using an approach similar to that of Koster (1957) the plane group consists of symmetry operators of the form $\{\hat{P}|\underline{R}\}$ which correspond to a point group coordinate transformation followed by a translation of coordinates:

$$\{\hat{P}|\underline{R}\}\ \underline{r} = \hat{P}\underline{r} + \underline{R} \qquad (2\text{-}2)$$

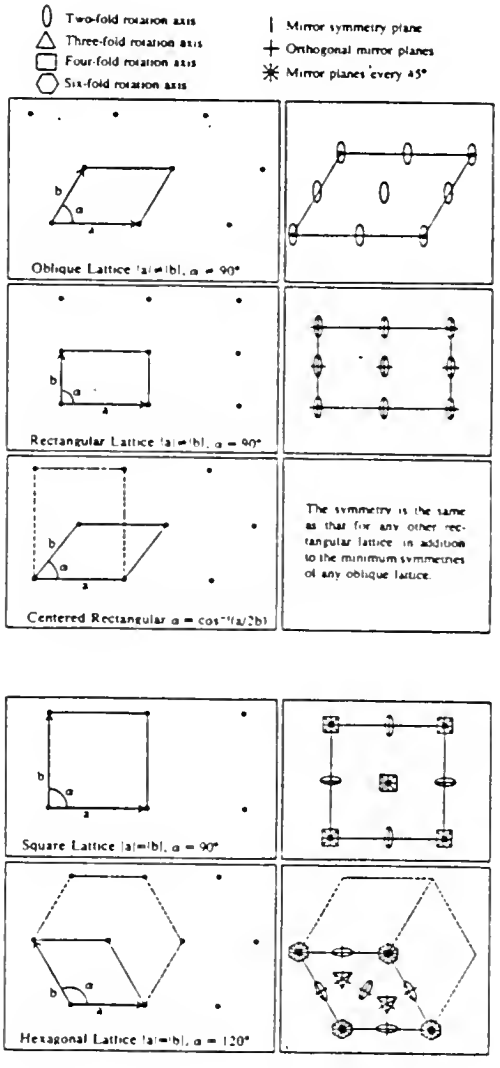

Figure 2-2. The five two-dimensional lattices and their symmetries. (From Solid State Physics by J. S. Blakemore. Copyright (c) 1969 by W. B. Saunders Company. Reprinted by permission of Holt, Rinehart, and Winston.)

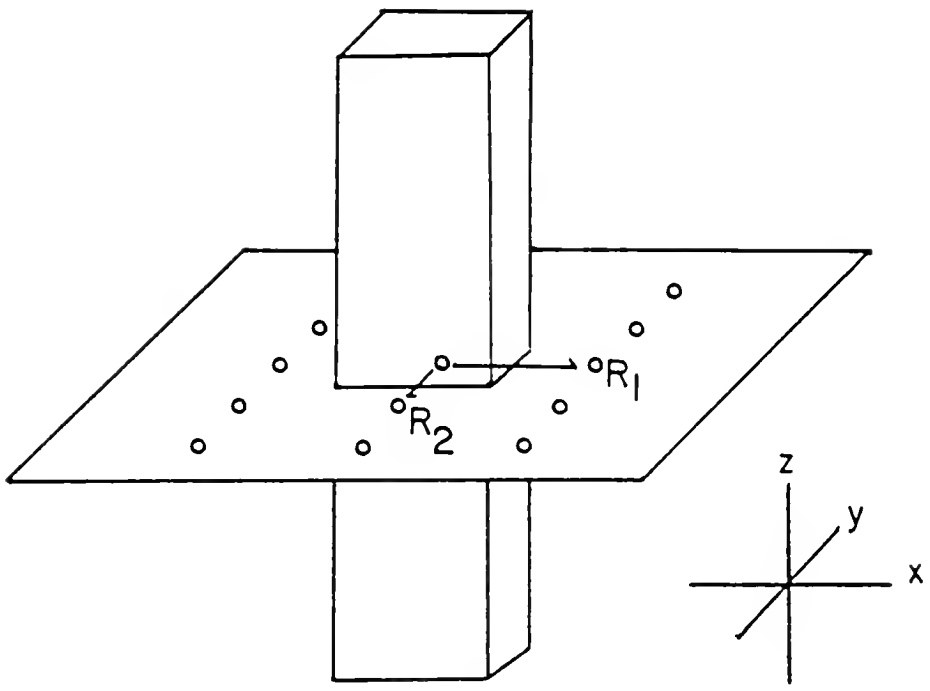

Figure 2-3. Illustration of parallelopiped unit cell for the two-dimensionally periodic monolayer. Note that the unit cell extends to infinite distance in both directions parallel to the z axis.

The operator $\{\hat{P}|\underline{R}\}$ can be seen to have the inverse operator $\{\hat{P}|\underline{R}\}^{-1}$ such that:

$$\{\hat{P}|\underline{R}\}^{-1} = \{\hat{P}^{-1}|-\hat{P}^{-1}\ \underline{R}\} \tag{2-3}$$

Given these definitions the operation of a symmetry operator upon a function $f(\underline{r})$ may be defined:

$$\{\hat{P}|\underline{R}\}\ f(\underline{r}) = f(\{\hat{P}|\underline{R}\}^{-1}\ \underline{r}) \tag{2-4}$$

Bloch's theorem applies to the two-dimensionally periodic thin film in a manner analogous to that for the three-dimensional crystalline case. From group theory (Tinkham, 1964) one can show that for an operator $\hat{M}$ which commutes with all the translation operators $\hat{R}$ (where $\hat{R}$ denotes the subgroup of translation operators of the plane group given by $\{\hat{E}|\underline{R}\}$, if $\hat{E}$ denotes the identity point group operator) the eigenfunctions of $\hat{M}$ can be chosen as members of the irreducible representations of the translation group. These irreducible representations may be labelled with wave vectors $\underline{k}_{//}$ that lie parallel to the plane of periodicity such that if the function $\Phi(\underline{r};\ \underline{k}_{//})$ belongs to the $\underline{k}_{//}$ irreducible representation, then:

$$\hat{R}\ \Phi(\underline{r};\ \underline{k}_{//}) = \Phi(\underline{r} - \underline{R};\ \underline{k}_{//}) = \exp(i\underline{k}_{//}\cdot\underline{R})\ \Phi(\underline{r};\ \underline{k}_{//}) \tag{2-5}$$

In a manner similar to the three-dimensional crystalline case, the set of wave vectors $\underline{k}_{//}$ is not a set of <u>unique</u> labels for each individual irreducible representation. For example, if the vector $\underline{c}$ is normal to both primitive lattice vectors $\underline{R}_1$ and $\underline{R}_2$ (e.g., $\underline{c} = \underline{R}_1 \times \underline{R}_2$), then two reciprocal lattice vectors may be defined as:

$$\underline{K}_1 = \frac{2\pi}{\underline{R}_1 \cdot (\underline{R}_2 \times \underline{c})} \quad (\underline{R}_2 \times \underline{c}) \tag{2-6}$$

and

$$\underline{K}_2 = \frac{2\pi}{\underline{R}_2 \cdot (\underline{R}_1 \times \underline{c})} \quad (\underline{R}_1 \times \underline{c}) \tag{2-7}$$

These reciprocal lattice vectors have the property that:

$$\underline{R}_i \cdot \underline{K}_j = 2\pi \, \delta_{ij} \tag{2-8}$$

Thus if we define a general reciprocal lattice vector $\underline{K}$ such that:

$$\underline{K} = h\underline{K}_1 + k\underline{K}_2 \tag{2-9}$$

then any two wave vectors $\underline{k}_{//}$ and $\underline{k}'_{//}$ related by:

$$\underline{k}'_{//} = \underline{k}_{//} + \underline{K} \tag{2-10}$$

label the same irreducible representation since:

$$\Phi(\underline{r} + \underline{R}; \underline{k}'_{//}) = \exp[i(\underline{k}_{//} + \underline{K}) \cdot \underline{R}] \; \Phi(\underline{r}; \underline{k}'_{//}) \tag{2-11}$$

$$= \exp[i\underline{k}_{//} \cdot \underline{R}] \; \Phi(\underline{r}; \underline{k}_{//})$$

Thus we may restrict our choice of wave vectors to the two-dimensional central Brillouin zone of wave vectors $\underline{k}_{//}$ closer to the origin than to any other point described by an arbitrary reciprocal lattice vector $\underline{K} \neq \underline{0}$.

With the Brillouin zone defined we may restate Bloch's theorem in a more straightforward form for use in solving finite secular matrix problems. The matrix elements of an operator $\hat{M}$, which commutes with all translation operators $\hat{R}$, will be zero for matrix elements between functions belonging to different irreducible representations labelled by $\underline{k}_{//}$ and $\underline{k}'_{//}$.

Recalling that the symmetry operators are unitary, or:

$$\langle \Phi_i(\underline{r}) | \hat{R}^{-1} \Phi_j(\underline{r}) \rangle = \langle \hat{R} \Phi_i(\underline{r}) | \Phi_j(\underline{r}) \rangle \tag{2-12}$$

We next consider the matrix element

$$\langle \Phi_i(\underline{r}; \underline{k}'_{//}) | \hat{M} \Phi_j(\underline{r}; \underline{k}_{//}) \rangle = \langle \Phi_i(\underline{r}; \underline{k}'_{//}) | \hat{R}^{-1} \hat{R} \hat{M} \Phi_j(\underline{r}; \underline{k}_{//}) \rangle \tag{2-13}$$

$$= \langle R \Phi_i(\underline{r}; \underline{k}'_{//}) | \hat{M} \hat{R} \Phi_j(\underline{r}; \underline{k}_{//}) \rangle$$

$$= \exp[i(\underline{k}'_{//} - \underline{k}_{//}) \cdot \underline{R}] \langle \Phi_i(\underline{r}; \underline{k}'_{//}) | \hat{M} \Phi(\underline{r}; \underline{k}_{//}) \rangle$$

Since $\underline{R}$ may represent any lattice point and by the hypothesis we are given that $\underline{k}'_{//} - \underline{k}_{//} \neq \underline{K}$, then the matrix element must equal zero:

$$\langle \Phi_i(\underline{r}; \underline{k}'_{//}) | \hat{M} \Phi_j(\underline{r}; \underline{k}_{//}) \rangle = 0 \tag{2-14}$$

A star of the wave vector $\underline{k}_{//}$ may be defined as the set of wave vectors generated by the operation of each symmetry operator in the point symmetry subgroup of the plane group of the thin film system on the wave vector $\underline{k}_{//}$. Since the wave vectors $\underline{k}_{//}$ are merely labels for the irreducible representations of the translation group, it is understood that if a symmetry operation yields a wave vector $\underline{k}''_{//}$ outside the central Brillouin zone then the wave vector $\underline{k}'_{//} = \underline{k}''_{//} + K$ equivalent to the wave vector $\underline{k}''_{//}$ is used as the member of the star. Thus it can be shown that the matrix elements of an operator $\hat{M}$ which commutes with the point group symmetry operators $\hat{P}$ (where $\hat{P}$ denotes $\{\hat{P}|\underline{0}\}$) have the property that:

$$\langle \Phi_i(\underline{r}; \underline{k}'_{//}) | \hat{M} \Phi_j(\underline{r}; \underline{k}_{//}) \rangle = \langle \Phi_i(\underline{r}; \underline{k}'_{//}) | \hat{P}^{-1} \hat{P} \hat{M} \Phi_j(\underline{r}; \underline{k}_{//}) \rangle \tag{2-15}$$

$$= \langle P\Phi_i(\underline{r}; \underline{k}'_{//}) | \hat{M} \hat{P} \Phi_j(\underline{r}; \underline{k}_{//}) \rangle$$

We notice that the new function $\hat{P}\Phi_i(\underline{r}; \underline{k}_{//})$ belongs to the irreducible representation labelled by $\hat{P}\underline{k}_{//}$, since if $\hat{R}$ is a general translation operator:

$$\hat{R}\,\hat{P}\,\Phi_i(\underline{r}; \underline{k}_{//}) = \hat{R}\,\Phi_i(\hat{P}^{-1}\,\underline{r}; \underline{k}_{//}) \tag{2-16}$$

$$= \Phi_i(\hat{P}^{-1}\,[\underline{r} - \underline{R}]; \underline{k}_{//})$$

$$= \exp[-i\underline{k}_{//}\cdot\hat{P}^{-1}\,\underline{R}]\;\Phi_i(\hat{P}^{-1}\,\underline{r}; \underline{k}_{//})$$

$$= \exp[-i(\hat{P}\underline{k}_{//})\cdot\underline{R}]\;\hat{P}\,\Phi_i(\underline{r}; \underline{k}_{//})$$

From group theory we recall that the eigenvectors of an operator $\hat{M}$ which commute with the operators of the symmetry group will be degenerate if a wave vector star possesses more than one unique member, since each irreducible representation $\underline{k}_{//}$ in the wave vector star will contain one degenerate eigenfunction. Equation 2-16 implies that this relationship is also true for the finite secular matrix problem if the basis sets are such that if the basis set for irreducible $\underline{k}_{//}$ contains a function $\Phi_i(\underline{r}; \underline{k}_{//})$, then the basis set for the $\hat{P}\underline{k}_{//}$ irreducible representation must contain the function $\hat{P}\Phi_i(\underline{r}; \underline{k}_{//})$.

2-2. The Xα Method

The Xα method is an approximate method for calculating the electronic structure of atoms, molecules, and extended systems using an approach originated by Slater (1951). The Born-Oppenheimer approximation (1927) is used to simplify the problem of finding the eigenvalues of the electronic Hamiltonian:

$$[\hat{H}(\underline{R}) - E(\underline{R})]\Psi(\underline{r}_i) = 0 \qquad (2\text{-}17)$$

where (using Hartree atomic units throughout):

$$\hat{H}(\underline{R}) = \sum_i \{-\frac{1}{2}\nabla^2_{\underline{r}_i} + \sum_{j>i}\frac{1}{r_{ij}} + \sum_m \frac{Z_m}{|\underline{r}_i - \underline{R}_n|} + \sum_{m>n}\frac{Z_m Z_n}{|\underline{R}_m - \underline{R}_n|}\} \qquad (2\text{-}18)$$

The coordinates $\underline{R}_m$ refer to nuclear coordinates and the coordinates $\underline{r}_i$ refer to electronic coordinates.

The Xα method originated as a means of approximating the Hartree-Fock model by replacing the non-local exchange terms with a local functional of the electron density (the origins of the Xα method are discussed at length in Slater (1974)). A different interpretation of the local exchange potential may be made using an approach based on the local density functional formalism of Kohn and Sham (1965). This local density functional formalism is based on the theorem by Hohenberg and Kohn (1964). The Hohenberg-Kohn theorem states that for a Hamiltonian of the general form

$$\hat{H} = \sum_i \{-\frac{1}{2}\nabla^2_{\underline{r}_i} + v(\underline{r}_i) + \sum_{j>i}\frac{1}{r_{ij}}\} \qquad (2\text{-}19)$$

there exists an energy functional $G[\rho]$ such that if $\rho(\underline{r})$ is the electron density resulting from $\Psi(\underline{r}_i)$, then

$$G[\rho] = \int d^{3n}r_i\ \Psi^*(\underline{r}_i)\ [\hat{H} - \sum_i v(\underline{r}_i)]\ \Psi(\underline{r}_i) \qquad (2\text{-}20)$$

Furthermore if $\rho_0(\underline{r})$ corresponds to the ground state $\Psi_0(\underline{r}_i)$ of the Hamiltonian H, then the total energy functional:

$$E[\rho] = G[\rho] + \int d^3r\ \rho(\underline{r})\ v(\underline{r}) \qquad (2\text{-}21)$$

has a variational minimum about the electron density $\rho_0(\underline{r})$.

If instead of considering just the electron density $\rho(\underline{r})$ but considering the first order density matrix $\rho(\underline{r};\ \underline{r}')$ which may without loss of generality be assumed to be of the form:

$$\rho(\underline{r};\ \underline{r}') = \sum_i n_i\ \Phi_i^*(\underline{r}')\ \Phi_i(\underline{r}) \tag{2-22}$$

where the functions Φ_i form an orthonormal basis and the occupation numbers have the property $0 \leq n_i \leq 1$, then we may define a new energy functional $E_{xc}[\rho]$:

$$E_{xc}[\rho] = G[\rho] - \int d^3r \int d^3r'\ \delta(\underline{r} - \underline{r}')[-\tfrac{1}{2}\nabla^2_{\underline{r}}]\ \rho(\underline{r};\ \underline{r}')$$

$$-\tfrac{1}{2}\int d^3r \int d^3r'\ \frac{\rho(\underline{r})\ \rho(\underline{r}')}{|\underline{r} - \underline{r}'|} \tag{2-23}$$

where $\rho(\underline{r}) = \rho(\underline{r};\ \underline{r})$. The second term on the right-hand side of Equation 2-23 corresponds to the expectation value of the kinetic energy of the first order density matrix $\rho(\underline{r};\ \underline{r}')$ and the third term corresponds to the Coulomb interaction of the charge density $\rho(\underline{r})$ with itself. Thus we see that the energy functional $E_{xc}[\rho]$ will correspond to the exchange and correlation energy components of the total energy.

The local density functional formalism is based on the approximation of the exchange correlation energy functional, which has an unknown analytic form, by a prescribed functional of the form:

$$E_{xc}[\rho] \simeq \int d^3r\ \{\rho\uparrow(\underline{r})\ V_{xc}(\rho\uparrow) + \rho\downarrow(\underline{r})\ V_{xc}(\rho\downarrow)\} \tag{2-24}$$

where $V_{xc}(\underline{r})$ is a function of the electron density of spin up for $\rho\uparrow$ and of the electron density of spin down for $\rho\downarrow$. The potential $V_{xc}(\underline{r})$ is most properly denoted as the exchange-correlation potential. However,

for brevity and historical continuity we shall refer to $V_{xc}(\underline{r})$ henceforth as the exchange potential.

In the Xα model the exchange potential V_{xc} is chosen to be of the form introduced by Slater (1951) with the addition of an adjustable parameter α with a value between 2/3 and 1 (Slater and Wood, 1971):

$$V_{x\alpha}(\rho\uparrow) = -\frac{9}{4}\alpha\left[\frac{3\rho\uparrow}{4\pi}\right]^{1/3} \tag{2-25}$$

For convenience we shall henceforth refer to an exchange potential operator $\hat{V}_{x\alpha}$ which when operating on $\rho(\underline{r})$ has the form:

$$\hat{V}_{x\alpha}\rho = V_{X\alpha}(\rho\uparrow)\rho\uparrow + V_{x\alpha}(\rho\downarrow)\rho\downarrow \tag{2-26}$$

This set of approximations yields an energy functional of the form:

$$E[\rho] = \frac{1}{2}\int d^3r \int d^3r' \left\{\delta(\underline{r} - \underline{r}')\,\nabla_r^2\,\rho(\underline{r};\,\underline{r}') + \frac{\rho(\underline{r})\,\rho(\underline{r}')}{|\underline{r} - \underline{r}'|}\right.$$

$$\left. + \int d^3r \left\{\hat{V}_{x\alpha} - \sum_m \frac{Z_m}{|\underline{r} - \underline{R}_m|}\right\}\rho(\underline{r}) + \sum_{m>n}\frac{Z_m Z_n}{|R_m - R_n|}\right. \tag{2-27}$$

where the total energy includes the nuclear repulsion term introduced by the Born-Oppenheimer approximation.

The orbitals $\Phi_i(\underline{r})$ are chosen by assuming as an approximate form the linear combination of a finite set of basis functions:

$$\Phi_i(\underline{r}) = \sum_m c_{mi}\,\psi_i(\underline{r}) \tag{2-28}$$

and the energy functional $E[\rho]$ is minimized using the variational principle subject to the constraint that the orbitals Φ_i are orthonormalized. This procedure yields the familiar secular equation:

$$\sum_n H_{mn}\,c_{ni} = \sum_n S_{mn}\,c_{ni}\,\varepsilon_i \tag{2-29}$$

where ε_i are the orbital eigenvalues and

$$S_{mn} = \int d^3r \; \psi_m^*(\underline{r}) \; \psi_n(\underline{r}) \tag{2-30}$$

$$H_{mn} = \int d^3r \; \psi_m^*(\underline{r}) \; \hat{H}_{eff}(\underline{r}) \; \psi_n(\underline{r}) \tag{2-31}$$

The one-electron Hamiltonian $H_{eff}(\underline{r})$ is given by:

$$\hat{H}_{eff}(\underline{r}) = -\frac{1}{2}\nabla^2 + \sum_m \frac{Z_m}{|\underline{r} - \underline{R}_m|} + \int d^3r' \frac{\rho(\underline{r}')}{|\underline{r} - \underline{r}'|} + \frac{4}{3} V_{X\alpha}(\rho_\sigma) \tag{2-32}$$

where ρ_σ corresponds to $\rho\uparrow$ if ψ_m and ψ_n correspond to spin up, and ρ_σ corresponds to $\rho\downarrow$ if ψ_m and ψ_n correspond to spin down.

2-3. LCAO Methods for Extended Systems

For infinitely extended systems the limit of the total energy of a finite section of the infinite system as the size of the finite section is systematically increased is not a useful definition of the total energy of the periodic system. It is easily seen that the total energy defined in this fashion will in most cases increase linearly with the cross-sectional area of the finite section (for two-dimensionally periodic systems as defined in Section 2-1) and thus will not have a convergent limit. The total energy per unit cell is a far more useful quantity that is usually convergent in the above mentioned limiting process for systems that possess zero total charge. In the Xα model the functional yielding the energy per unit cell may be expressed:

$$E[\rho] = -\frac{1}{2}\int_{\Omega} d^3r \int d^3r' \; \delta(\underline{r} - \underline{r}') \; \nabla_r^2 \; \rho(\underline{r}; \underline{r}')$$

$$+ \frac{1}{2}\int_{\Omega} d^3r \int d^3r' \; \frac{\rho(\underline{r}) \; \rho(\underline{r}')}{|\underline{r} - \underline{r}'|} - \sum_{\underline{R}} \int_{\Omega} d^3r \; \rho(\underline{r}) \sum_{m} \frac{Z_m}{|\underline{r} - \underline{R}_m - \underline{R}|}$$

$$+ \int_{\Omega} d^3r \; V_{x\alpha}(\underline{r}) + \frac{1}{2} \sum_{\underline{R}} {\sum_{m,n}}' \frac{Z_m Z_n}{|\underline{R}_m - \underline{R}_n - \underline{R}|} \qquad (2\text{-}33)$$

where the primed summation over the indices m and n indicates that the terms corresponding to $m = n$ when $\underline{R} = \underline{0}$ are to be omitted. The integrations over the region Ω denote an integration over one three-dimensional unit cell (as defined in Section 2-1).

For computational convenience we assume Born-von Karman (1912) periodic boundary conditions, such that all eigenfunctions of periodic operators are periodic over translations of the general form $M\,\underline{R}_1 + N\,\underline{R}_2$, where M and N are integers and $\underline{R}_1$ and $\underline{R}_2$ are the primitive lattice vectors for the system of interest. Periodic boundary conditions reduce the problem involving an infinite number of electrons to the problem of a finite number of electrons contained in M by N unit cells, such that the orbitals obey periodic boundary conditions. This yields a procedure which is effectively a cluster calculation on an M by N unit cell system with an external environment outside being a periodically repeated version of the internal system rather than empty space.

Let us approximate the orbitals $\Phi_i(\underline{r})$ by a linear combination of a finite number of orbitals $\psi_m(\underline{r})$. The spin-up one-electron effective Hamiltonian for this procedure may be expressed,

$$H^{\uparrow}_{eff}(\underline{r}) = -\frac{1}{2}\nabla^2 + \frac{1}{2}\int d^3r' \; \frac{\rho(\underline{r}')}{|\underline{r} - \underline{r}'|} - \sum_{\underline{R}} \sum_{m} \frac{Z_m}{|\underline{r} - \underline{R}_m - \underline{R}|} - 3\alpha\left[\frac{3\rho^{\uparrow}}{4\pi}\right]^{1/3} \qquad (2\text{-}34)$$

with the spin down effective Hamiltonian having an analogous form. From equation 2-14 we see that the logical choice of basis functions will be Bloch functions $\psi_m(\underline{r};\ \underline{k}_{//})$, or now labelling functions with the wave vector $\underline{k}_{//}$:

$$\rho(\underline{r};\ \underline{r}') = \sum_i \sum_{\underline{k}_{//}} n_i(\underline{k}_{//})\ \Phi_i^*(\underline{r};\ \underline{k}_{//})\ \Phi_i(\underline{r};\ \underline{k}_{//}) \tag{2-35}$$

$$\Phi_i(\underline{r};\ \underline{k}_{//}) = \sum_m c_{im}(\underline{k}_{//})\ \psi_m(\underline{r};\ \underline{k}_{//}) \tag{2-36}$$

We see that the Born-von Karman periodic boundary conditions require that the orthonormalization condition be expressed:

$$\int_{\Omega'} d^3r\ \psi_i^*(\underline{r};\ \underline{k}'_{//})\ \psi_j(\underline{r};\ \underline{k}'_{//}) = \delta_{ij}\ \delta_{\underline{k}_{//},\underline{k}'_{//}} \tag{2-37}$$

where the integration region Ω' corresponds to the region defined by the M by N unit cells. The periodic boundary conditions also restrict the choice of wave vectors to a discrete set, since

$$\psi_i(\underline{r} + M\underline{R}_1 + N\underline{R}_2;\ \underline{k}_{//}) = \exp[i\underline{k}_{//}\cdot(M\underline{R}_1 + N\underline{R}_2)]\ \psi_i(\underline{r};\ \underline{k}_{//}) \tag{2-38}$$

$$= \psi_i(\underline{r};\ \underline{k}_{//})$$

This implies

$$\underline{k}_{//} = \frac{m}{M}\underline{K}_1 + \frac{n}{N}\underline{K}_2, \quad (m \text{ and } n \text{ integers}) \tag{2-29}$$

are the only allowed choices of $\underline{k}_{//}$, in addition to the condition that we only consider wave vectors in the central Brillouin zone.

The Bloch basis functions $\psi_i(\underline{r};\ \underline{k}_{//})$ may be constructed from localized functions $U_i(\underline{r})$:

$$\psi_i(\underline{r};\ \underline{k}_{//}) = \sum_{\underline{R}} \exp[i\underline{k}_{//}\cdot\underline{R}]\ U_i(\underline{r} - \underline{R}) \tag{2-40}$$

This yields a secular equation of the form

$$\sum_n H_{mn}(\underline{k}_{//})\, c_{ni}(\underline{k}_{//}) = \varepsilon_i \sum_n S_{mn}(\underline{k}_{//})\, c_{ni}(\underline{k}_{//}) \tag{2-41}$$

where

$$S_{mn}(\underline{k}_{//}) = \sum_{\underline{R}} \exp[i\underline{k}_{//}\cdot\underline{R}] \int d^3r\, U_m^*(\underline{r}+\underline{R})\, U_n(\underline{r}) \tag{2-42}$$

$$H_{mn}(\underline{k}_{//}) = \sum_{\underline{R}} \exp[i\underline{k}_{//}\cdot\underline{R}] \int d^3r\, U_m^*(\underline{r}+\underline{R})\, \hat{H}_{eff}(\underline{r})\, U_n(\underline{r}) \tag{2-43}$$

2-4. Fitting Methods for Thin Films

The effective Hamiltonian in Equation 2-41 contains a term proportional to $\rho^{1/3}$; one cannot usually express integrals involving this term in an analytic closed form. One way of alleviating this difficulty for molecular systems is the approximation of the functions $\rho^{1/3}(\underline{r})$ by a linear combination of fitting functions $\tilde{G}_m(\underline{r})$, henceforth referred to as the exchange fit,

$$\rho^{1/3}(\underline{r}) \simeq \sum_m g_m\, \tilde{G}_m(\underline{r}) \tag{2-44}$$

This approach to solving the problems involving the analytic behavior of $\rho^{1/3}$ was originally suggested by Sambe and Felton (1975) with extensions to the formalism and computational method later introduced by Dunlap, Connolly, and Sabin (1977) and Mintmire (1979). In these previous works the total charge density $\rho(\underline{r})$ was also approximated using a linear combination of a set of charge fitting functions $\tilde{F}_m(\underline{r})$, this procedure being henceforth referred to as the charge fit,

$$\rho(\underline{r}) \simeq \sum_m f_m\, \tilde{F}_m(\underline{r}) \tag{2-45}$$

The rationale behind approximating $\rho(\underline{r})$ is to reduce the number of analytic integrals which must be computed, thus achieving a savings in computational effort.

For extended systems the fitting functions $\tilde{G}_m(\underline{r})$ and $\tilde{F}_m(\underline{r})$ are composed of periodic sums of localized functions $G_m(\underline{r})$ and $F_m(\underline{r})$, (where a localized function has the property that $\lim_{r\to\infty} r^3 G_m(\underline{r}) = 0$), that may be expressed:

$$\tilde{G}_m(\underline{r}) = \sum_{\underline{R}} G_m(\underline{r} - \underline{R}) \tag{2-46}$$

$$\tilde{F}_m(\underline{r}) = \sum_{\underline{R}} F_m(\underline{r} - \underline{R}) \tag{2-47}$$

The exchange fitting coefficients g_m are chosen using a least squares fitting procedure in which the set of conditions

$$\frac{\partial}{\partial g_i}\left[\int_\Omega d^3r \{\rho^{1/3}(\underline{r}) - \sum_m g_m \tilde{G}_m(\underline{r})\}^2 \right] = 0 \tag{2-48}$$

yield the matrix equation

$$\sum_n G_{mn} g_n = x_m \tag{2-49}$$

where

$$G_{mn} = \sum_{\underline{R}} \int d^3r \; G_m(\underline{r}) \; G_n(\underline{r} - \underline{R}) \tag{2-50}$$

and

$$x_m = \int_\Omega d^3r \; \rho^{1/3}(\underline{r}) \; \tilde{G}_m(\underline{r}) \tag{2-51}$$

$$= \int d^3r \; \rho^{1/3}(\underline{r}) \; G_m(\underline{r})$$

The matrix elements G_{mn} may be evaluated in analytic form if we choose the functions $G_m(\underline{r})$ to be some analytic function such as Hermite-Gaussian functions. The integrals x_m, however, require numerical integration for most cases where only the charge density is known as a linear combination of analytic functions. This procedure does allow a reduction of the total number of numerical integrations required compared to a process not using fitting by an approximate factor of N^2/N_x, where N is the number of orbital basis functions and N_x is the number of exchange fitting functions $G_m(\underline{r})$.

The total charge density $\rho(\underline{r})$ is also approximated using a linear combination of analytic functions such as Hermite-Gaussian functions. The rationale for fitting the charge density as well as $\rho^{1/3}$ is that the fitting process will reduce the total number of computationally time consuming integrals necessary for computing the Coulomb contributions to the total energy and the secular matrix by an approximate factor of N^2/N_c, where N_c is the number of charge fitting functions $F_m(\underline{r})$. Since the value of N_c is typically the same order of magnitude as N, approximating the density may produce a substantial saving in computational time.

Before explaining the procedure for choosing the coefficients f_m, let us digress for a moment to the problem of approximating charge densities in the general case using the methods introduced for molecular claculations by Dunlap (Dunlap, Connolly, and Sabin, 1979a) and by Mintmire (1979). Consider a prototypical molecular charge density $\rho(\underline{r})$ such that ρ decreases more rapidly than r^{-3} in the limit of large r. Then define the electrostatic interaction U of a charge density with itself to be $U = \frac{1}{2}[\rho|\rho]$, where

$$[\rho_1|\rho_2] = \int d^3r \int d^3r' \frac{\rho_1(\underline{r})\ \rho_2(\underline{r}')}{|\underline{r} - \underline{r}'|} \tag{2-52}$$

If the specified charge density ρ is approximated by another density $\tilde{\rho}$ which is dependent upon several parameters which may be varied independently, and if

$$\rho(\underline{r}) = \tilde{\rho}(\underline{r}) + \Delta\rho(\underline{r}) \tag{2-53}$$

then

$$[\rho|\rho] = 2[\rho|\tilde{\rho}] - [\tilde{\rho}|\tilde{\rho}] + [\Delta\rho|\Delta\rho] \tag{2-54}$$

Let us define an approximate electrostatic interaction energy $\tilde{U}$ in terms of the approximate density $\tilde{\rho}$ and the exact charge density ρ:

$$\tilde{U} = [\rho|\tilde{\rho}] - \frac{1}{2}[\tilde{\rho}|\tilde{\rho}] \tag{2-55}$$

Since the difference $\Delta U = U - \tilde{U} = \frac{1}{2}[\Delta\rho|\Delta\rho]$ is greater than or equal to zero for any choice of $\tilde{\rho}$, a reasonable criterion for choosing $\tilde{\rho}$ is the minimization of ΔU. This constraint will be satisfied if the variation of ΔU with respect to allowed variations of $\tilde{\rho}$ is zero:

$$\delta\Delta U = \delta\tilde{U} = 0 \tag{2-56}$$

leading to the relationship expressed in terms of $\delta\tilde{\rho}$:

$$\delta\tilde{U} = [\rho|\delta\tilde{\rho}] - [\tilde{\rho}|\delta\tilde{\rho}] = 0 \tag{2-57}$$

We see that if a variation of the form $\delta\rho = \tilde{\rho}\ d\varepsilon$ is possible within the range of variations allowed to $\tilde{\rho}$ and $d\varepsilon$ arbitrary, then the additional relationship

$$\{[\rho|\tilde{\rho}] - [\tilde{\rho}|\tilde{\rho}]\}\, d\varepsilon = 0 \tag{2-58}$$

is valid. This equation implies the equality

$$[\rho|\tilde{\rho}] = [\tilde{\rho}|\tilde{\rho}] \tag{2-59}$$

which shows that for the choice of $\tilde{\rho}$ satisfying Equation 2-57, then

$$\tilde{U} = \frac{1}{2}\,[\rho|\tilde{\rho}] = \frac{1}{2}\,[\tilde{\rho}|\tilde{\rho}] \tag{2-60}$$

For $\tilde{\rho}$ expressed as a linear combination of fitting functions $F_m(\underline{r})$:

$$\tilde{\rho}(\underline{r}) = \sum_m f_m F_m(\underline{r}) \tag{2-61}$$

we may restate Equation 2-57 in terms of the quantities f_m and $F_m(\underline{r})$:

$$\delta\tilde{U} = \sum_m \{[\rho|\frac{\partial\tilde{\rho}}{\partial f_m}] - [\tilde{\rho}|\frac{\partial\tilde{\rho}}{\partial f_m}]\}\, \delta f_m \tag{2-62}$$

$$= \sum_m \{[\rho|F_m] - \sum_n f_n\,[F_n|F_m]\}\, \delta f_m = 0$$

Since the variations δf_m are arbitrary and independent, each term in the summation over the index m must equal zero. Rearranging terms yields:

$$\sum_n [F_m|F_n]\, f_n = [F_m|\rho] \tag{2-63}$$

or

$$\sum_n B_{mn}\, f_n = a_n \tag{2-64}$$

where

$$B_{mn} = [F_m|F_n] \tag{2-65}$$

$$a_m = [F_m|\rho]$$

With the proper choice of fitting functions $F_m(\underline{r})$ and form of the charge density ρ, these integrals may be evaluated analytically.

Extension of these methods to extended systems requires a few modifications. The fitting functions are now the periodic fitting functions $\tilde{F}_m(\underline{r})$ formed from the periodic sum of the localized functions $F_m(\underline{r})$ as stated in Equation 2-47. The charge interaction expression $[\rho_1|\rho_2]$ must also be redefined in order to avoid dealing with infinite terms. The most convenient definition of this term, if ρ_1 and ρ_2 are periodic extended charge densities, is the electrostatic interaction per unit cell:

$$[\rho_1|\rho_2] = \int_\Omega d^3r \int d^3r' \frac{\rho_1(\underline{r})\ \rho_2(\underline{r}')}{|\underline{r} - \underline{r}'|} \tag{2-66}$$

The charge interaction term $[\rho_1|\rho_2]$ is still non-negative for $\rho_1 = \rho_2$ and ρ_1 having no singularities. In addition, this expression is still symmetric with respect to the order of ρ_1 and ρ_2 (both of which are periodic), since

$$[\rho_1|\rho_2] = \int_\Omega d^3r \int d^3r' \frac{\rho_1(\underline{r})\ \rho_2(\underline{r}')}{|\underline{r} - \underline{r}'|} \tag{2-67}$$

$$= \sum_{\underline{R}} \int_\Omega d^3r \int_\Omega d^3r' \frac{\rho_1(\underline{r})\ \rho_2(\underline{r}' - \underline{R})}{|\underline{r} - \underline{r}' + \underline{R}|}$$

$$= \sum_{\underline{R}} \int_\Omega d^3r \int_\Omega d^3r' \frac{\rho_1(\underline{r} + \underline{R})\ \rho_2(\underline{r}')}{|\underline{r} + \underline{R} - \underline{r}'|}$$

$$= \int_\Omega d^3r' \int_\Omega d^3r \frac{\rho_2(\underline{r}')\ \rho_1(\underline{r})}{|\underline{r} - \underline{r}'|} = [\rho_2|\rho_1]$$

This expression for the charge interaction is also convenient because it satisfies two conditions:

1) for $\tilde{F}_m(\underline{r})$ a periodic function formed from the periodic sum of of localized functions $F_m(\underline{r})$ as in Equation 2-47, then

$$[\tilde{F}_m|\tilde{F}_n] = \sum_{\underline{R}} \int d^3r \int d^3r' \frac{F_m(\underline{r})\, F_n(\underline{r} - \underline{R})}{|\underline{r} - \underline{r}'|} \tag{2-68}$$

which is analytically integrable in closed form for $F_m(\underline{r})$ being a Hermite-Gaussian function;

2) $[\rho_1|\rho_2]$ is finite if and only if one or both of the charge distributions ρ_1 and ρ_2 satisfy the charge neutrality condition:

$$\int_\Omega d^3r\ \rho(\underline{r}) = 0 \tag{2-69}$$

The first condition is evident upon inspection. The second condition follows from consideration of a limiting procedure which begins with a finite assembly of identical unit cells. The initial assembly is constructed with no embedded voids. The limiting process then consists of arbitrary enlargement of the finite assembly, with the infinitely periodic (in two-dimensions) slab the ultimate result. Any such finite assembly has a periodic charge density which satisfies the explicit constraint on asymptotic behavior required by the definition of the molecular charge density interaction $[\rho_1|\rho_2]$ of Equation 2-52. It then follows from Equation 2-52 that the charge interaction for such a finite assembly with the charge density belonging to a <u>single</u> unit cell is

$$[\rho_1|\rho_2] = \sum_{\underline{R}}{}' \int_\Omega d^3r \int_\Omega d^3r' \frac{\rho_1(\underline{r})\, \rho_2(\underline{r}')}{|\underline{r} - \underline{r}' + \underline{R}|} \tag{2-70}$$

where the primed summation indicates a finite number of terms. In order to carry through a physically reasonable limiting process the single unit cell is conceived as being the most nearly central unit cell of the

finite assembly. Similarly the origin of coordinates is associated, for convenience, with the central unit cell. Then for each term of Equation 2-70 save for the one corresponding to $\underline{R} = \underline{0}$ the contribution may be exactly as a multipole expansion (see Appendix B for a more detailed discussion). If the charge neutrality condition is not satisfied then the leading term in the multipole expansion will be a monopole-monopole interaction term proportional to R^{-1}. For a two-dimensional lattice of vectors $\underline{R}$ an infinite sum of monopole-monopole interactions is not convergent. Therefore in the limit of an arbitrarily extended slab, the charge neutrality condition is necessary if the charge interaction is to converge to finite limit. Similarly if the charge neutrality condition is satisfied, the leading term in the multipole expansion for given $\underline{R}$ is a monopole-dipole term proportional to R^{-2}. It is shown in Appendix B, however, that this multipole term has zero total contribution to the charge interaction term for two-dimensional lattices with inversion symmetry. Thus the leading order term with a non-zero contribution to the charge interaction term will be a term proportional to R^{-3}, which leads to a convergent sum in Equation 2-70 in the infinite limit under consideration.

Thus the second condition leads immediately to the observation that Equations 2-63 through 2-65 as derived are not usable in a direct manner, since the density involved is purely electronic and manifestly not neutral. However, Equation 2-65 is valid for the extended system so long as charge densities neutral by cells are employed. For any finite system Equation 2-63 may be rewritten trivially as

$$[\tilde{F}_m|\rho - \sum_n f_n \tilde{F}_n] = 0 \qquad (2\text{-}71)$$

irrespective of charge neutrality. In the limit described above, however, the charge interaction expression becomes that of Equation 2-67 and the necessary and sufficient conditions on charge neutrality come into play with the result that if at least one of the $\tilde{F}_m$ is not charge neutral, then the right-hand factor in Equation 2-71 must be charge neutral, where

$$\int_\Omega d^3r\ \rho(\underline{r}) = \sum_n f_n \int_\Omega d^3r\ \tilde{F}_n(\underline{r}) = \sum_n f_n \int d^3r\ F_n(\underline{r}) \tag{2-72}$$

or expressed differently

$$\sum_n f_m\ \eta_m = 1 \tag{2-73}$$

where

$$\eta_m = \{\int d^3r\ F_m(\underline{r})\} \ /\ \{\int_\Omega d^3r\ \rho(\underline{r})\} \tag{2-74}$$

We can produce a matrix equation equivalent to Equation 2-64 if we introduce a nuclear lattice charge ρ_N to each electronic density, thereby giving the requisite cell-by-cell neutrality, to the interaction term in Equation 2-64 and then subtract out terms contained in Equation 2-71 and analyze the identity

$$[\tilde{F}_m - \eta_m\rho_N|\rho - \rho_N] - [\tilde{F}_m - \eta_m\rho_N|\sum_n f_n(\tilde{F}_n - \eta_n\rho_N)] \tag{2-75}$$

$$= [\tilde{F}_m|\rho - \sum_n f_n\tilde{F}_n] - \{1 - \sum_n f_n\eta_n\}[\tilde{F}_m - \eta_m\rho_N|\rho_N] - \eta_m[\rho_N|\rho - \sum_n f_n\tilde{F}_n]$$

The first term of the right hand side of Equation 2-75 is zero according to Equation 2-71. Since Equation 2-73 states that $\{1 - \sum_n f_n\eta_n\} = 0$ and in addition we see that $[\tilde{F}_m - \eta_m\rho_N|\rho_N]$ is finite, then the second term of

the right-hand side of Equation 2-75 must equal zero. The term $[\rho_N|\rho - \sum_n f_n\tilde{F}_n]$ must also be finite (again by charge neutrality) for thin films; therefore Equation 2-75 reduces to:

$$\{\sum_n f_n[\tilde{F}_m - \eta_m\rho_N|\tilde{F}_n - \eta_n\rho_N]\} - [\tilde{F}_m - \eta_m\rho_N|\rho - \rho_N] = \eta_m\lambda \qquad (2\text{-}76)$$

where

$$\lambda = [\rho_N|\rho - \sum_n f_n\tilde{F}_n] \qquad (2\text{-}77)$$

is an undetermined constant independent of the index m in Equation 2-76. Restating Equation 2-76 in matrix notation yields:

$$\sum_n B_{mn} f_n = a_m + \lambda\eta_m \qquad (2\text{-}78)$$

where

$$B_{mn} = [\tilde{F}_m - \eta_m\rho_N|\tilde{F}_n - \eta_n\rho_N] \qquad (2\text{-}79)$$

$$a_m = [\tilde{F}_m - \eta_m\rho_N|\rho - \rho_N] \qquad (2\text{-}80)$$

This set of equations is similar to the equations resulting from a least-squares fitting procedure which includes a linear constraint equation. Thus we may solve for λ by rearranging Equation 2-78:

$$f_m - \sum_n \{B^{-1}\}_{mn} a_n = \lambda \sum_n \{B^{-1}\}_{mn} \eta_n \qquad (2\text{-}81)$$

$$\sum_m \eta_m f_m - \sum_m \sum_n \eta_m \{B^{-1}\}_{mn} a_n = \lambda \sum_{mn} \eta_m \{B^{-1}\}_{mn} \eta_n \qquad (2\text{-}82)$$

resulting in the value of

$$\lambda = \{1 - \sum_m \sum_n \eta_m \{B^{-1}\}_{mn} a_n\} / \{\sum_m \sum_n \eta_m \{B^{-1}\}_{mn} \eta_n\} \qquad (2\text{-}83)$$

The solution for the coefficients f_m is then given by

$$f_m = \sum_n \{B^{-1}\}_{mn} \cdot (a_n + \lambda \eta_n) \tag{2-84}$$

We see that the approximate electrostatic interaction energy defined in Equation 2-55 now has the form:

$$\tilde{U} = \sum_n f_n a_n - \frac{1}{2} \sum_m \sum_n f_n \{B^{-1}\}_{mn} f_n \tag{2-85}$$

$$= [\tilde{\rho}|\rho] - \frac{1}{2}[\tilde{\rho}|\tilde{\rho}] - [\rho|\rho_N] + \frac{1}{2}[\rho_N|\rho_N] \tag{2-86}$$

which is the electrostatic energy of the combined electronic and nuclear charges with only the electron repulsion term being replaced by an approximate interaction.

2-5. Self-Consistent Solution of the Secular Equation

The orbital coefficients $c_{ni}(\underline{k}_{//})$ are obtained by solving the secular equation in Equation 2-41. Since the matrix elements $H_{mn}(\underline{k}_{//})$ are dependent upon the coefficients $c_{ni}(\underline{k}_{//})$ for which we seek a solution, Equation 2-41 is solved using the familiar iterative procedure known as the self-consistent field (SCF) method, described by Slater (1963) for atomic and molecular systems. In the SCF method one starts with an initial choice of $c_{ni}(\underline{k}_{//})$ to generate the matrix elements $H_{mn}(\underline{k}_{//})$. The secular equation is then solved to yield a new set of values for the coefficients $c_{ni}(\underline{k}_{//})$ which is used to begin a new iteration. This process is repeated until some predetermined criterion of convergence for the iterative process is satisfied.

Due to the introduction of the fitting procedures, the secular equation defined in Equations 2-41 through 2-43 will not use the effective Hamiltonian as it stands in Equation 2-34. Instead the effective Hamiltonian will be of the form (for the spin up effective Hamiltonian):

$$\hat{H}^{\uparrow}_{eff}(\underline{r}) = -\frac{1}{2}\nabla^2 + \sum_m f_m \int d^3r' \frac{\tilde{F}_m(\underline{r}')}{|\underline{r} - \underline{r}'|} - \sum_{\underline{R}} \sum_a \frac{Z_a}{|\underline{r} - \underline{R}_a - \underline{R}|}$$

$$- 3\alpha\left[\frac{3}{4\pi}\right]^{1/3} \sum_m g_m \tilde{G}_m(\underline{r}) \qquad (2\text{-}87)$$

Thus given an initial choice of $c_{ni}(\underline{k}_{//})$ and $n_i(\underline{k}_{//})$, the logical order of each iteration will be:

1) Compute the fitting coefficients f_m and g_m;

2) Use the fitting coefficients to generate the secular matrix defined in Equation 2-87;

3) Solve the secular Equation 2-41 to yield a new set of coefficients $c_{ni}(\underline{k}_{//})$ and occupation numbers $n_i(\underline{k}_{//})$.

Since this procedure differs from those of typical LCAO calculations in the use of a fitting formalism, we present briefly a discussion of the necessary equations for the above-mentioned procedure for each iteration, beginning with an initial set of coefficients $c_{ni}(\underline{k}_{//})$ and occupation numbers $n_i(\underline{k}_{//})$.

First the charge density ρ of Equation 2-35 is used with the fitting scheme of Equations 2-78 through 2-84 to compute the charge fitting coefficients f_m. The B_{mn} matrix elements of Equation 2-79 are evaluated directly while the values for a_m are constructed:

$$a_m = \{\sum_i \sum_{\underline{k}_{//}} n_i(\underline{k}_{//}) \sum_j \sum_k c^*_{ji}(\underline{k}_{//})\, c_{ki}(\underline{k}_{//})\, V_{jkm}(\underline{k}_{//})\} - C_m \qquad (2\text{-}88)$$

where

$$V_{jkm}(\underline{k}_{//}) = \sum_{\underline{R}} \sum_{\underline{R}'} \exp[i\underline{k}_{//}\cdot\underline{R}] \int d^3r\ U_j^*(\underline{r} + \underline{R})\ U_k(\underline{r})$$

$$\times \{\int d^3r' \frac{F_m(\underline{r}' - \underline{R}')}{|\underline{r} - \underline{r}'|} - \eta_m \sum_a \frac{Z_a}{|\underline{r}' - \underline{R}_a - \underline{R}'|}\} \qquad (2\text{-}89)$$

and

$$C_m = \sum_{\underline{R}} \{[\int d^3r\ F_m(\underline{r} - \underline{R}) \sum_a \frac{Z_a}{|\underline{r} - \underline{R}_a|}] - \eta_m \sum_a \sum_b{}' \frac{Z_a Z_b}{|\underline{R}_a - \underline{R}_b - \underline{R}|}\} \qquad (2\text{-}90)$$

The primed summation indicates that nuclear self-interaction terms for which $\underline{R}$ is the zero vector and indices a and b denote identical nuclear sites are to be omitted.

Next the cube root of the density is fit using Equation 2-49. The G_{mn} matrix elements are evaluated in the form given in Equation 2-50. The x_m integrals are evaluated using a numerical integration procedure. For each numerical grid point $\underline{r}_i$ the value of the density $\rho(\underline{r}_i)$ is generated from the precalculated values of Bloch functions $\psi_j(\underline{r}_i;\ \underline{k}_{//})$ and the exchange functions $\tilde{G}_m(\underline{r}_i)$:

$$\rho(\underline{r}_i) = \sum_{\ell} \sum_{\underline{k}_{//}} n_\ell(\underline{k}_{//}) \left| \sum_j c_{j\ell}(\underline{k}_{//})\ \psi_j(\underline{r}_i;\ \underline{k}_{//}) \right|^2 \qquad (2\text{-}91)$$

which is then used to compute $\rho^{1/3}(\underline{r}_i)$. The numerical cube root of the density is used then with the values of the exchange fitting functions $\tilde{G}_m(\underline{r}_i)$ to evaluate x_m integral numerically:

$$x_m = \sum_i w_i\ \rho^{1/3}(\underline{r}_i)\ \tilde{G}_m(\underline{r}_i) \qquad (2\text{-}92)$$

where the weights w_i and the grid points $\underline{r}_i$ are appropriately chosen

grid points for a three-dimensional numerical integration over the unit cell volume Ω.

The fitting coefficients f_m and g_m are then used to evaluate the elements of the secular matrix defined by Equation 2-43. Using the expression for the effective Hamiltonian of Equation 2-87, the matrix elements for the spin up effective Hamiltonian have the form:

$$H_{ij}(\underline{k}_{//}) = T_{ij}(\underline{k}_{//}) + \sum_m f_m V_{ijm}(\underline{k}_{//}) - 3\alpha\left[\frac{3}{4\pi}\right]^{1/3} \sum_m g_m X_{ijm}(\underline{k}_{//}) \quad (2\text{-}93)$$

where

$$T_{ij}(\underline{k}_{//}) = \sum_{\underline{R}} \exp[i\underline{k}_{//}\cdot\underline{R}] \int d^3r\, U_i^*(\underline{r} + \underline{R})\{-\frac{1}{2}\nabla^2\} U_j(\underline{r}) \quad (2\text{-}94)$$

and

$$X_{ijm}(\underline{k}_{//}) = \sum_{\underline{R}} \exp[i\underline{k}_{//}\cdot\underline{R}] \sum_{\underline{R}'} \int d^3r\, U_i^*(\underline{r} + \underline{R})\, U_j(\underline{r})\, G_m(\underline{r} - \underline{R}') \quad (2\text{-}95)$$

This form of the secular matrix is diagonalized and new occupation numbers $n_i(\underline{k}_{//})$ are computed, using the eigenvalues of the secular equation to find the lowest eigenstates of the effective Hamiltonian to occupy. At this point the agreement between the current orbital coefficients $c_{ni}(\underline{k}_{//})$ and those present at the beginning of the current iteration is tested for convergence of the iterative sequence. If the convergence criteria are not satisfied, a new iteration begins.

CHAPTER III
COMPUTATIONAL METHODS

3-1. Choice of Basis Sets

In any atomic, molecular, or solid state calculation of electronic structure using a linear combination of a finite set of basis functions as approximate orbitals, the particular choice of functions is a critical part of the computational procedure. The first decision in choosing basis functions that must be made is the type of functions to be used. This work is based on the use of Hermite-Gaussian functions, which are described in Appendix A. These functions are specific linear combinations of the more familiar Cartesian Gaussians of the form $x^l y^m z^n \exp(-ar^2)$, where l, m, and n are nonnegative integers and the exponent coefficient a (commonly denoted the "orbital exponent") is constant for all Cartesian Gaussians which are components of the Hermite-Gaussian. That is, all Hermite-Gaussians may be expressed as $P(x,y,z)\exp(-ar^2)$, where $P(x,y,z)$ is a polynomial of finite order of the coordinate variables x, y, and z.

The total number of Hermite-Gaussian functions in the basis and the choice of the orbital exponents a_i is also a critical choice. Fortunately there is an extensive literature of results of atomic and molecular calculations using Cartesian Gaussian functions that may be consulted in making these decisions so that Cartesian basis sets may be converted to Hermite-Gaussian basis sets. The conversion for most systems from Cartesian Gaussian basis sets to Hermite-Gaussian basis sets is usually

trivial, since s and p type Cartesian Gaussian functions correspond to equivalent Hermite-Gaussian basis functions. Cartesian d type functions cannot be expressed as a single Hermite-Gaussian function; instead they must be expressed as a sum of two Hermite-Gaussian functions. This is not a serious problem, since we may include both Hermite-Gaussian functions and contract them to yield the Cartesian Gaussian. Thus we may use Cartesian Gaussian basis sets expressed as contracted Hermite-Gaussians if necessary. The charge fitting and exchange fitting basis sets are then chosen using the method described by Dunlap, Connolly, and Sabin (1979a) for atomic and molecular calculations.

3-2. Overlap and Kinetic Energy Integrals

The overlap matrix elements $S_{ij}(\underline{k}_{//})$ between normalized Hermite-Gaussian basis functions will be of the form:

$$S_{ij}(\underline{k}_{//}) = (N_i N_j)^{-1/2} \sum_{\underline{R}} \exp[i\underline{k}_{//}\cdot\underline{R}]$$

$$\int d^3r\ f(\hat{n}_i, a_i, \underline{A}_i - \underline{R};\ \underline{r})\ f(\hat{n}_j, a_j, \underline{A}_j;\ \underline{r}) \qquad (3\text{-}1)$$

where N_i and N_j are normalization constants for the localized Hermite-Gaussians. The kinetic energy matrix elements $T_{ij}(\underline{k}_{//})$ are evaluated at the same time as the overlap matrix elements since they are of the same general form as the overlap matrix elements such that:

$$T_{ij}(\underline{k}_{//}) = (N_i N_j)^{-1/2} \sum_{\underline{R}} \exp[i\underline{k}_{//}\cdot\underline{R}]$$

$$\frac{1}{2} \sum_{s=1}^{3} \int d^3r\ f(\hat{n}_i + 2\hat{u}_s, a_i, \underline{A}_i - \underline{R};\ \underline{r})\ f(\hat{n}_j, a_j, A_j;\ \underline{r}) \qquad (3\text{-}2)$$

where the integer sets $\hat{u}_s$ refer to the sets (1,0,0), (0,1,0), and (0,0,1) for values of s equal to 1, 2, and 3 respectively. For values of a and b such that $(a+b)R^2_{max}$ is greater than 1 (the value of 1 is rather arbitrary and may be adjusted in order to speed computational time as more computational benchmarks are accumulated) these integrals will be evaluated using direct lattice sums of integrals of the form given in Equation A-5 in Appendix A. For values of $(a+b)R^2_{max}$ (where R_{max} is the greater of $\underline{R}_1$ and $\underline{R}_2$, the primitive lattice vectors) less than or equal to 1, the overlap matrix elements and kinetic energy matrix elements are evaluated using reciprocal lattice space techniques described in Appendix C using expansions of the form given by Equation C-8.

Löwdin orthonormalization (Löwdin, 1956) is used to transform the matrix elements of the secular matrix to an orthonormal basis so that the $\underset{\sim}{S}$ matrix in the secular equation will be the unit matrix. First the unitary matrix $\underset{\sim}{U}$ is found which diagonalizes the overlap matrix:

$$\underset{\sim}{U}^{\dagger}\ \underset{\sim}{S}\ \underset{\sim}{U} = \underset{\sim}{d} \tag{3-3}$$

The overlap matrix may then be transformed to the unit matrix by use of the matrix $\underset{\sim}{T}$:

$$\underset{\sim}{T}^{\dagger}\ \underset{\sim}{S}\ \underset{\sim}{T} = \underset{\sim}{1} \tag{3-4}$$

where

$$\underset{\sim}{T} = \underset{\sim}{U}\ \underset{\sim}{d}^{-1/2} \tag{3-5}$$

The secular equation of Equation 2-41 then transforms according to

$$\underset{\sim}{T}^{\dagger}\ \underset{\sim}{H}\ \underset{\sim}{T}\ (\underset{\sim}{T}^{-1}\ \underset{\sim}{C}) = (\underset{\sim}{T}^{-1}\ \underset{\sim}{C})\ \underset{\sim}{\varepsilon} \tag{3-6}$$

Approximate linear dependencies (which arise from the limits to precision inherent in any computational procedure) in the basis may be handled by excluding eigenvectors of the overlap matrix which have eigenvalues less than some specified tolerance (for the purposes of this work the tolerance was chosen to be 10^{-5}).

3-3. Fitting Function Integrals

The integrals B_{ij}, C_j, $V_{ijm}(\underline{k}_{//})$, and $X_{ijm}(\underline{k}_{//})$ currently are evaluated using direct lattice expansion techniques as discussed in Appendix A. The matrix elements B_{ij}, defined in Equation 2-79, may be reduced to the form:

$$B_{ij} = \sum_{\underline{R}} \{ (-1)^{n_j} \frac{2\pi^{5/2}}{a_i a_j (a_i+a_j)^{1/2}} R(\hat{n}_i+\hat{n}_j, \frac{a_i a_j}{a_i+a_j}, \underline{A}_i-\underline{R}-\underline{A}_j)$$

$$- \sum_a 2\pi Z_a [\frac{n_i}{a_j} R(\hat{n}_j, a_j, \underline{A}_j+\underline{R}-\underline{R}_a) + \frac{n_j}{a_i} R(\hat{n}_i, a_i, \underline{A}_i-\underline{R}-\underline{R}_a)]$$

$$+ n_i n_j \sum_a \sum_b{}' \frac{Z_a Z_b}{|\underline{R}_a-\underline{R}-\underline{R}_b|} \} \qquad (3\text{-}7)$$

using Equations A-40 and A-46. The C_j integrals, defined in Equation 2-90, may be reduced to

$$C_j = \sum_{\underline{R}} \{ \sum_a \frac{2\pi Z_a}{a_j} R(\hat{n}_j, a_j, \underline{A}_j-\underline{R}-\underline{R}_a) - n_j \sum_a \sum_b{}' \frac{Z_a Z_b}{|\underline{R}_a-\underline{R}-\underline{R}_b|} \} \qquad (3\text{-}8)$$

Equations A-41 and A-47 may be used to convert the matrix elements $V_{ijm}(\underline{k}_{//})$ to the form:

$$V_{ijm}(\underline{k}_{//}) = (N_i N_j)^{-1/2} \sum_{\underline{R}} \exp[i\underline{k}_{//}\cdot\underline{R}] \sum_{\hat{K}} g(\hat{K},\hat{n}_i,\hat{n}_j,a_i,a_j)$$

$$f(\hat{K},\frac{a_i a_j}{a_i+a_j},\underline{A}_i-\underline{R}-\underline{A}_j;\ \underline{0}) \sum_{\underline{R}'} \{(-1)^{n_m} \frac{2\pi^{5/2}}{(a_i+a_j)a_m(a_i+a_j+a_m)^{1/2}}$$

$$R(\hat{n}_i+\hat{n}_j+\hat{n}_m-\hat{K},\ \frac{(a_i+a_j)a_m}{a_i+a_j+a_m},\ \frac{a_i(\underline{A}_i-\underline{R})+a_j\underline{A}_j}{a_i+a_j} - \underline{A}_m-\underline{R}')$$

$$-\sum_a Z_a \frac{2\pi\eta_m}{a_i+a_j} R(\hat{n}_i+\hat{n}_j-\hat{K},\ a_i+a_j,\ \frac{a_i(\underline{A}_i-\underline{R})+a_j\underline{A}_j}{a_i+a_j} - \underline{R}_a-\underline{R}')\}$$

(3-9)

For the direct lattice expansions displayed in Equations 3-7 and 3-8 and the inner lattice sum over $\underline{R}'$ in Equation 3-9, multipole expansion techniques as described in Appendix B are used to increase the computational speed of evaluating these integrals.

The exchange fitting integrals $X_{ijm}(\underline{k}_{//})$, defined in Equation 2-95, are also evaluated in a double lattice sum having the form:

$$X_{ijm}(\underline{k}_{//}) = (N_i N_j)^{-1/2} \sum_{\underline{R}} \exp[i\underline{k}_{//}\cdot\underline{R}] \sum_{\hat{K}} g(\hat{K},\hat{n}_i,\hat{n}_j,a_i,a_j)$$

$$f(\hat{K},\ \frac{a_i a_j}{a_i+a_j},\ \underline{A}_i-\underline{R}-\underline{A}_j;\ 0) \sum_{\underline{R}'} \left(\frac{\pi}{a_i+a_j+a_m}\right)^{3/2} (-1)^{n_m}$$

$$f(\hat{n}_i+\hat{n}_j+\hat{n}_m-\hat{K},\ \frac{(a_i+a_j)a_m}{a_i+a_j+a_m},\ \frac{a_i(\underline{A}_i-\underline{R})-a_j\underline{A}_j}{a_i+a_j} - \underline{A}_m-\underline{R}';\ 0)$$

(3-10)

All of the above integrals could also be evaluated using reciprocal lattice expansions as discussed in Appendix C. Since $V_{ijm}(\underline{k}_{//})$ and $X_{ijm}(\underline{k}_{//})$ each contain two lattice sums as expressed in Equations 3-9 and 3-10, we may choose to convert one or both of the direct lattice summations to reciprocal lattice expansions. An approach using double reciprocal lattice expansions has been tested for the case of all spherically symmetric Gaussian functions for the $V_{ijm}(\underline{k}_{//})$ and $X_{ijm}(\underline{k}_{//})$ integrals (which are the computationally most time consuming integrals to evaluate). The results from these tests indicate that the large number of sine and cosine function evaluations required make the double lattice reciprocal lattice expansion algorithm at best equal in computational time to the direct lattice expansion algorithm for integrals involving diffuse Gaussian functions, which is the case requiring the most computer time using the direct lattice expansion algorithm. For Gaussian functions which were not extremely diffuse, the double reciprocal lattice expansion algorithms required considerably more computational time than algorithms using the double direct lattice expansions.

Another approach would be to convert only the inner lattice sums over $\underline{R}'$ in Equations 3-9 and 3-10 to reciprocal lattice expansions. The formulas necessary for incorporating this approach into computational algorithms are derived in Appendix C. This approach has not yet been incorporated into the computer code, leaving open one avenue for increasing the computational speed of the computer code for calculating the thin layer electronic structure.

3-4. Numerical Integration Techniques

In order to fit the exchange potential [or more precisely, the function $\rho^{1/3}(\underline{r})$] to a linear combination of fitting functions $\tilde{G}_m(\underline{r})$ we must numerically integrate the expression:

$$x_m = \int_\Omega d^3r\ \rho^{1/3}(\underline{r})\ \tilde{G}_m(\underline{r}) \tag{3-11}$$

This leads to the approximate form of x_m:

$$x_m \simeq \sum_i w_i \rho^{1/3}(\underline{r}_i)\ \tilde{G}_m(\underline{r}_i) \tag{3-12}$$

The integration points $\underline{r}_i$ and weights w_i, which are chosen for numerical integration over the parallelopiped primitive unit cell defined in Section 2-1, are discussed in Appendix D.

The values of the primitive orbitals $\psi_j(\underline{r}_i;\ \underline{k}_{//})$ and the values of the periodic fitting functions $\tilde{G}_m(\underline{r}_i)$ must be evaluated at each integration point. For a primitive Bloch orbital $\psi(\underline{r}_i;\ \underline{k}_{//})$ constructed from localized Hermite-Gaussian functions:

$$\psi(\underline{r}_i;\ \underline{k}_{//}) = N^{-1/2} \sum_{\underline{R}} \exp[i\underline{k}_{//}\cdot\underline{R}]\ f(\hat{n},a,\underline{A}+\underline{R};\ \underline{r}_i) \tag{3-13}$$

we may evaluate $\psi(\underline{r}_i;\ \underline{k}_{//})$ either by using the above direct lattice expansion or by using the reciprocal lattice expansion:

$$\psi(\underline{r}_i;\ \underline{k}_{//}) = \frac{\pi}{a\Omega} N^{-1/2}\ a^{n_3/2}\ H_{n_3}[a^{1/2}(z-A_z)]$$

$$\sum_{\underline{K}} (-i)^{n_1+n_2}\ (K_x+k_{//x})^{n_1}\ (K_y+k_{//y})^{n_2}$$

$$\exp[-(\underline{K}+\underline{k}_{//})^2/4a]\ \exp[i(\underline{K}+\underline{k}_{//})\cdot(\underline{r}_i-\underline{A})] \tag{3-14}$$

discussed in Appendix C. Evaluation of the periodic fitting function $\tilde{G}_m(\underline{r}_i)$, defined in Equation 2-46, is equivalent in form to that of a Bloch function with a wave vector $\underline{k}_{//}$ equal to the zero vector. Thus we may evaluate the fitting function with either a direct lattice expansion or a reciprocal lattice expansion:

$$\tilde{G}(\underline{r}_i) = \sum_{\underline{R}} f(\hat{n},a,\underline{A}_i\underline{r}_i) \tag{3-15}$$

$$= \frac{\pi}{a\Omega} a^{n_3/2} H_{n_3}[a^{1/2}(z-A_z)] \sum_{\underline{K}} (-i)^{n_1+n_2}$$

$$K_x^{n_1} K_y^{n_2} \exp[-K^2/4a] \exp[i\underline{K}\cdot(\underline{r}_i-\underline{A})]$$

The matrix elements G_{mn}, defined in Equation 2-50, may be evaluated either analytically or numerically. We have chosen to evaluate G_{mn} numerically using the same integration grid as used for the evaluation of x_m. This particular choice of the same numerical integration grid is advantageous since the use of G_{mn} in Equation 2-49 evaluated as

$$G_{mn} = \sum_i w_i \tilde{G}_m(\underline{r}_i) \tilde{G}_n(\underline{r}_i) \tag{3-16}$$

is equivalent to a least-squares fitting procedure over a weighted discrete set of points. That is to say, the use of G_{mn} as it is expressed in Equation 3-16 in the solution of Equation 2-49 yields a set of coefficients for the exchange fitting functions g_m which minimize the quantity:

$$\Delta = \sum_i w_i \{\rho^{1/3}(\underline{r}_i) - \sum_m g_m \tilde{G}_m(\underline{r}_i)\}^2 \tag{3-17}$$

We find that this particular means of evaluating G_{mn} yields a method which requires fewer integration points (and thus less computational time) for the same precision in the exchange fitting procedure than if

we evaluate G_{mn} analytically. This is not difficult to understand when one considers that the process which uses the numerically evaluated values of G_{mn} will solve the least-squares fitting procedure over a discrete set of points with an error of the order of the precision of the evaluated values of $\psi_j(\underline{r}_i; \underline{k}_{//})$ and $\tilde{G}_m(\underline{r}_i)$, which are typically of the order 10^{-5} to 10^{-8}. The use of an analytically evaluated G_{mn} matrix yields a process which will have an error of the order of the precision of the numerical integration, which is typically of the order 10^{-1} to 10^{-3}. As long as the number of grid points exceeds the number of fitting functions $\tilde{G}_m(\underline{r})$ such that the discrete least-squares fitting procedure is not capable of yielding solutions with severe oscillations between the discrete set of grid points, it appears that the use of a numerically integrated value of G_{mn} is preferable.

CHAPTER IV
RESULTS

4-1. Atomic Hydrogen Monolayer

The atomic hydrogen monolayer was chosen as the initial test case for the approach outlined in Chapters 2 and 3 for calculating the electronic structure of thin films because atomic hydrogen possesses only one electron and may be treated adequately using only a small number of basis functions. Calculations have been performed on two different lattice structures: a square lattice and a hexagonal lattice. Preliminary calculations were performed (Mintmire and Sabin, 1980b) using a minimal basis set consisting of three s-type Gaussian functions taken from van Diujneveldt (1971) for the orbital basis. The basis set used for fitting the charge density contains three s-type Gaussian functions with exponents equal to twice the exponents used in the orbital basis. The basis set used for fitting the exchange potential similarly contained three s-type Gaussian functions with exponents equal to one-third the exponents used in the charge fitting basis. This set will henceforth be referred to as Basis 1. Table 4-1 presents the orbital exponents used in the orbital basis set as well as the orbital exponents for the Gaussian functions used to fit the charge density and the exchange potential.

The value of 2/3 was used for α in all calculations in this work, except where explicitly noted. Other values of α could of course be used, such as the α_{vt} or α_{HF} values for the atomic systems given by Schwarz (1972).

Table 4-1. Basis sets for the atomic hydrogen monolayer.

Type of basis	Function[a] Type	Exponents Basis 1	Basis 2
Orbital	s	0.151398	0.151398
	s	0.681440	0.681440
	s	4.50180	4.50180
	x	-	1.000
	y	-	1.000
	z	-	1.000
Charge fitting	s	0.302796	0.302796
	s	1.362888	1.362888
	s	9.00360	9.00360
	x^2+y^2	-	2.000
Exchange fitting	s	0.100932	0.100932
	s	0.454296	0.454296
	s	3.00120	3.00120
	x^2+y^2	-	1.666667

[a]The nomenclature for the function type is of the form $x^{n_1}y^{n_2}z^{n_3}$ for non-spherically symmetric Hermite-Gaussians. The superscripts n_1, n_2, and n_3 refer to the set of integers $\hat{n} = (n_1, n_2, n_3)$ which define the Hermite-Gaussian function and do not represent the Cartesian Gaussian function one would normally associate with this nomenclature. Expressions of the form "x^2+y^2" are to be interpreted as the sum of two Hermite-Gaussian functions of type x^2 and y^2.

The formalism described in this work assumes that the value of α is constant over all regions of space as opposed to the muffin-tin multiple-scattering Xα method described by Johnson (1973), where α may have different values in different regions of space. Since one of the ultimate goals of this method is to describe the electronic structure of systems containing more than one type of atomic center, we feel that it is simpler at this time to avoid the complicated question of what value of α is appropriate for a particular system and use the value of α resulting from the original derivation of the local density functional formalism approach of Kohn and Sham (1965) and Gaspar (1954).

The values of the wave vector $\underline{k}_{//}$ were chosen such that all orbitals were periodic over a translation equal to four times that of any primitive lattice translation, which is equivalent to a Born-von Karman region equal to a four by four array of contiguous primitive unit cells. Thus this choice yields sixteen evenly spaced non-equivalent (by translation symmetry) wave vectors in the central Brillouin zone. For the square lattice, point group symmetry reduces the number of non-equivalent wave vectors to seven. The Brillouin zone of the square lattice is depicted in Figure 4-1, with the irreducible region of the Brillouin zone defined by the triangle (ΓXM). Figure 4-2 illustrates the location of the seven non-equivalent wave vectors used in the calculations. The hexagonal lattice has only four non-equivalent wave vectors in the Brillouin zone. The hexagonal Brillouin zone and the four non-equivalent wave vectors are illustrated in Figures 4-3 and 4-4. The cohesive energies per particle were calculated by taking the difference of the total energy at a given lattice constant and the energy of atomic hydrogen calculated using the molecular LCAO-Xα program (Mintmire, 1979). These results for the

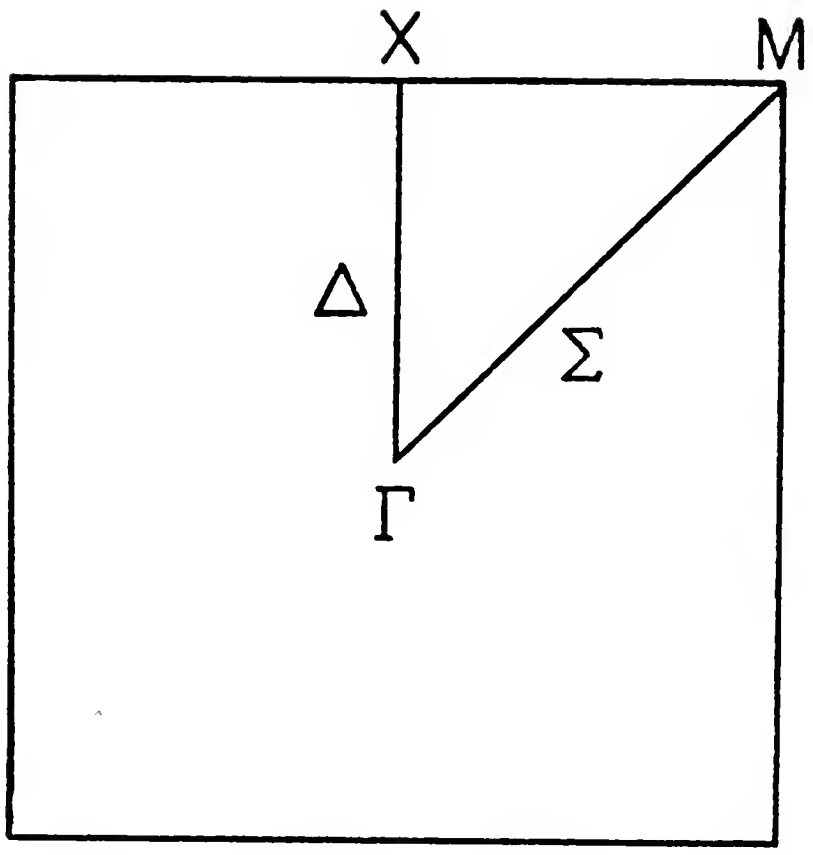

Figure 4-1. Central Brillouin zone for the square lattice.

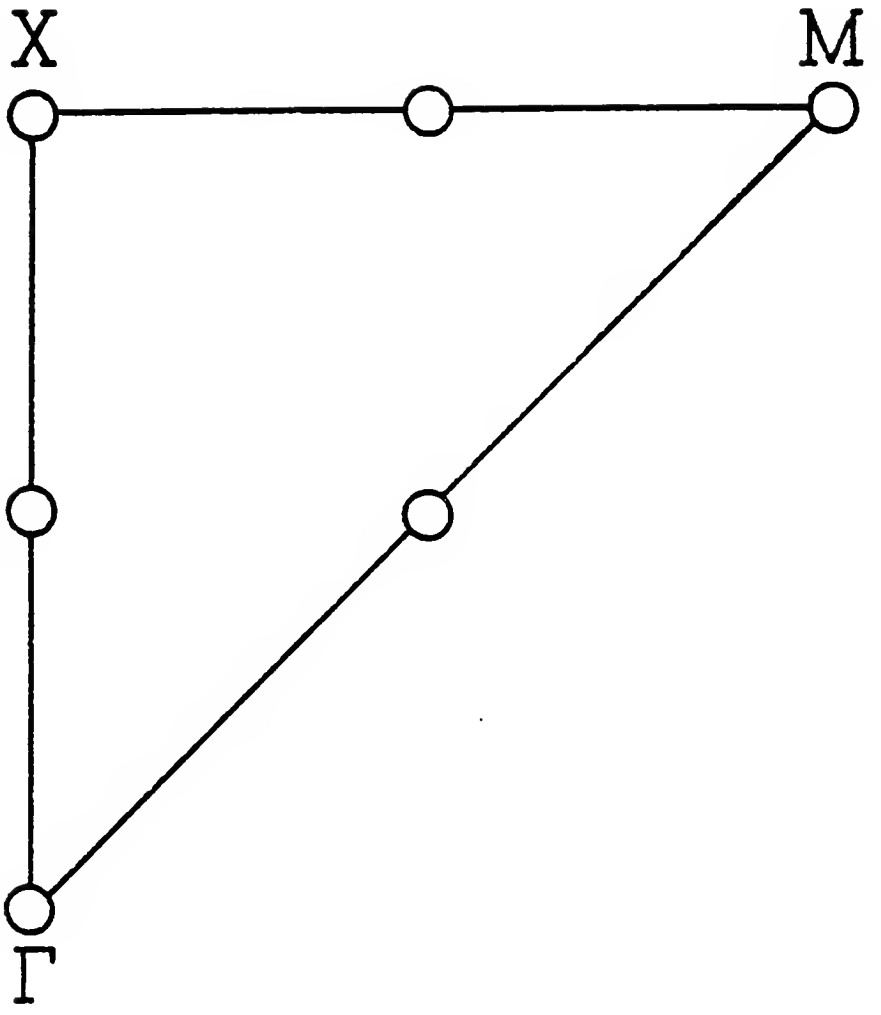

Figure 4-2. Seven representative points in the irreducible triangle of the central Brillouin zone for the square lattice.

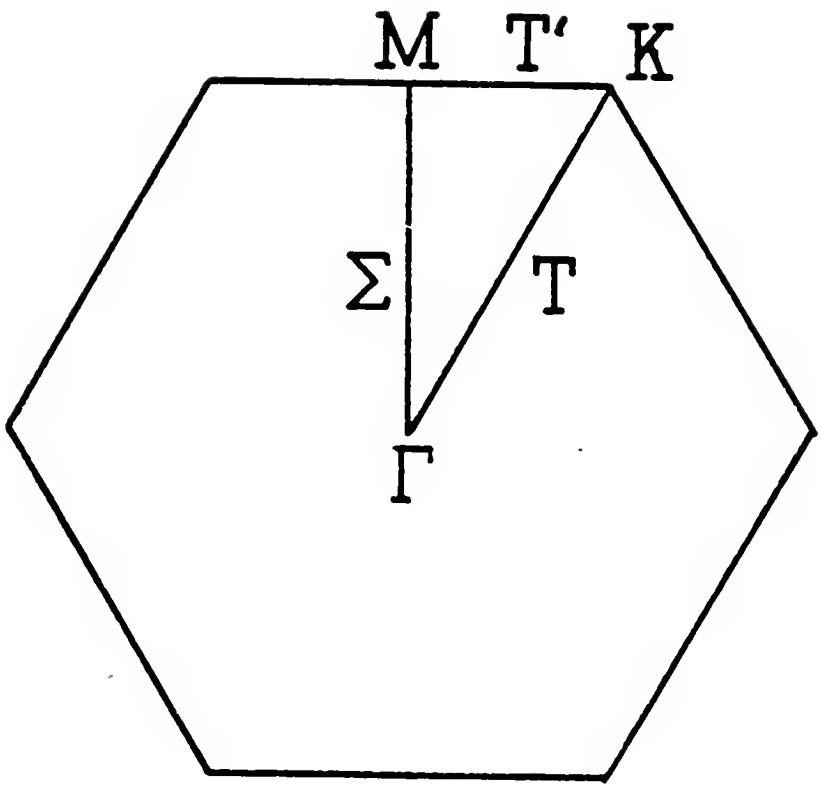

Figure 4-3. Central Brillouin zone for the hexagonal lattice.

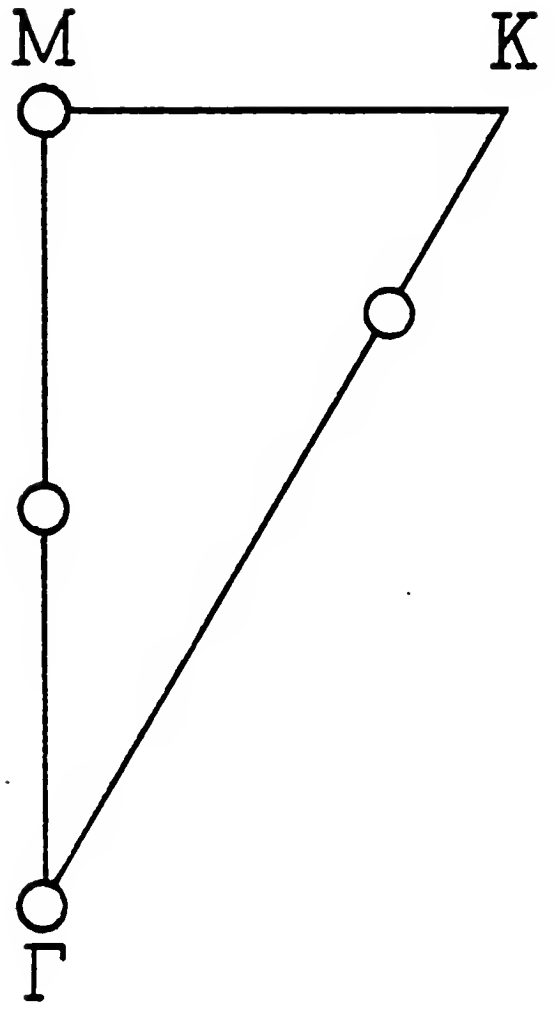

Figure 4-4. Four representative points of the irreducible triangle of the central Brillouin zone for the hexagonal lattice.

cohesive energies per particle versus the lattice constant are depicted in Figure 4-5. Initially these results were interpreted to imply that the square lattice structure possessed a lower equilibrium cohesive energy per particle (-0.035 Hartrees versus -0.005 Hartrees) and thus a more stable equilibrium geometry relative to the hexagonal structure.

The effects of the choice of α were tested by first using the molecular LCAO-Xα program to find the value of α which yields a total energy of atomic hydrogen equal to -0.5 Hartrees using Basis 1. Further calculations were performed using this value of α (equal to 0.781508) and it was found that the cohesive energy curve underwent only minimal changes, with the equilibrium cohesive energy per particle of the square structure changing by less than 0.001 Hartrees with respect to the equilibrium cohesive energy per particle of 0.035 Hartrees for the square lattice calculations with α equal to 2/3.

More extensive calculations were performed using a (3s,1p) basis set for the orbital basis set where p-type functions with exponents equal to 1.0 were added to Basis 1 as polarization functions. This basis set (henceforth referred to as Basis 2) is presented in Table 4-1 along with Basis 1. In addition to the slight improvement in the basis set, a finer grid of wave vectors was used in the Brillouin zone, increasing the number of non-equivalent (by translation symmetry) points in the central Brillouin to 256. This increases the number of non-equivalent points, when point group symmetry is considered, in the Brillouin zone from 4 points to 30 points for the hexagonal lattice and from 7 points to 45 points for the square lattice. Figures 4-6 and 4-7 display these two sets of points in their irreducible regions of the Brillouin zone for the square and hexagonal lattices respectively.

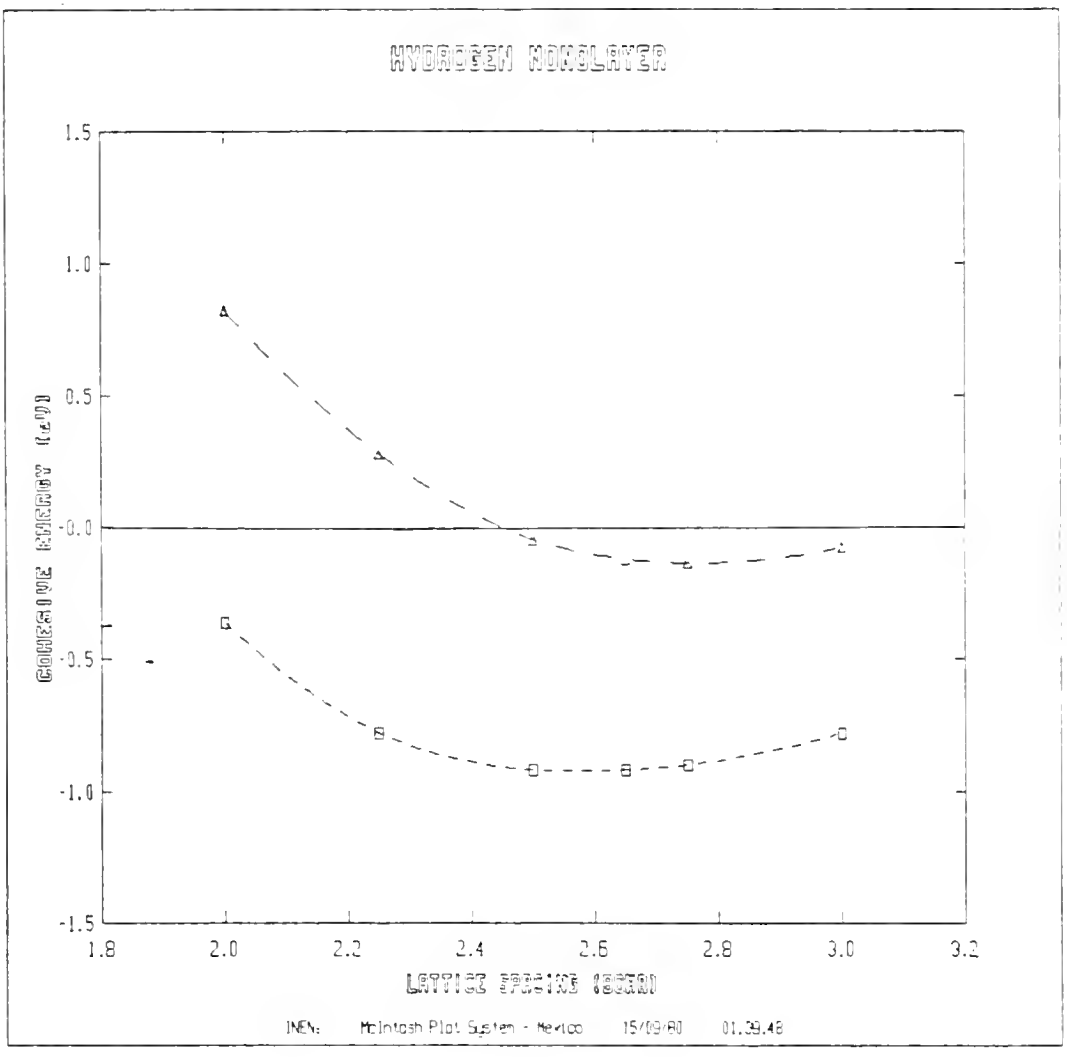

Figure 4-5. Cohesive energy per particle versus lattice constant for square (□) and hexagonal (△) lattices.

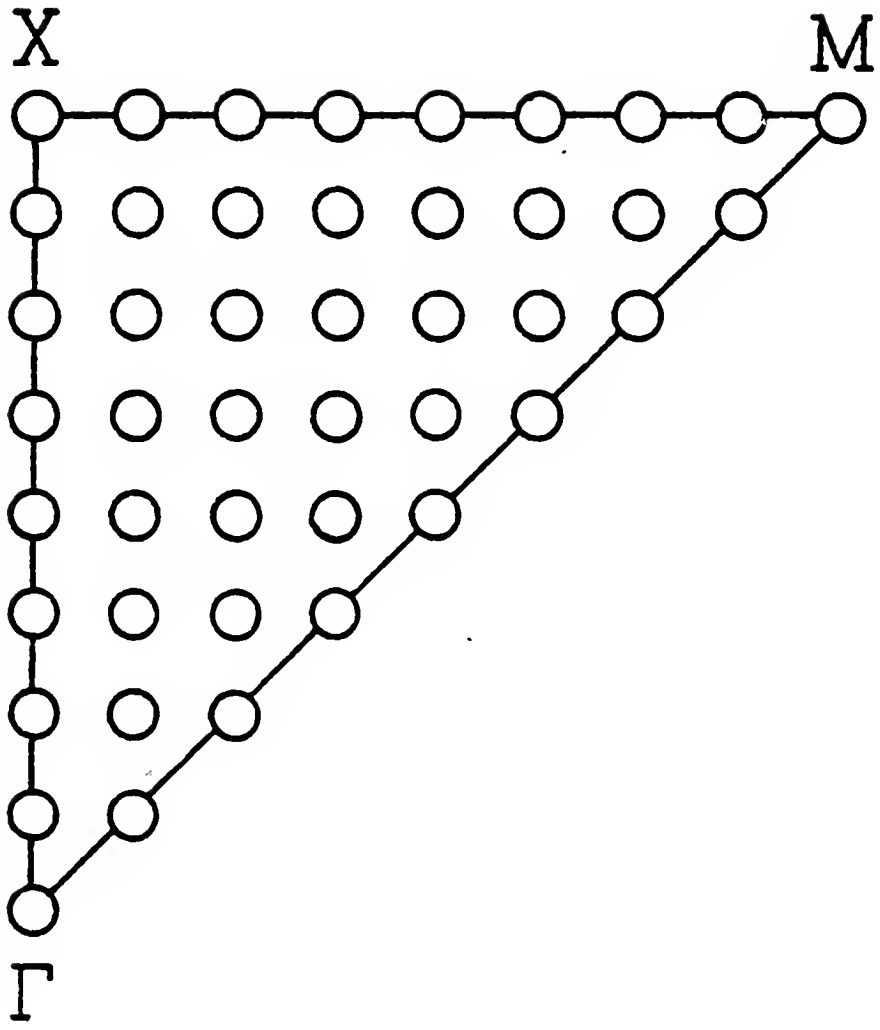

Figure 4-6. Forty-five representative points of the irreducible triangle of the Brillouin zone for the square lattice.

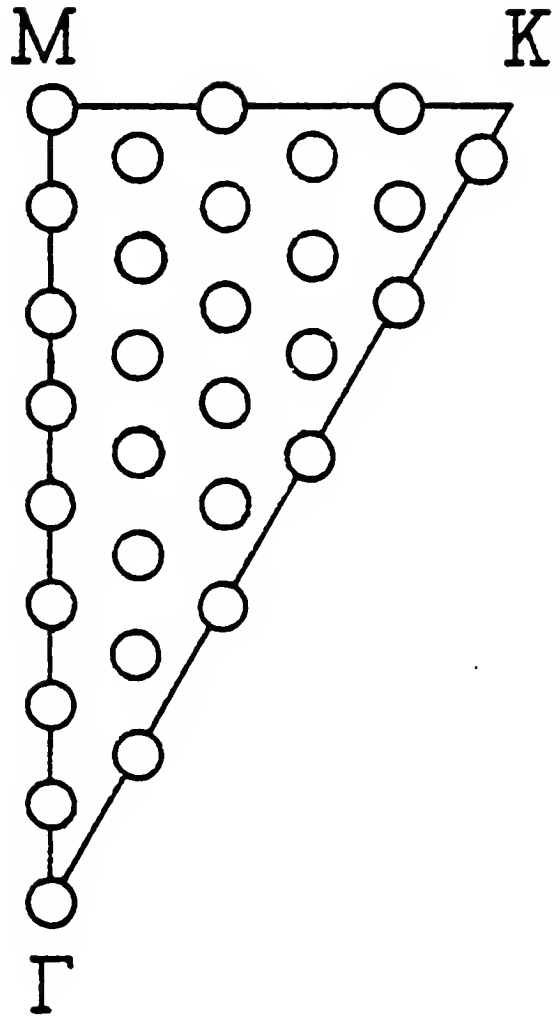

Figure 4-7. Thirty representative points of the irreducible triangle of the Brillouin zone for the hexagonal lattice.

The resulting cohesive energies per particle and virial ratios are presented as a function of the lattice constant for the square and hexagonal lattices in Tables 4-2 and 4-3 respectively. A graphical display of the cohesive energies per particle is made in Figure 4-8. The cohesive energies are calculated as the total energy minus the energy of the atomic monolayer at a lattice separation of 100 a.u. As can be easily seen, these results differ markedly from the results of our preliminary calculations. Our earlier inference that the square lattice is the energetically preferred geometry at equilibrium is obviously refuted by these more recent results. In fact by plotting the cohesive energy per particle versus the square root of the area of the cross section in the periodic plane of the parallelopiped unit cell defined in Section 2-1 (thus giving the cohesive energy per particle as a function of the density of the lattice sites) as displayed in Figure 4-9, we see that the results for the two different geometries are almost indistinguishable. Most of the difference between the two sets of results may be attributed to the increase in the number of Brillouin zone points, since the improvement in the basis from a (3s) basis to a (3s,1p) basis is only a modest improvement compared to the increase of the total number of points in the Brillouin zone from 16 to 256.

It is to be noted that both Table 4-2 and Table 4-3 contain two sets of results for the lattice constant of 5.0 a.u. Using the spin-polarized version of the computer code at this particular lattice separation (and only at this particular choice) leads to two stable (in the self-consistent iterative procedure) solutions that correspond to a non-spin-polarized (NSP) and completely spin-polarized (SP) solutions. Which result is obtained depends on the initial choice of fitting coefficients to generate

Table 4-2. Calculated results for the square atomic hydrogen monolayer.

Lattice Separation (a.u.)	Total Energy (Hartrees)	-V/T	Binding Energy (Hartrees)	Binding Energy (eV)
2.25	-0.4883	1.867	-0.0354	-0.963
2.50	-0.4921	1.995	-0.0391	-1.065
2.65	-0.4918	2.062	-0.0389	-1.057
2.75	-0.4909	2.103	-0.0380	-1.033
3.00	-0.4868	2.188	-0.0338	-0.920
5.00[a]	-0.4327	2.187	+0.0202	+0.550
5.00[b]	-0.4521	1.934	+0.0009	+0.024
100.00	-0.4530	1.972	-	-

[a] non-spin-polarized solution

[b] spin-polarized solution

Table 4-3. Calculated results for the hexagonal atomic hydrogen monolayer.

Lattice Separation (a.u.)	Total Energy (Hartrees)	-V/T	Binding Energy (Hartrees)	Binding Energy (eV)
2.25	-0.4823	1.784	-0.0293	-0.797
2.50	-0.4917	1.919	-0.0382	-1.040
2.65	-0.4924	1.990	-0.0394	-1.073
2.75	-0.4922	2.033	-0.0392	-1.066
3.00	-0.4892	2.131	-0.0363	-0.987
5.00[a]	-0.4378	2.229	+0.0151	+0.412
5.00[b]	-0.4503	1.923	+0.0027	+0.072
100.00	-0.4530	1.971	-	-

[a] non-spin-polarized solution

[b] spin-polarized solution

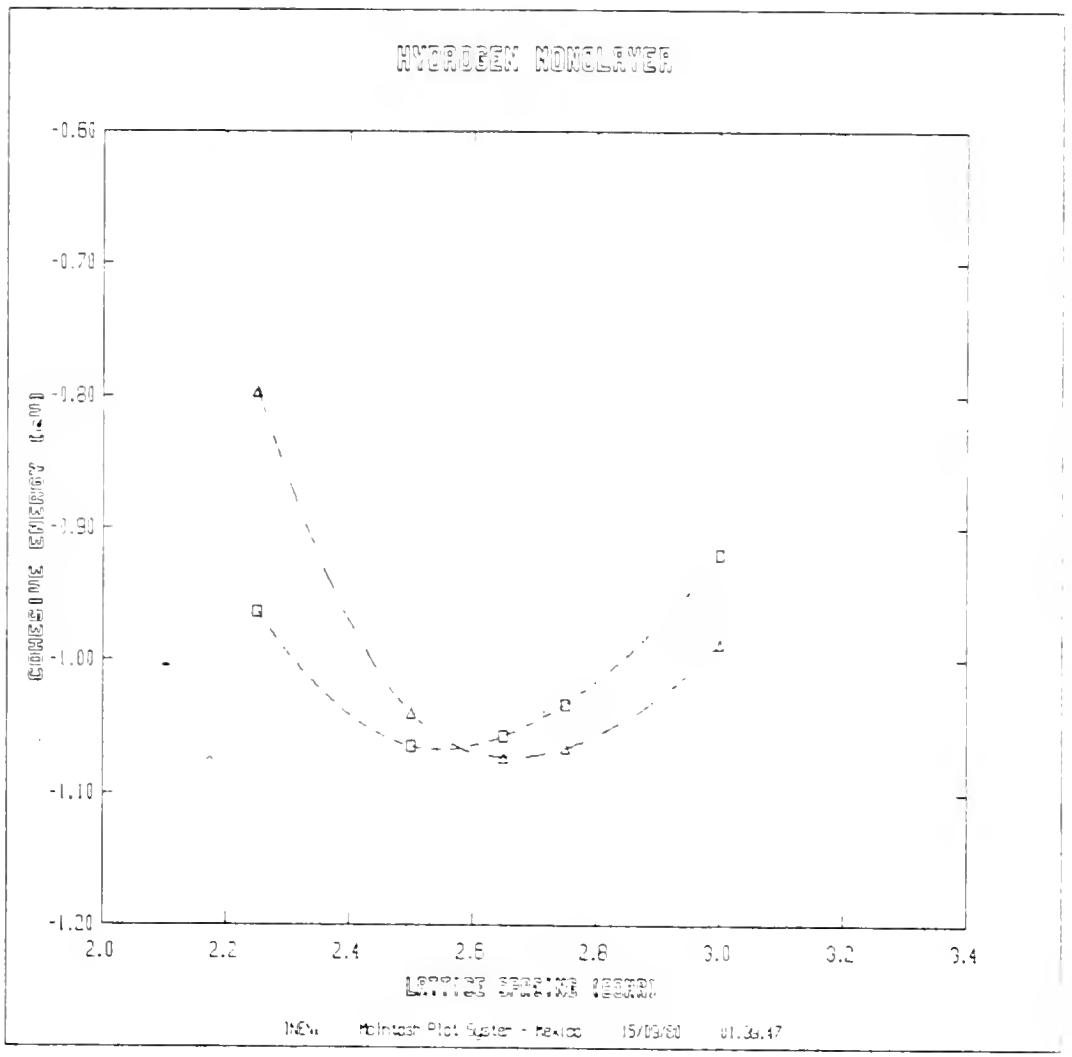

Figure 4-8. Cohesive energy per particle versus lattice constant for square (□) and hexagonal (△) lattices.

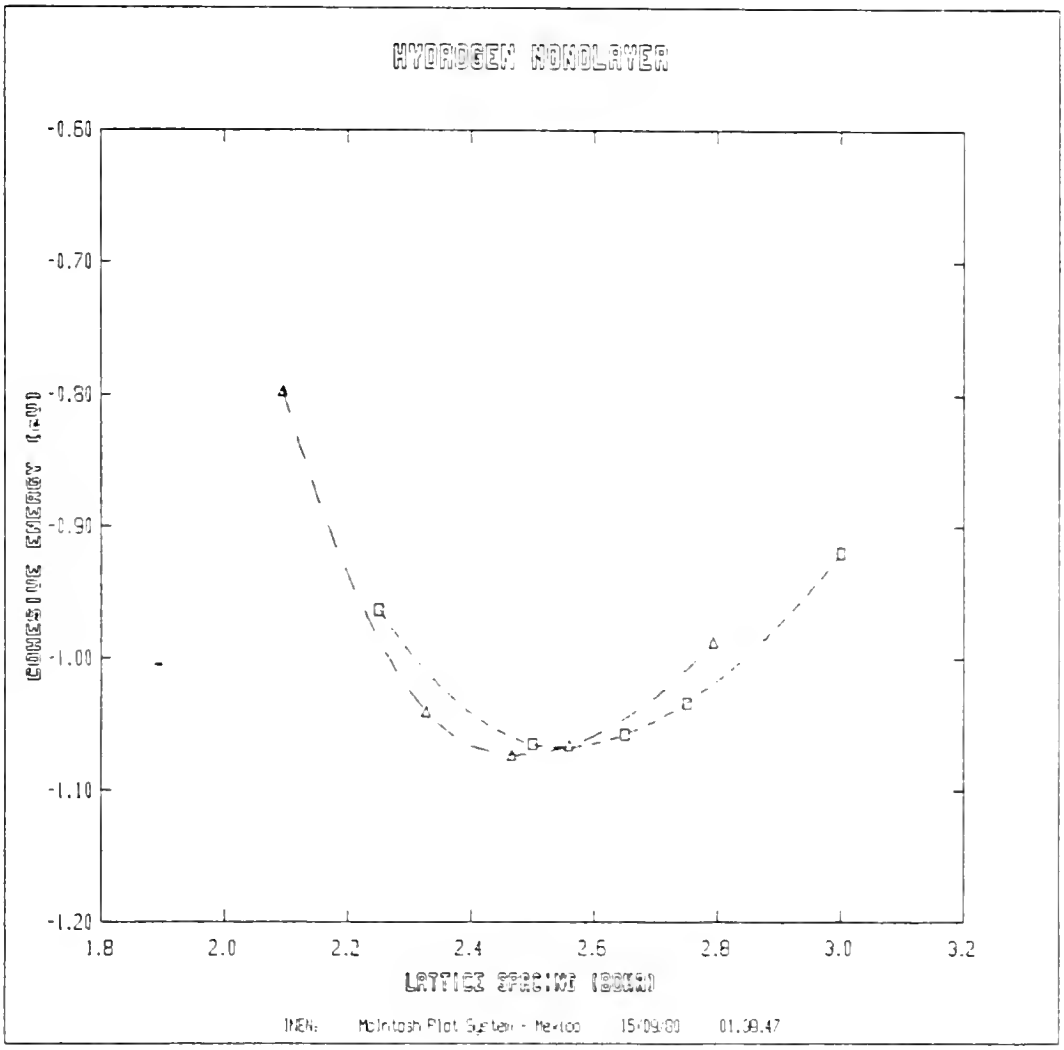

Figure 4-9. Cohesive energy per particle versus modified lattice constant for square (□) and hexagonal (△) lattices.

the effective potential, since using fitting coefficients corresponding to an SP system of overlapping atomic potentials yields the SP result, while starting with coefficients from the NSP state at 3.0 a.u. yields the NSP result. For the NSP results in general, it was necessary to rerun the calculation in the NSP mode of the computer code in order to confirm this assertion, since technical details involving choosing occupation numbers at wave vectors near the Fermi surface prevented the SP version from converging on a totally NSP result. The NSP results calculated in both the NSP and SP modes of the computer code differed by less than 10^{-5} Hartrees in the total energy. The NSP and SP results at a lattice constant equal to 5.0 a.u. evidently indicate that the bands corresponding to the different spins collapse at a lattice constant slightly less than 5.0 a.u. This contention was tested by calculating the cohesive energies per particle for both the NSP and SP modes at lattice constants equal to 6.0 a.u., 8.0 a.u., and 12.0 a.u. Figure 4-10 illustrates the results for these calculations and demonstrates the apparent crossing of the NSP state and the SP state at a lattice constant between 4.0 a.u. and 5.0 a.u. A similar phenomenon has been reported for the crystalline vanadium system (Hattox, Conklin, Slater, and Trickey, 1973) which exhibits the same collapse of bands of different spins to a doubly degenerate band as the lattice constant is decreased from the atomic limit.

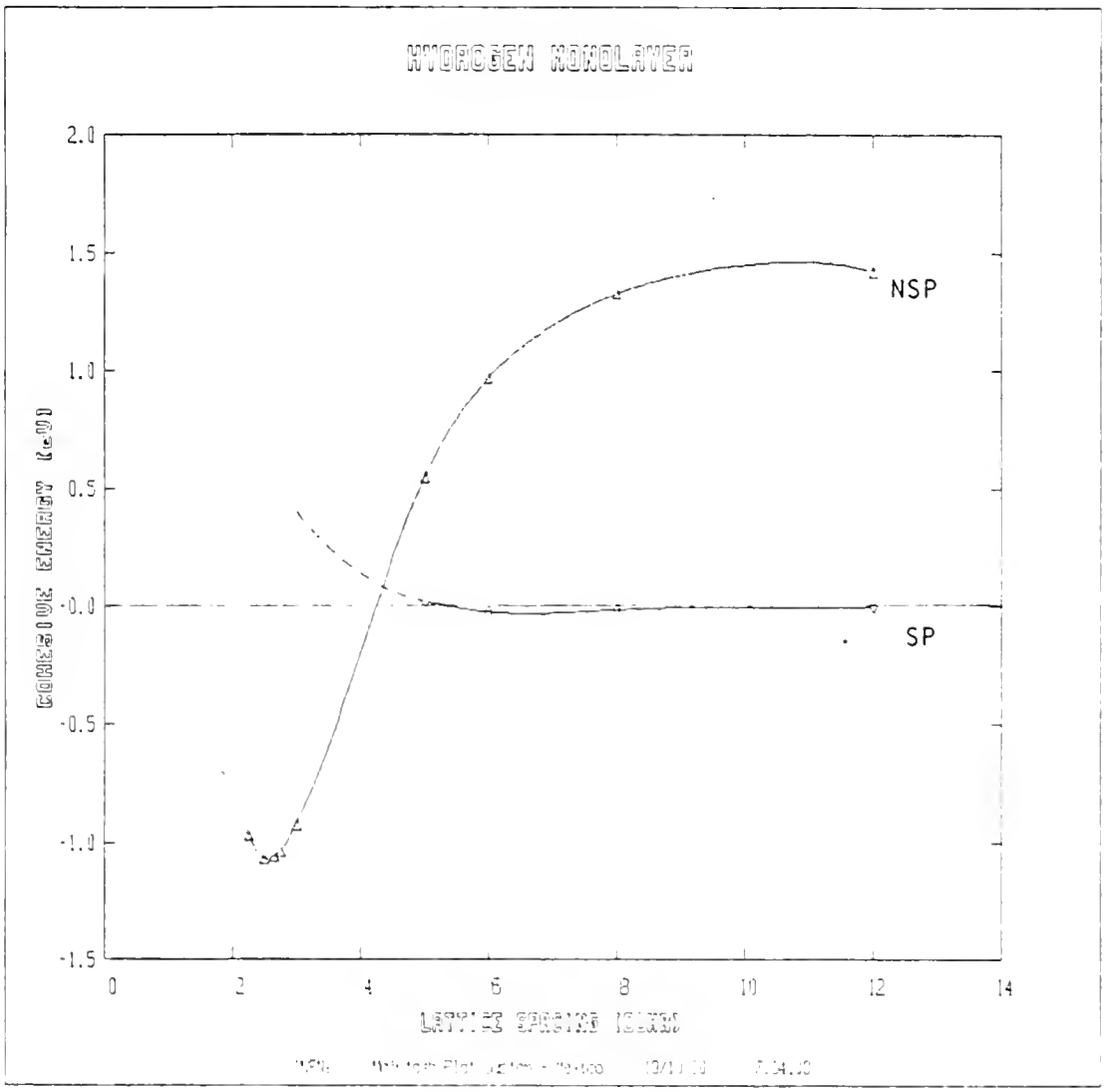

Figure 4-10. Spin-polarized and non-spin-polarized solution cohesive energies per particle versus lattice constant for the square lattice. Dashed portion of spin-polarized curve is extrapolated from the solid portion of the line.

4-2. Atomic Beryllium Monolayer

Beryllium is an interesting system to study using the methods described in this work for several reasons. Recent experimental measurements of the work function of the (0001) surface of beryllium by Green and Bauer (1978) indicate that beryllium has a work function of 5.1 eV, a value much higher than previous measurements had indicated. Until the results of Green and Bauer the recommended value of the work function according to the standard reference (Fomenko, 1966) was only 3.92 eV. Although Green and Bauer attribute this discrepancy in the work function to possible oxidation of the beryllium surface in the earlier work, these differences in experimental results pose a question worthy of theoretical investigation. The interpretation of certain peaks in the Auger spectra of beryllium (Suleman and Pattinson, 1971) also poses questions appropriate for theoretical investigation using surface electronic structure computational methods.

In addition to the questions resulting from experimental study, beryllium is an interesting prototype system for studying the surface of metals. With only four electrons per atom, beryllium should require relatively modest amounts of computational effort for an adequate treatment of the surface. Also beryllium is only weakly bound as a dimer, with a dissociation energy which is experimentally estimated to be about 0.7 eV (Gaydon, 1968). The weak binding of the dimer is also indicated by theoretical calculations such as the configuration interaction calculations by Bender and Davidson (1967), which yield a strictly repulsive ground state potential energy curve, and the self-consistent electron pair/coupled electron pair approximation (SCEP/CEPA) calculations by Dykstra, Schaefer, and

Meyer (1977) which leads them to estimate the calculated dissociation energy to be about 0.03 eV at an equilibrium separation of about 8.5 bohr. Hartree-Fock calculations by Bauschlicher, Liskow, Bender, and Schaefer (1975) and by Jordan and Simons (1977) indicate the smallest cluster that exhibits appreciable binding (0.46 eV per atom) contains four beryllium atoms. This indicates that the cohesive energy of the solid (and presumably the monolayer) may be primarily due to the delocalization of the electron charge over a collection of sites. The full effect of this delocalization will be investigated by comparing cohesive energies of the infinitely extended monolayer using the methods described in this work with the binding energies calculated by Bauschlicher (1976) on beryllium clusters and with experimental results for the real surface.

We have performed calculations on the atomic beryllium monolayer using the (6s, 2p) basis given in Table 4-4. The 6 s-type functions are taken from van Diujneveldt's (1971) 6s basis for beryllium. The 2 p-type functions are the same as used by Bauschlicher (1976) in his cluster calculations where the p-type functions were used with van Duijneveldt's 9s basis for beryllium. The p-type functions are introduced as polarization functions, since no p orbitals will be occupied in the ground state of the beryllium atom. However since beryllium contains the greatest number of electrons of the elements that have only s orbitals occupied, we may anticipate that the p functions will have a greater contribution than equivalent calculations for hydrogen, helium, or lithium. Thus questions of the balance between the s functions and p functions should be considered. In his study of basis set effects, van Diujneveldt (1971) states that s/p ratios greater than 5/2 (for 2 p-type functions) lead to unbalanced behavior in Hartree-Fock calculations on the nitrogen dimer. Since

Table 4-4. Basis sets for the beryllium monolayer.

Orbital basis		Charge fitting basis		Exchange fitting basis	
Type	Exponent	Type	Exponent	Type	Exponent
s	0.067376	s	0.134752	s	0.0449173
s	0.198210	s	0.396420	s	0.132140
s	1.767558	s	3.535116	s	1.178372
s	6.819528	s	13.639056	s	4.546352
s	30.827597	s	61.655194	s	20.551731
s	204.906144	s	409.81229	s	136.604096
x	0.509	s	1.018	s	0.33933
x	0.118	s	0.236	s	0.079667
y	0.509	x^2+y^2	1.018	x^2+y^2	0.33933
y	0.118	x^2+y^2	0.236	x^2+y^2	0.079667
z	0.509	z^2	1.018	z^2	0.33933
z	0.118	z^2	0.236	z^2	0.079667

beryllium has no occupied p orbitals in the atomic ground state (while nitrogen does) we feel that our 6s/2p ratio is acceptable, especially in the light of the results by Bauschlicher (1976) that a 9s/2p ratio yields reasonable results. Preliminary calculations on the dimer were performed with the above basis using the molecular LCAO-Xα program (Mintmire, 1979) and a plot of the binding energy versus the nuclear separation is presented in Figure 4-11. These results are consistent with the previously mentioned results of Dykstra, Schaefer, and Meyer and demonstrate the weak binding of the beryllium dimer as well as provide a check on the balance of the (6s, 2p) basis set.

Since beryllium possesses a hexagonal close packed structure in the solid, the calculations were performed on a hexagonal lattice of beryllium atoms. This structure is equivalent to a single layer from the (0001) surface of the crystalline solid. The beryllium lattice possesses a Brillouin zone with the same symmetry as that of the hexagonal atomic hydrogen monolayer previously displayed in Figure 4-3. We used the same array of 30 non-equivalent points in the Brillouin zone for the beryllium as for the hexagonal atomic hydrogen monolayer calculations.

Table 4-5 presents some results of our calculations giving the cohesive energies and virial ratios of the beryllium monolayer as a function of the lattice spacing. These results and Figure 4-12 imply that the beryllium monolayer has an equilibrium lattice separation of 4.1 bohrs and an equilibrium cohesive energy of -2.64 eV per particle. Since the virial theorem is valid for the Xα method (Slater, 1972b), the virial ratio -V/T should equal 2 at the minimum of the cohesive energy curve where the derivative of the cohesive energy with respect to the lattice spacing equals zero. We see in Table 4-5 that the location of the cohesive energy

Table 4-5. Calculated results for the atomic beryllium monolayer.

Lattice Separation (a.u.)	Total Energy (Hartrees)	-V/T	Binding Energy (Hartrees)	Binding Energy (eV)
3.80	-14.293628	1.99370	-0.092185	-2.5084
3.90	-14.296508	1.99553	-0.095065	-2.5867
4.00	-14.298019	1.99880	-0.096576	-2.6278
4.10	-14.298351	2.00149	-0.096908	-2.6369
4.25	-14.297454	2.00586	-0.096011	-2.6125
4.321	-14.296885	2.00566	-0.095442	-2.5970
4.50	-14.293275	2.00837	-0.091832	-2.4987
5.00	-14.275816	2.01493	-0.074373	-2.0237
6.00	-14.234844	2.01263	-0.033401	-0.9088
100.00	-14.201443	1.99901	-	-

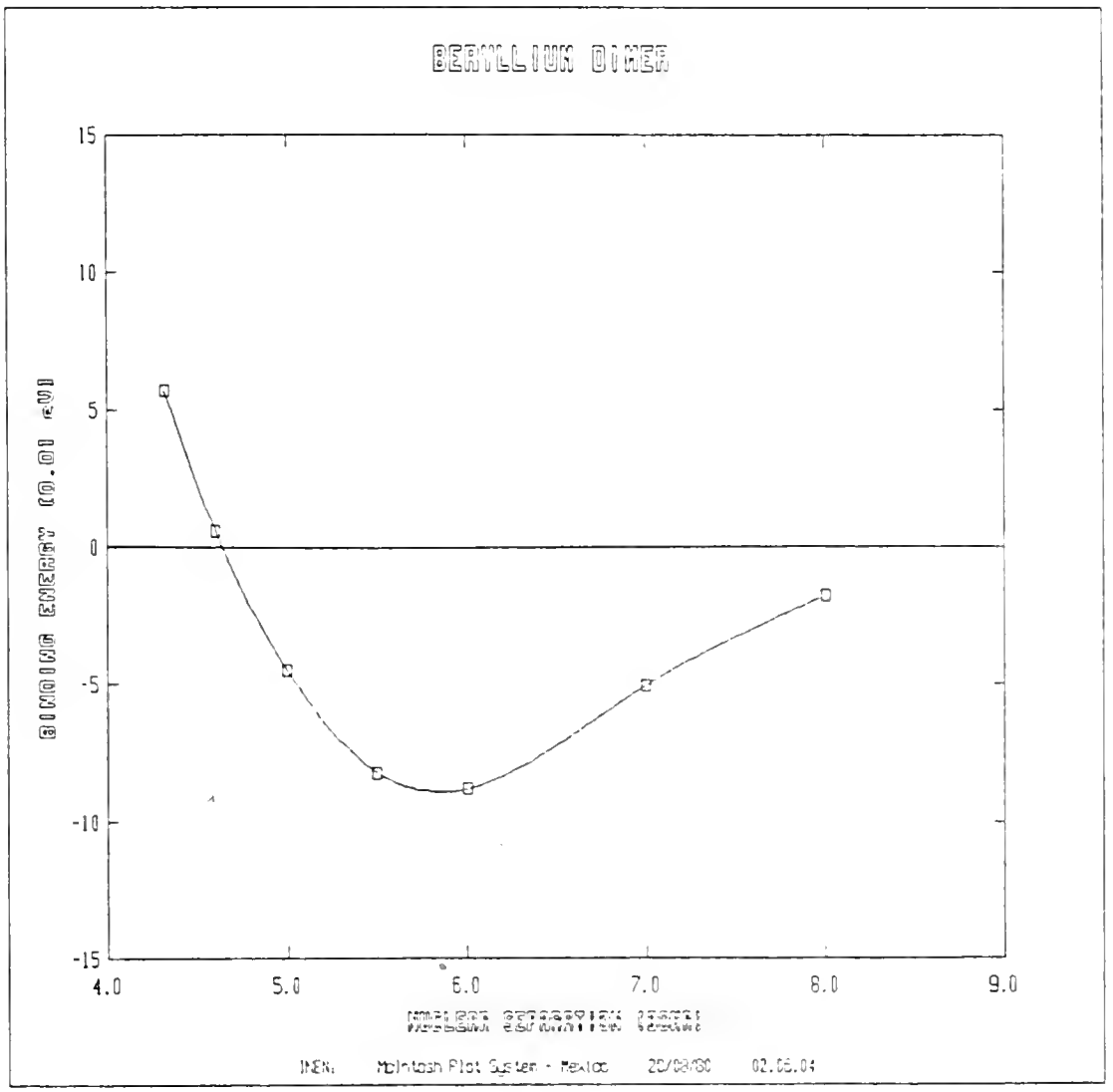

Figure 4-11. Binding energy versus internuclear separation for the beryllium dimer.

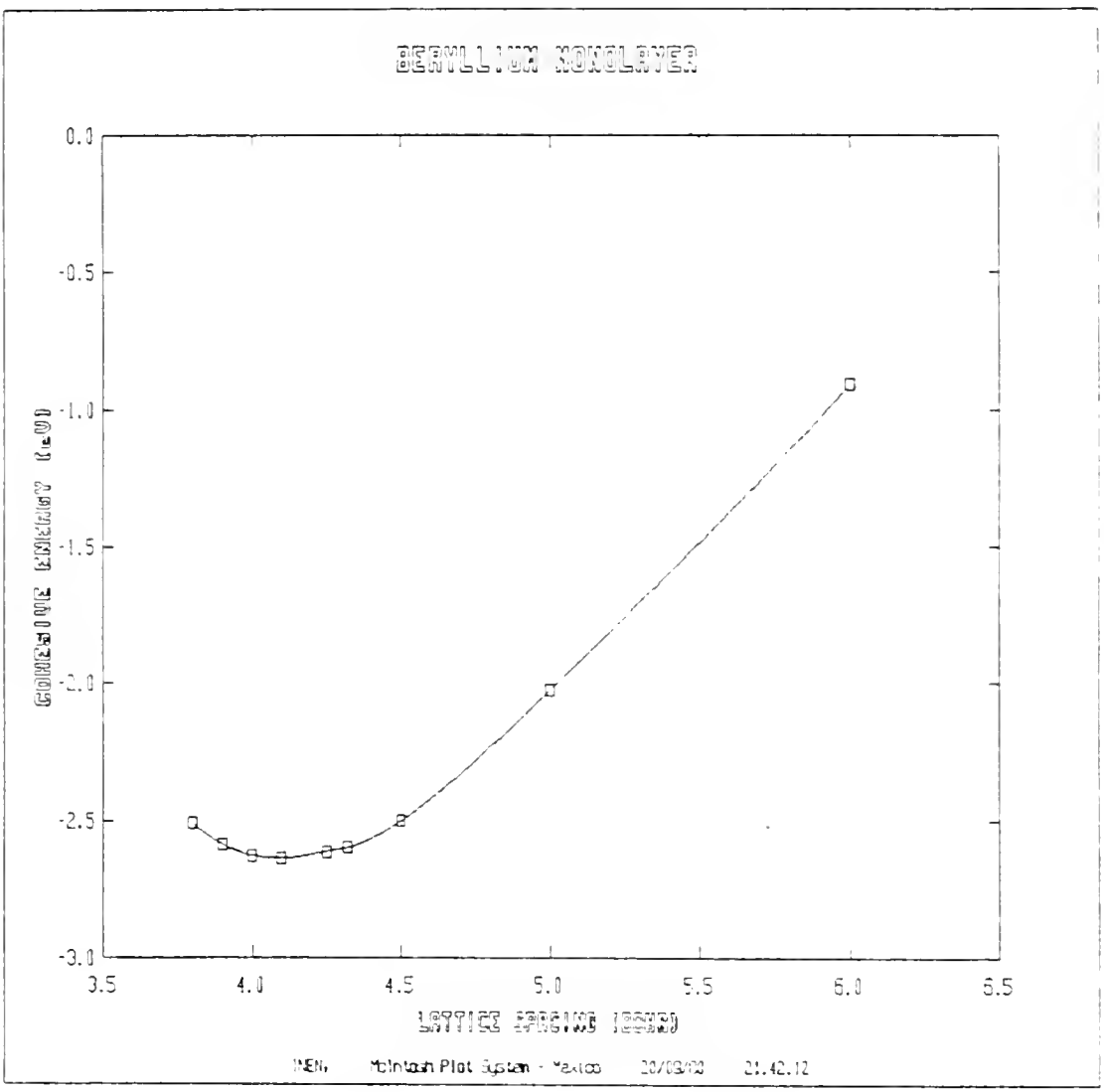

Figure 4-12. Cohesive energy per particle versus lattice constant for the hexagonal beryllium monolayer.

minimum (predicted by interpolation of the virial ratios to yield a predicted lattice constant of 4.05 a.u. and an estimated cohesive energy per particle at that lattice constant of -2.63 eV) is in close agreement with that predicted by the actual cohesive energy curve. These equilibrium results differ slightly from the bulk equilibrium separation of 4.321 bohrs and equilibrium cohesive energy of -3.32 eV per particle (Kittel, 1976), but not more than could be attributed to the difference between monolayer and bulk solid beryllium. Bauschlicher (1976) has performed calculations using the Hartree-Fock method on various size beryllium clusters with the same internuclear separation as the bulk solid. For the various monolayer clusters, Bauschlicher reports binding energies of +0.22 eV per particle for a three atom cluster, +0.07 eV per particle for a six atom cluster, -0.16 eV per particle for a seven atom cluster, and -0.63 eV per particle for a fourteen atom cluster. The largest cluster Bauschlicher considered was a twenty-two atom cluster in two layers which yielded a computed binding energy of -0.89 eV per particle. These cluster results apparently indicate a trend in binding energies as the cluster size increases which should be consistent with our equilibrium cohesive energy of -2.64 eV per particle, although one may infer that much larger clusters are necessary for a proper treatment of the cohesive energy of the beryllium monolayer. This is a point in favor of our earlier contention that a primary cause of the binding energy of the beryllium monolayer is the delocalization of the electronic charge over many nuclear sites.

Band energies were interpolated for 4096 points in the Brillouin zone using a scheme adapted from the method proposed by Monkhorst and Pack (1976) for three-dimensional Brillouin zone interpolations. This method uses a discrete Fourier transform over the 256 evenly spaced points in the

complete Brillouin zone for which the band energies are computed. Band energies at intermediate points were then evaluated using the resulting Fourier expansion. Figure 4-13 displays the valence bands and lower empty bands computed for the beryllium monolayer at a lattice spacing of 4.10 a.u. The shape of the bands resemble qualitatively the bands reported by Loucks and Cutler (1964) for crystalline beryllium, if we compare our results with the solid energy bands for wave vectors lying in planes parallel to the plane of periodicity of the monolayer. One may assume that the discrepancy between our bands and those of Loucks and Cutler is due to the differences between the monolayer and the crystal, and that the addition of more layers would lead to multilayer bands more in agreement with those of the crystalline beryllium solid. Further work is currently progressing in the direction of calculations involving more than one layer of beryllium.

We may estimate the work function of beryllium from the negative of the Fermi energy of our calculations (Kittel, 1976). We find that our Fermi energy for the monolayer of -3.80 eV agrees quite well with the recommended value of Fomenko (1966). However the discussion by Trickey and Worth (1977) indicates that while the choice of α equal to 2/3 will yield reasonable cohesive energies and band widths, one expects that this value of α will lead to underestimating band gaps and the Fermi energy. Thus the fact that we anticipate our Fermi energy to underestimate the work function, and that increasing the number of layers will probably change the Fermi energy in a manner not easily predictable, our estimated work function of 3.80 eV is not necessarily in conflict with the reported experimental work function of 5.10 eV (Green and Bauer, 1978).

The density of states for the beryllium monolayer was computed using the interpolated set of band energies and is presented in Figure 4-14.

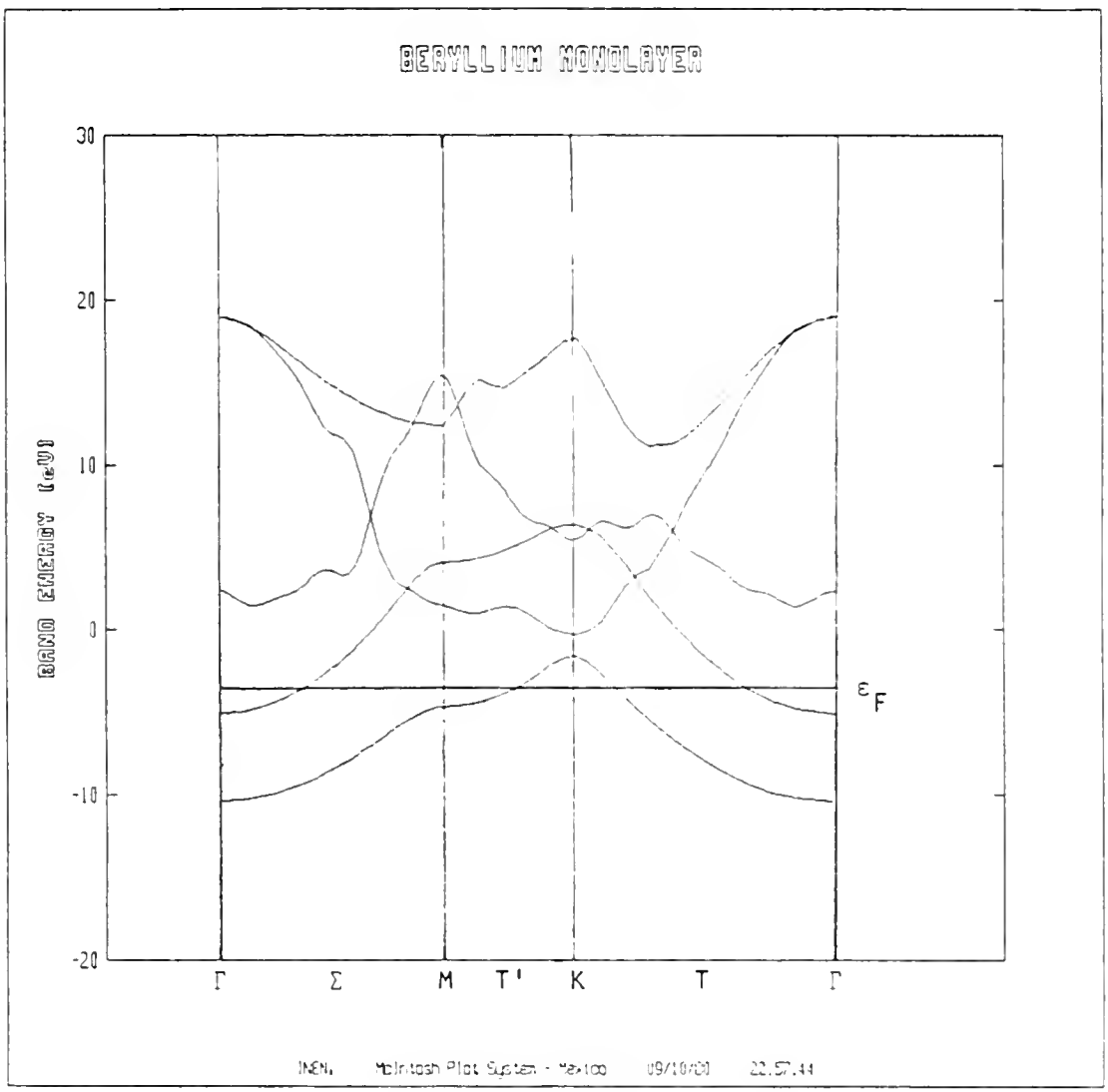

Figure 4-13. Band energies for the hexagonal beryllium monolayer. The core band located at -100.93 eV is omitted.

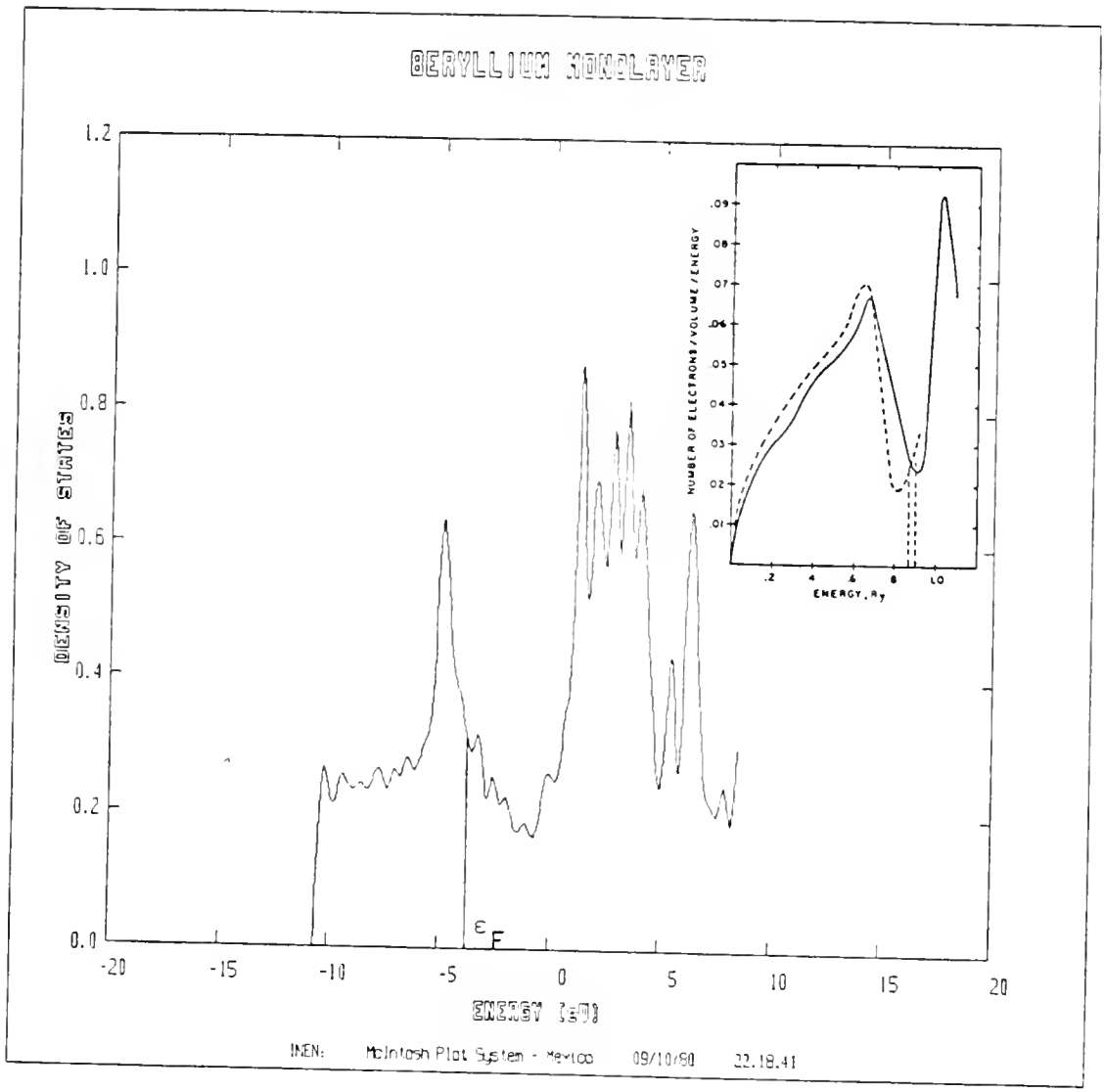

Figure 4-14. Total density of states for the hexagonal beryllium monolayer. The solid line shown in the inset is the total density of states computed for crystalline beryllium by Loucks and Cutler (1964).

The results are also consistent and in qualitative agreement with the density of states computed for the crystalline beryllium solid (Loucks and Cutler, 1964). The relatively flat region in the density of states at energies around -10. eV in Figure 4-14 is understandable when one notices that the bands in Figure 4-13 are nearly free electron like in character. One can demonstrate that the density of states for a two-dimensional electron gas will be a step function. Thus the flat region of our density of states is due to the nearly free electron like behavior of the bottom of the lowest band in Figure 4-12.

Musket and Fortner (1971) have reported Auger Electron Spectra (AES) results for beryllium indicating two peaks at 92 eV and 104 eV. Later work by Suleman and Pattinson (1971) indicates that the AES peak at 92 eV was evidently due to impurities on the beryllium surface, although they agreed with the earlier conclusion of Musket and Fortner that the peak at 104 eV was due to a (2p, 2p) KVV transition at the solid surface. The energy of this transition will equal the energy difference of an electron in the 2p band (ε_{2p}) and the energy of the hole it fills in the core K shell (ε_K) minus the energy required to excite an electron from some different location in the 2p band (ε'_{2p}). We may thus find an estimate for the peak of the above mentioned transition by taking the difference $\Delta\varepsilon = \varepsilon_{2p} + \varepsilon'_{2p} - \varepsilon_K$. To find appropriate bounds for our estimate (since we do not anticipate monolayer results more accurate than 2 or 3 eV in the light of our previous discussion of the effects of adding more layers to the beryllium system) we may consider ε_{2p} and ε'_{2p} jointly equal either to the bottom of the second band in Figure 4-13, which corresponds to the $2p_z$ band, or to the Fermi energy. Since we anticipate that the band energy for the core band will not be very accurate, we will use the reported

results of -111 eV plus the work function (Siegbahn, et al., 1967). Depending upon whether we use the experimental work function or our estimated work function, we find a range of 105 to 109 eV for our estimate of the (2p, 2p) KVV Auger peak. Thus we find one more source of agreement of our monolayer results with those of the bulk solid, indicating that even these simple monolayer calculations provide useful information for describing the surface of the bulk solid.

These calculations were performed on an Amdahl V7 computer and required approximately 20 minutes of CPU time for each value of the lattice constant. Preliminary calculations have been attempted for the beryllium double layer with relaxed precision tolerances in order to reduce the CPU time required. Unfortunately these preliminary calculations required approximately 4 hours of CPU time per lattice constant for the double layer and yielded unsatisfactory results due to precision problems involving the more diffuse basis functions. It is felt that the inclusion of routines to incorporate the mixed lattice expansion algorithm for evaluating the $V_{ijk}(\underline{k}_{//})$ and $X_{ijk}(\underline{k}_{//})$ integrals described in Chapter III will both reduce the total required computational time and increase the precision of the evaluated integrals involving diffuse functions. Steps are currently being taken to incorporate these techniques into the computer code in order to perform calculations on the beryllium double layer and other more complex two-dimensionally periodic systems.

CHAPTER V
SUMMARY

The primary purpose of this work has been to develop and test a new approach for calculating the electronic structure of thin films, with the ultimate objective of studying the electronic properties of solid surfaces. The calculations presented in this dissertation hopefully have indicated some of the possible applications of our approach, although a complete understanding of the strengths and weaknesses of the approach outlined in this dissertation will require much more extensive testing. The basic approach discussed herein has relied on the following assumptions:

1) Properties characteristic of the surface can be reliably studied using a thin layer model;
2) the coupling of nuclear motion and electronic motion may be neglected so that electronic properties can be calculated reliably within the Born-Oppenheimer approximation; and
3) the local density functional ($X\alpha$) formalism yields results which are useful in understanding the electronic properties of surfaces.

The first assumption is intuitively reasonable given sufficiently many layers in the film, and its use is supported by work on d-band metals which indicates that the surface effects exhibited by films 15 to to 20 layers thick accurately simulate the effects of the bulk surface (Cooper, 1977). The Born-Oppenheimer approximation is a common one in

both molecular and solid state calculations, and barring evidence to the contrary for a particular case, we may assume this approximation to be reasonable. The third assumption has been shown empirically to yield results in reasonable agreement with experiment in a multitude of cases (for a review of applications of the $X\alpha$ formalism see Slater, 1974, and Connolly, 1976). The final test of all three assumptions, of course, is that of comparison of results for a series of different systems using the above model with the experimental results for those systems.

In addition to the previously mentioned assumptions used in establishing the mathematical model, various approximations have been made in finding a computational solution for the model. These approximations, which are capable of refinement to any limit of precision (or at least to the limit of precision of the computational equipment) with a corresponding increase in computational time, fall in four basic categories:

1) the representation of orbitals with a finite basis (the LCAO approximation);
2) the general computational approximation of evaluating quantities to within some predetermined tolerance;
3) the procedure for fitting the charge density and the cube root of the charge density; and
4) the approximate treatment of the Brillouin zone introduced through the use of periodic boundary conditions.

Of these approximations, the first two are well known and no detailed discussion of these points will be made. The effects of finite basis sets are discussed by Schaefer (1972, pp. 56-83) while the effects of precision tolerances are discussed by Clementi and Mehl (1971). No attempts have been made to optimize basis sets, although bases optimized for atomic

hydrogen and beryllium in other works have been used in our reported calculations. Appropriate tolerances were found so that the total energies were calculated to an estimated precision of 10^{-5} Hartrees. The effects of using different numbers of points in the Brillouin zone has been examined briefly for the hydrogen monolayer, with the conclusion that an insufficient number of points can yield radically different cohesive energies from results using an adequate number of Brillouin zone points. Examining the difference of band energies between adjacent points in the Brillouin zone for the beryllium calculations using 256 points in the Brillouin zone yields an upper bound to the error in the total energy of about 0.05 Hartrees for this particular source of error. No testing has been made of the errors introduced by the charge density fitting procedures, although we anticipate that errors in the total energy due to this source of error will be less than 0.001 Hartrees if the fitting scheme for thin films behaves similarly to the fitting scheme for the molecular case (Dunlap, Connolly, and Sabin, 1979a).

The physically reasonable results produced for the hydrogen monolayer indicate that there are no inherent flaws in the mathematical formalism. The beryllium monolayer results further indicate the feasibility of our approach as well as demonstrating the applicability to experimentally interesting systems. The comparison of our theoretically estimated values for the equilibrium lattice spacing, equilibrium cohesive energy per particle, and work function with the experimentally determined quantities for the beryllium system and with other calculated results indicate that even such a simple model as the monolayer yields useful results. The primary difficulty with our approach at this time is the amount of computer time required to produce adequately precise results for systems

larger than the atomic beryllium monolayer. Current work to incorporate the reciprocal lattice expansion techniques described in Appendix C as well as structural changes in the computer code to optimize the order of operation should lead to a substantial reduction in required computer time.

In summary we may state that this dissertation hopefully represents the beginning of an extended study of the electronic properties of surfaces. Needless to say, the methods presented herein are not a finished product, but rather the first stage of development of what we believe to be a line of study that can be extremely fruitful in terms of understanding the basic properties of solid surfaces.

APPENDIX A
HERMITE-GAUSSIAN FUNCTIONS AND INTEGRALS

A-1. Definition of Hermite-Gaussian Functions

The basis functions used in this work are functions which are composed of specific combinations of Cartesian Gaussians (which are of the form $x^l\ y^m\ z^n\ \exp(-ar^2)$, where l, m, and n are non-negative integers). These functions may be referred to as Hermite-Gaussian functions, which is the nomenclature introduced by Zivkovic and Maksic (1968) in their discussion of the use of these functions for molecular calculations. A Hermite-Gaussian function $f(\hat{n}, a, \underline{A}; \underline{r})$ is defined:

$$f(\hat{n}, a, \underline{A}; \underline{r}) = \partial_{\underline{A}}^{\hat{n}} \exp(-a|\underline{r} - \underline{A}|^2) \qquad \text{(A-1)}$$

where $\hat{n}$ refers to a set of three non-negative integers (n_1, n_2, n_3) which define the operation $\partial_{\underline{A}}^{\hat{n}}$:

$$\partial_{\underline{A}}^{\hat{n}} = \frac{\partial^{n_1}}{\partial A_x^{n_1}} \frac{\partial^{n_2}}{\partial A_y^{n_2}} \frac{\partial^{n_3}}{\partial A_z^{n_3}} \qquad \text{(A-2)}$$

This notation is consistent with that of Zivkovic and Maksic, although other workers (Golebiewski and Mrozek, 1973; McMurchie and Davidson, 1978) have introduced slightly different notations. The term "Hermite-Gaussian functions" derives from the fact that given the form of the Hermite polynomials:

$$H_n(x) = (-1)^n \exp(x^2)\ \partial_x^n \exp(-x^2) \qquad \text{(A-3)}$$

the Hermite-Gaussian function $f(\hat{n}, a, \underline{A}; \underline{r})$ may be expressed:

$$f(\hat{n}, a, \underline{A}; \underline{r}) = a^{n/2} H_{n_1}[a^{1/2}(x-A_x)]\ H_{n_2}[a^{1/2}(y-A_y)]$$
$$H_{n_3}[a^{1/2}(z-A_z)]\ \exp(-a|\underline{r} - \underline{A}|^2) \qquad \text{(A-4)}$$

where n denotes the sum of the components of $\hat{n}$ (i.e., $n = n_1 + n_2 + n_3$). These functions are useful in computation since they enable us to perform the calculation of integrals and other numerical data, as pointed out by Zivkovic and Maksic (1968), in three steps:

1) for any integration or summation which does not involve $\underline{A}$ and is linear in $f(\hat{n}, a, \underline{A}; \underline{r})$, bring the differentiation operator outside the integration or summation;
2) calculate the appropriate integral or sum for spherically symmetric Gaussians in closed form; and
3) apply the differentiation operator to the analytic form of the resultant expression.

As an example we may compute the overlap integral between two Hermite-Gaussian functions centered on two different centers $\underline{A}$ and $\underline{B}$.

$$d^3r\ f(\hat{n},a,\underline{A}; \underline{r})\ f(\hat{n}',b,\underline{B}; \underline{r})$$
$$= \partial_{\underline{A}}^{\hat{n}}\ \partial_{\underline{B}}^{\hat{n}'} \int d^3r \exp[-a|\underline{r}-\underline{A}|^2 - b|\underline{r}-\underline{B}|^2] \qquad \text{(A-5)}$$
$$= \partial_{\underline{A}}^{\hat{n}}\ \partial_{\underline{B}}^{\hat{n}'}\ [\pi/(a+b)]^{3/2} \exp[-\,ab|\underline{A} - \underline{B}|^2/(a+b)]$$
$$= (-1)^{n'}\ [\pi/(a+b)]^{3/2}\ f(\hat{n}+\hat{n}',\ ab/(a+b),\ \underline{A}-\underline{B};\ \underline{0})$$

A-2. Products of Two Hermite-Gaussian Functions

The overlap integrals of Equation A-5 are a simple example of integrals which involve the product of two Hermite-Gaussian functions. Such integrals may be evaluated with less complexity by decomposing the product of two Hermite-Gaussian functions into two factors. Consider the product of two Hermite-Gaussian functions:

$$f(\hat{n}, a, \underline{A}; \underline{r})\ f(\hat{n}', b, \underline{B}; \underline{r})$$

$$= \partial_{\underline{A}}^{\hat{n}}\, \partial_{\underline{B}}^{\hat{n}'} \exp[-a|\underline{r} - \underline{A}|^2] \exp[-b|\underline{r} - \underline{B}|^2] \qquad \text{(A-6)}$$

$$= \partial_{\underline{A}}^{\hat{n}}\, \partial_{\underline{B}}^{\hat{n}'} \exp\left[\frac{-ab}{a+b}\,|\underline{A}-\underline{B}|^2\right] \exp\left[-(a+b)\left|\underline{r} - \frac{a\underline{A} + b\underline{B}}{(a+b)}\right|^2\right]$$

Defining the quantitities $\underline{P}$ and $\underline{Q}$:

$$\underline{P} = \underline{A} - \underline{B} \qquad \text{(A-7)}$$

and

$$\underline{Q} = (a\underline{A} + b\underline{B}) / (a + b) \qquad \text{(A-8)}$$

we may express the product of two Hermite-Gaussian functions in terms of functions $g(\underline{P})$ and $h(\underline{r} - \underline{Q})$:

$$f(\hat{n}, a, \underline{A}; \underline{r})\ f(\hat{n}', b, \underline{B}; \underline{r}) = \partial_{\underline{A}}^{n}\, \partial_{\underline{B}}^{n'}\, g(\underline{P})\, h(\underline{r} - \underline{Q}) \qquad \text{(A-9)}$$

where

$$g(\underline{P}) = \exp\left[\frac{-ab}{a+b}\,|P|^2\right] \qquad \text{(A-10)}$$

and

$$h(\underline{r} - \underline{Q}) = \exp[-(a+b)|\underline{r} - \underline{Q}|^2] \qquad \text{(A-11)}$$

Repeated taking of derivatives yields:

$$\partial_{\underline{A}}^{\hat{n}}\,\partial_{\underline{B}}^{\hat{n}'}\,g(\underline{P})\,h(\underline{r}-\underline{Q}) = \sum_{k_1=0}^{n_1}\sum_{k_2=0}^{n_2}\sum_{k_3=0}^{n_3}\sum_{k_1'=0}^{n_1'}\sum_{k_2'=0}^{n_2'}\sum_{k_3'=0}^{n_3'}$$

$$\times \binom{n_1}{k_1}\binom{n_2}{k_2}\binom{n_3}{k_3}\binom{n_1'}{k_1'}\binom{n_2'}{k_2'}\binom{n_3'}{k_3'}\{\partial_{\underline{A}}^{\hat{k}}\,\partial_{\underline{B}}^{\hat{k}'}\,g(\underline{P})\}$$

$$\times \{\partial_{\underline{A}}^{\hat{n}-\hat{k}}\,\partial_{\underline{B}}^{\hat{n}'-\hat{k}'}\,h(\underline{r}-\underline{Q})\} \qquad \text{(A-12)}$$

We may rearrange the sums over the indices k_i and k_i', using the new indices K_i and K_i', where

$$K_i = k_i + k_i' \qquad \text{(A-13)}$$

and

$$K_i' = k_i' \qquad \text{(A-14)}$$

This rearrangement yields the expression:

$$\int \partial_{\underline{A}}^{\hat{n}}\,\partial_{\underline{B}}^{\hat{n}'}\,g(\underline{P})\,h(\underline{r}-\underline{Q}) = \sum_{K_1=0}^{n_1+n_1'}\sum_{K_2=0}^{n_2+n_2'}\sum_{K_3=0}^{n_3+n_3'}$$

$$\times \sum_{K_1'=\max[0,K_1-n_1]}^{\min[n_1',K_1]}\ \sum_{K_2'=\max[0,K_2-n_2]}^{\min[n_2',K_2]}\ \sum_{K_3'=\max[0,K_3-n_3]}^{\min[n_3',K_3]}$$

$$\times \binom{n_1}{K_1-K_1'}\binom{n_2}{K_2-K_2'}\binom{n_3}{K_3-K_3'}\binom{n_1'}{K_1'}\binom{n_2'}{K_2'}\binom{n_3'}{K_3'}$$

$$\times \{\partial_{\underline{A}}^{\hat{K}-\hat{K}'}\,\partial_{\underline{B}}^{\hat{K}'}\,g(\underline{P})\}\{\partial_{\underline{A}}^{\hat{n}-\hat{K}+\hat{K}'}\,\partial_{\underline{B}}^{\hat{n}'-\hat{K}'}\,h(\underline{r}-\underline{Q})\} \qquad \text{(A-15)}$$

Using the relationships

$$\frac{\partial g}{\partial P_i} = \frac{\partial g}{\partial A_i} = -\frac{\partial g}{\partial B_i} \qquad \text{(A-16)}$$

and

$$\frac{\partial h}{\partial Q_i} = \frac{a+b}{a}\frac{\partial h}{\partial A_i} = \frac{a+b}{b}\frac{\partial h}{\partial B_i} \tag{A-17}$$

we may rewrite Equation A-15:

$$\partial_{\underline{A}}^{\hat{n}}\,\partial_{\underline{B}}^{\hat{n}'}\, g(\underline{P})\, h(\underline{r}-\underline{Q}) = \sum_{\hat{K}} g(\hat{K}, \hat{n}, \hat{n}', a, b)\, \{\partial_{\underline{P}}^{\hat{K}}\, g(\underline{P})\}$$

$$\times\ \{\partial_{\underline{Q}}^{\hat{n}+\hat{n}'-\hat{K}}\, h(\underline{r}-\underline{Q})\} \tag{A-18}$$

The function $g(\hat{K}, \hat{n}, \hat{n}', a, b)$ is defined:

$$g(\hat{K}, \hat{n}, \hat{n}', a, b) = \prod_{i=1}^{3} \{ \sum_{K_i'} \frac{a^{n-K+K'} b^{n'-K'}}{(a+b)^{n+n'-K}} \binom{n_i}{K_i - K_i'} \binom{n_i'}{K_i'} \} \tag{A-19}$$

where the indices K_i' have as their respective ranges:

$$\max[0, K_i - n_i] \le K_i' \le \min[n_i', K_i] \tag{A-20}$$

Furthermore we may use the relationships:

$$\partial_{\underline{P}}^{\hat{K}}\, g(\underline{P}) = f(\hat{K}, ab/(a+b), \underline{P}; \underline{0}) \tag{A-21}$$

and

$$\partial_{\underline{Q}}^{\hat{n}+\hat{n}'-\hat{K}}\, h(\underline{r}-\underline{Q}) = f(\hat{n}+\hat{n}'-\hat{K}, a+b, \underline{Q}; \underline{r}) \tag{A-22}$$

to yield the expression

$$f(\hat{n}, a, \underline{A}; \underline{r})\, f(\hat{n}', b, \underline{B}; \underline{r})$$

$$= \sum_{\hat{K}} g(\hat{K}, \hat{n}, \hat{n}', a, b)\, f(\hat{K}, ab/(a+b), \underline{P}; \underline{0})$$

$$f(\hat{n}+\hat{n}'-\hat{K}, a+b, \underline{Q}; \underline{r}) \tag{A-23}$$

Thus we see that Equation A-23 may be used to reduce integrals involving the product of two Hermite-Gaussian functions of the same coordinate $\underline{r}$ to a sum of integrals involving a single Hermite-Gaussian function of the coordinate $\underline{r}$.

A-3. Nuclear Attraction Integrals

The electrostatic interaction integral of a charge distribution described by a Hermite-Gaussian function $f(n, a, \underline{A}; \underline{r})$ with a nuclear center of charge $Z_{\underline{C}}$ located at the position vector $\underline{C}$ may be denoted:

$$[f(\hat{n},a,\underline{A};\underline{r}) \mid Z_{\underline{C}}] = Z_{\underline{C}} \int d^3r \; f(n,a,\underline{A};\underline{r}) \frac{1}{|\underline{r} - \underline{C}|} \tag{A-24}$$

We may use Boys' (1950) relation for spherically symmetric Gaussian functions:

$$[f(\hat{0},a,\underline{A};\underline{f}) \mid Z_{\underline{C}}] = \lambda \; F_0(aT^2) \tag{A-25}$$

to evaluate this integral, where λ is the constant:

$$\lambda = 2\pi \; Z_{\underline{C}} \; / \; a \tag{A-26}$$

and $F_0(s)$ is the incomplete gamma function:

$$F_0(s) = \int_0^1 du \; \exp[-su^2] \tag{A-27}$$

The vector $\underline{T}$ is defined as

$$\underline{T} = \underline{A} - \underline{C} \tag{A-28}$$

Thus the electrostatic interaction integral in Equation A-34 may be

expressed:

$$[f(\hat{n}, a, \underline{A}; \underline{r}) \mid Z_{\underline{C}}] = \partial_{\underline{A}}^{\hat{n}} F_0(aT^2) \tag{A-29}$$

McMurchie and Davidson (1978) have introduced the function $R(\hat{n}, a, \underline{r})$:

$$R(\hat{n}, a, \underline{r}) = \partial_{\underline{r}}^{\hat{n}} F_0(ar^2) \tag{A-30}$$

where we have employed slightly different notation from that of McMurchie and Davidson. This function may be expressed in the expansion:

$$R(\hat{n}, a, \underline{r}) = \sum_{\hat{k}} a^{n-k} 2^{n-2k} (-1)^k x^{n_1-2k_1} y^{n_2-2k_2} z^{n_3-2k_3} F_{n-k}(ar^2)$$

$$\frac{\hat{n}_1!}{\hat{k}_1!\ (\hat{n}_1-2\hat{k}_1)!} \frac{\hat{n}_2!}{\hat{k}_2!\ (\hat{n}_2-2\hat{k}_2)!} \frac{\hat{n}_3!}{\hat{k}_3!\ (\hat{n}_3-2\hat{k}_3)!} \tag{A-31}$$

where the incomplete gamma functions $F_n(s)$ may be defined:

$$F_n(s) = \int_0^1 du\ u^{2n} \exp[-su^2] \tag{A-32}$$

and the interval over which the indices k_i range is:

$$0 \le 2k_i \le n_i \tag{A-33}$$

The function $R(\hat{n}, a, \underline{r})$ may be evaluated using recursion relationships if we define the quantity $T_{n,l,m,j}$:

$$T_{n,l,m,j} = (-\sqrt{a})^{n+l+m} \int_0^1 du\ \{H_n[ux\sqrt{a}]\ H_l[uy\sqrt{a}]\ H_m[uz\sqrt{a}]$$

$$u^{n+l+m+2j} \exp[-ar^2]\} \tag{A-34}$$

This quantity satisfies the following relationships:

$$T_{0,0,0,j} = F_j(ar^2) \tag{A-35}$$

and

$$T_{n_1,n_2,n_3,0} = R(\hat{n}, a, \underline{r}) \tag{A-36}$$

If we use the method described by McMurchie and Davidson (1978) to evaluate the incomplete gamma functions $F_n(s)$, the functions $R(\hat{n}, a, \underline{r})$ may be evaluated using the recursion relationships:

$$T_{n_1,n_2,n_3+1,j} = -2a \{zT_{n_1,n_2,n_3,j+1} + n_3 T_{n_1,n_2,n_3-1,j+1}\} \tag{A-37}$$

$$T_{n_1,n_2+1,n_3,j} = -2a \{yT_{n_1,n_2,n_3,j+1} + n_2 T_{n_1,n_2-1,n_3,j+1}\} \tag{A-38}$$

and

$$T_{n_1+1,n_2,n_3,j} = -2a \{xT_{n_1,n_2,n_3,j+1} + n_1 T_{n_1-1,n_2,n_3,j+1}\} \tag{A-39}$$

Thus we see that the electrostatic interaction integral of a Hermite-Gaussian function with a nuclear center may be expressed:

$$[f(\hat{n},a,\underline{A};\underline{r}) \mid Z_{\underline{C}}] = (2\pi/a)\, Z_{\underline{C}}\, R(\hat{n}, a, \underline{A} - \underline{C}) \tag{A-40}$$

Using the relationship expressed in Equation A-23 we may also express the electrostatic interaction integral of the product of two Hermite-Gaussian functions with a nuclear center:

$$[f(\hat{n},a,\underline{A};\underline{r})\ f(\hat{n}',b,\underline{B};\underline{r})\,|\,Z_{\underline{C}}] = \frac{2\pi}{(a+b)}\ Z_{\underline{C}}\ \sum_{\hat{K}}\ g(\hat{K},\hat{n},\hat{n}',a,b)$$

$$f(\hat{K},ab/(a+b),\underline{A}-\underline{B};\underline{0})\ R(\hat{n}+\hat{n}'-\hat{K},a+b,\underline{Q}-\underline{C}) \qquad \text{(A-41)}$$

where $\underline{Q}$ is the vector defined in Equation A-8.

A-4. Electron Repulsion Integrals

The electrostatic interaction integral of two Hermite-Gaussian functions with each other may be expressed:

$$[f(\hat{n},a,\underline{A};\underline{r})\ |\ f(\hat{n}'',c,\underline{C};\underline{r}')] = \int d^3r \int d^3r' \frac{1}{|\underline{r}-\underline{r}'|}$$

$$f(\hat{n},a,\underline{A};\underline{r})\ f(\hat{n}'',c,\underline{C};\underline{r}') \qquad \text{(A-42)}$$

We may again use the relationships derived by Boys (1950) for spherically symmetric Gaussians:

$$[f(\hat{0},a,\underline{A};\underline{r})\ |\ f(\hat{0},c,\underline{C};\underline{r}')] = \lambda\ F_0(\ acT^2/[a+c]) \qquad \text{(A-43)}$$

where λ is now the new constant

$$\lambda = 2\pi^{5/2}\ /\ \{ac\ (a+c)^{1/2}\} \qquad \text{(A-44)}$$

and the vector $\underline{T}$ is defined:

$$\underline{T} = \underline{A} - \underline{C} \qquad \text{(A-45)}$$

The methods used in Section A-3 for evaluating the nuclear interaction integrals may be extended trivially to yield:

$$[f(\hat{n}, a, \underline{A}; \underline{r}) \mid f(\hat{n}'', c, \underline{C}; \underline{r}')] = (-1)^{n''} \{2\pi^{5/2}/[ac\ (a+c)^{1/2}]\}$$

$$R(\hat{n}+\hat{n}'', ac/(a+c), \underline{A} - \underline{C}) \qquad \text{(A-46)}$$

Similarly Equation A-23 may be used to evaluate the electrostatic interaction integral of two Hermite-Gaussian functions with a single Hermite-Gaussian function:

$$[f(\hat{n}, a, \underline{A}; \underline{r}) f(\hat{n}', b, \underline{B}; \underline{r}) \mid f(\hat{n}'', c, \underline{C}; \underline{r}')]$$

$$= (-1)^{n''} \{2\pi^{5/2}/[(a+b)c\ (a+b+c)^{1/2}]\} \sum_{\hat{K}} g(\hat{K}, \hat{n}, \hat{n}', a, b)$$

$$f(\hat{K}, ab/(a+b), \underline{A}-\underline{B}; \underline{0})\ R\left(\hat{n}+\hat{n}'+\hat{n}''-\hat{K}, \frac{(a+b)c}{a+b+c}, \underline{Q}-\underline{C}\right) \qquad \text{(A-47)}$$

This procedure could be extended straightforwardly to the case of two Hermite-Gaussian functions interacting with the product of two other Hermite-Gaussian functions. This has not been done since no integrals of this form are necessary for the current work.

APPENDIX B
MULTIPOLE EXPANSIONS OF COULOMB INTEGRALS

B-1. Multipole Expansions of Electrostatic Interactions

Consider the sum of electrostatic interaction terms of a charge density $\rho_1(\underline{r})$ centered about the origin and a charge density $\rho_2(\underline{r})$ centered about a lattice site $\underline{R}$ of a two-dimensionally periodic Bravais lattice:

$$U = \sum_{\underline{R}} \int d^3r_1 \int d^3r_2 \; \rho_1(\underline{r}_1) \; \rho_2(\underline{r}_2) \; \frac{1}{|\underline{r}_1 - \underline{r}_2 - \underline{R}|} \qquad (B\text{-}1)$$

where the coordinates $\underline{r}_1$ and $\underline{r}_2$ are illustrated in Figure B-1. These charge densities are assumed to be localized about their respective centers, such that $\rho(\underline{r})$ goes to zero faster than any polynomial of $|\underline{r}|$ in the asymptotic limit as $|\underline{r}|$ tends toward infinity. This condition may be more restrictive than necessary, but it is easily satisfied by the Gaussian functions used in this work as well as by exponential functions. If this expansion is summed in order of increasing $|\underline{R}|$, the convergence of the Coulomb terms is usually slow so that many terms must be included in a truncated expansion so that the sum may be computed within a specified precision.

Piela and Delhalle (1978) have found that the use of a multipole expansion as an approximation for all terms having $|\underline{R}|$ greater than some radius R' for one-dimensionally periodic systems such as polymers is an effective method for speeding the computational procedure. The multipole expansion considered in this work uses the bipolar expansion of the

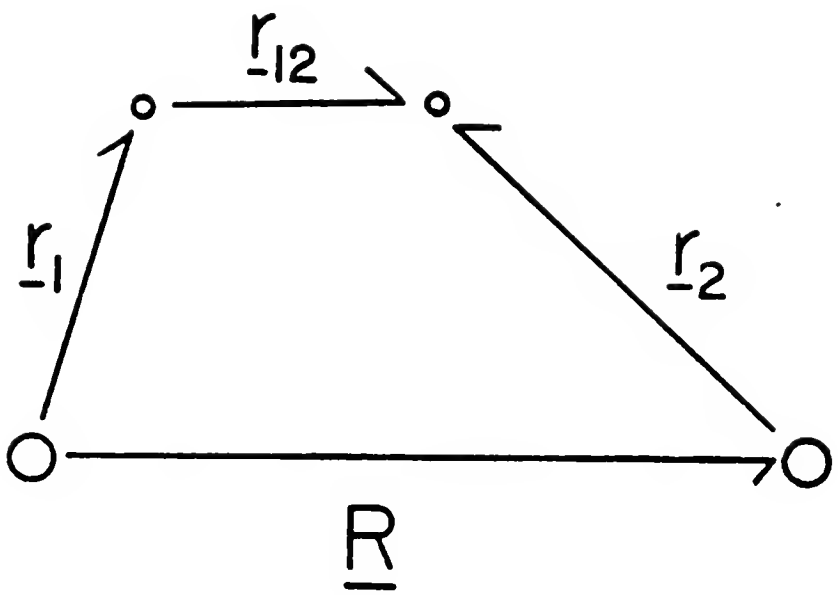

Figure B-1. Coordinate system for the multipole expansion.

inverse of the interelectronic separation $|\underline{r}_1 - \underline{r}_2 - \underline{R}|^{-1}$, as presented by Steinborn and Ruedenberg (1973):

$$\frac{1}{|\underline{r}_1 - \underline{r}_2 - \underline{R}|} = \sum_{\ell,m} \sum_{\ell',m'} (-1)^{\ell'+m+m'} \hat{y}^m_\ell(\underline{r}_1) \hat{y}^{m'}_{\ell'}(\underline{r}_2) \hat{z}^{-m-m'}_{\ell+\ell'}(\underline{R}) \tag{B-2}$$

The functions $\hat{y}^m_\ell(\underline{r})$ and $\hat{z}^m_\ell(\underline{r})$ are the modified regular and irregular solid spherical harmonics respectively (all notation and phase conventions are consistent with those used in Steinborn and Ruedenberg, 1973):

$$\hat{y}^m_\ell(\underline{r}) = r^\ell \, Y^m_\ell(\theta,\phi) \, [(2\ell+1) \, (\ell-m)! \, (\ell+m)! \, / \, 4\pi]^{-1/2} \tag{B-3}$$

and

$$\hat{z}^m_\ell(\underline{r}) = r^{-(\ell+1)} \, Y^m_\ell(\theta,\phi) \, [4\pi \, (\ell-m)! \, (\ell+m)! \, / \, (2\ell+1)]^{1/2} \tag{B-4}$$

Equation B-2 will be valid for values of $\underline{r}_1$ and $\underline{r}_2$ for which one of the following two conditions is satisfied:

1) $|\underline{r}_1| < |\underline{r}_2 + \underline{R}|$ and $|\underline{r}_2| < |\underline{R}|$; or

2) $|\underline{r}_2| < |\underline{r}_1 - \underline{R}|$ and $|\underline{r}_1| < |\underline{R}|$.

The multipole expansion technique approximates the electrostatic interaction with the truncated expression:

$$\int d^3r_1 \int d^3r_2 \frac{\rho_1(\underline{r}_1) \, \rho_2(\underline{r}_2)}{|\underline{r}_1 - \underline{r}_2 - \underline{R}|} = \sum_{L=0}^{L_{max}} \sum_{M} \hat{z}^M_L(\underline{R}) \sum_{\ell=0}^{L} \sum_{m=\max[-\ell,M+\ell-L]}^{\min[\ell,M+L-\ell]} (-1)^{L+M-\ell} \, M_1(\ell,m) \, M_2(L-\ell,M-m) \tag{B-5}$$

where the expressions $M_1(\ell,m)$ and $M_2(L-\ell,M-m)$ refer to the multipole moments of $\rho_1(\underline{r})$ and $\rho_2(\underline{r})$:

$$M_i(\ell,m) = \int d^3r \, \hat{y}^m_\ell(\underline{r}) \, \rho_i(\underline{r}) \tag{B-6}$$

Stolarczyk and Piela (1979) have demonstrated that the truncated expansion in Equation B-5 will be invariant to translations and rotations of the coordinate system as long as $|\underline{R}|$ remains constant. Since all omitted terms in Equation B-5 for the multipole expansion will be of the order of $|\underline{R}|^{-(L_{max}+2)}$ in the asymptotic limit as $|\underline{R}|$ tends toward infinity, the convergence of a lattice sum using the truncated expansion implies that the exact expansion will also be convergent.

Thus we will choose an approximation, to any desired precision, of the exact lattice sum U in Equation B-1. This approximation will be of the form:

$$U' = \sum_{|\underline{R}|<R'} \int d^3r_1 \int d^3r_2 \frac{\rho_1(\underline{r}_1)\,\rho_2(\underline{r}_2)}{|\underline{r}_1 - \underline{r}_2 - \underline{R}|} + \sum_{|\underline{R}|>R'} \sum_{L=0}^{L_{max}} \sum_{M} \hat{z}_L^M(\underline{R}) \sum_{\ell=0}^{L} \sum_{m} (-1)^{L+M-\ell} M_1(\ell,m) M_2(L-\ell,M-m) \tag{B-7}$$

where R' is chosen according to some as yet unspecified criterion. This leads to a computational savings since this sum may be evaluated as two terms: One term is the sum of multipole expansions terms for all lattice sites except the origin ($\underline{R} = \underline{0}$):

$$U_{mult} = \sum_{L} \sum_{M} \{ \sum_{|\underline{R}|>0} \hat{z}_L^M(\underline{R}) \} \sum_{\ell} \sum_{m} (-1)^{L+M-\ell} M_1(\ell,m) M_2(L-\ell,M-m) \tag{B-8}$$

where the indices range over the same intervals as those given in Equation B-5. The value of R' is chosen by summing in order of increasing $|\underline{R}|$ the difference between the exact electrostatic integral contained in the left-hand side of Equation B-5 and the truncated multipole expansion in the right-hand side of Equation B-5 until the difference is less than

some specified tolerance. This sum, including the exact electrostatic integral for the zero lattice vector, yields the expression:

$$U_{diff} = \int d^3r_1 \int d^3r_2 \frac{\rho_1(\underline{r}_1)\,\rho_2(\underline{r}_2)}{|\underline{r}_1 - \underline{r}_2|} + \sum_{|\underline{R}|>0}^{R'}$$

$$\{ \int d^3r_1 \int d^3r_2 \frac{\rho_1(\underline{r}_1)\,\rho_2(\underline{r}_2)}{|\underline{r}_1 - \underline{r}_2 - \underline{R}|} - \sum_L \sum_M \hat{z}_L^M(\underline{R})$$

$$\sum_\ell \sum_m (-1)^{L+M-\ell} M_1(\ell,m)\, M_2(L-\ell,M-m) \} \qquad \text{(B-9)}$$

Summing the expressions in Equations B-8 and B-9 results in the expression given in Equation B-7. The evaluation of U_{mult} will be considered shortly.

B-2. Evaluation of the Modified Irregular Solid Spherical Harmonics

The lattice vectors $\underline{R}$ will have a zero component in the z direction since the z direction is chosen as the normal to the plane of periodicity. Thus the modified irregular solid spherical harmonics $\hat{z}_\ell^m(\underline{R})$ may be expressed:

$$\hat{z}_\ell^m(\underline{R}) = (-1)^m\, (\ell-m)!\, P_\ell^m(0)\, R^{-(\ell+1)}\, e^{im\phi} \qquad \text{(B-10)}$$

where ϕ defines the angle between $\underline{R}$ and the x axis. The Legendre polynomial $P_\ell^m(0)$ will be nonzero only for $\ell-m$ even, such that $\ell-m = 2k$. where k is an integer. If this condition is satisfied, the Legendre polynomial will equal:

$$P_\ell^m(0) = (-1)^k\, (\ell+m)!\, /\, \{2^\ell\, k!\, (k+m)!\} \qquad \text{(B-11)}$$

Since every Bravais lattice will possess inversion symmetry, we may consider the sum of modified irregular solid spherical harmonics for both $\underline{R}$ and $-\underline{R}$. Thus we may utilize the relationship

$$\hat{z}_{\ell}^{m}(-\underline{R}) = (-1)^{\ell}\, \hat{z}_{\ell}^{m}(\underline{r}) \tag{B-12}$$

to yield the expression

$$\hat{z}_{\ell}^{m}(\underline{R}) + \hat{z}_{\ell}^{m}(-\underline{R}) = \frac{(-1)^{k}\ (\ell+m)!\ (\ell-m)!}{2^{\ell-1}\ k!\ (k+m)!\ R^{\ell+1}}\ e^{im\phi} \tag{B-13}$$

for even values of ℓ and m such that $2k = \ell-m$. If either ℓ or m is odd then this sum instead will equal zero. In the present work, L_{max} has the value of six and thus fifteen real numbers must be evaluated for the values of the modified irregular solid spherical harmonics. These fifteen real numbers correspond to the real values of $\hat{z}_{2}^{0}$, $\hat{z}_{4}^{0}$, and $\hat{z}_{6}^{0}$, and to the real and imaginary parts of $\hat{z}_{2}^{2}$, $\hat{z}_{4}^{2}$, $\hat{z}_{4}^{4}$, $\hat{z}_{6}^{2}$, $\hat{z}_{6}^{4}$, and $\hat{z}_{6}^{6}$. No value is computed for $\hat{z}_{0}^{0}$ since no multipole expansions will contain a nonzero monopole-monopole interaction. No additional values are computed for $\hat{z}_{\ell}^{-m}$ since these may be generated from the relationship

$$\hat{z}_{\ell}^{-m}(\underline{R}) = (-1)^{m}[\hat{z}_{\ell}^{m}(\underline{R})]^{*} \tag{B-14}$$

The value of the sum of $\hat{z}_{\ell}^{m}(\underline{R})$ for all $|\underline{R}|>0$ is computed by summing all lattice site contributions for a finite number of lattice sites up to a maximum radius R''. The sum of lattice site terms for $|\underline{R}|$ greater than R'' is approximated by the integral:

$$\sum_{|\underline{R}|>R''} \hat{z}_{\ell}^{m}(\underline{R}) \simeq \Omega^{-1} \int_{R''}^{\infty} r\, dr \int_{0}^{2\pi} \hat{z}_{\ell}^{m}(\underline{r})\, d\phi \tag{B-15}$$

$$= (-1)^{k} 2\pi(\ell!/k!)^{2}\delta_{m0} \,/\, \{2^{\ell}\Omega(\ell-1)(R''^{\ell-1})\}$$

where $k=\ell-m$ and Ω is the area of the two-dimensional unit cell of the two-dimensional Bravais lattice.

B-3. Evaluation of Multipole Moments

The evaluation of the multipole moments of the nuclear charge is uncomplicated. A nuclear center having a total charge Z_i located at a position vector $\underline{A}$ will have the multipole moment $M(\ell,m)$:

$$M(\ell,m) = Z_i\, \hat{y}_{\ell}^{m}(\underline{A}) \tag{B-16}$$

The multipole moments of a charge distribution represented by a Hermite-Gaussian function $f(\hat{n}, a, \underline{A}; \underline{r})$ may be evaluated using the relationship for modified regular solid spherical harmonics (Steinborn and Reudenberg, 1973):

$$\hat{y}_{\ell}^{m}(\underline{r}_1+\underline{r}_2) = \sum_{\ell'=0}^{\ell} \sum_{m'} \hat{y}_{\ell'}^{m'}(\underline{r}_1)\, \hat{y}_{\ell-\ell'}^{m-m'}(\underline{r}_2) \tag{B-17}$$

Setting $\underline{r}_1 = \underline{r} - \underline{A}$ and $\underline{r}_2 = \underline{A}$, we see that

$$\int d^3r\, f(\hat{n},a,\underline{A};\underline{r})\, \hat{y}_{\ell}^{m}(\underline{r}) = \partial_{\underline{A}}^{\hat{n}} \sum_{\ell'} \sum_{m'} \hat{y}_{\ell-\ell'}^{m-m'}(\underline{A}) \int d^3r\, \hat{y}_{\ell'}^{m'}(\underline{r}-A)\exp[-a|\underline{r}-\underline{A}|^2] \tag{B-18}$$

Since the Gaussian function is spherically symmetric about $\underline{A}$, the integrals on the right-hand side of Equation B-18 will be nonzero only for

the term where ℓ' is equal to zero. Using the definition of the modified regular solid spherical harmonics given in Equation B-3, we may evaluate the integral for the term where ℓ' is equal to zero:

$$\int d^3r\ f(\hat{n},a,\underline{A};\underline{r})\ \hat{y}_\ell^m(\underline{r}) = \partial_{\underline{A}}^{\hat{n}}\ \hat{y}_\ell^m(\underline{A})\ [\pi/a]^{3/2} \tag{B-19}$$

If the charge density $\rho(\underline{r})$ has the form of the product of two Hermite-Gaussian functions:

$$\rho(\underline{r}) = f(\hat{n},\ a,\ \underline{A};\ \underline{r})\ f(\hat{n}',\ b,\ \underline{B};\ \underline{r}) \tag{B-20}$$

we may use the relationship expressed in Appendix A in Equation A-23 in conjunction with Equation B-19 to yield the multipole moments of charge densities which have the form described in Equation B-20:

$$M(\ell,m) = \sum_{\hat{K}}\ (\hat{K},\hat{n},\hat{n}',a,b)\ f(\hat{K},ab/[a+b],\underline{A}-\underline{B};\underline{0})\ [\pi/(a+b)]^{3/2}$$

$$\cdot\ \partial_{\underline{Q}}^{\hat{n}+\hat{n}'-\hat{K}}\ \hat{y}_\ell^m(\underline{Q}) \tag{B-21}$$

where $\underline{Q}$ is as defined in Equation A-8.

The functions $\hat{y}_\ell^m(\underline{A})$ may be evaluated by considering the following expansion of the spherical harmonics $Y_\ell^m(\hat{r})$ multiplied by a factor of r^ℓ, where m is greater than or equal to zero:

$$r^\ell\ Y_\ell^m(\hat{r}) = \frac{(-1)^m r^\ell}{2^\ell\ \ell!}\ [\frac{(2\ell+1)}{4\pi}\ \frac{(\ell-m)!}{(\ell+m)!}]^{1/2}\ e^{im\phi}\ (1-\zeta^2)^{m/2}\ \frac{d^{\ell+m}}{d\zeta^{\ell+m}}\ (\zeta^2-1)^\ell \tag{B-22}$$

where $\zeta = \cos\theta$. We may expand a factor of the above equation in the following form:

$$r^m(1-\zeta^2)^{m/2}\ e^{im\phi} = \sum_{k=0}\ \binom{m}{k}\ i^k\ y^k\ x^{m-k} \tag{B-23}$$

We may also expand the factor:

$$r^{\ell-m} \frac{d^{\ell+m}}{d\zeta^{\ell+m}} (\zeta^2-1)^{\ell} = \sum_{0\le 2j\le \ell-m} (-1)^j \binom{\ell}{j} \frac{(2\ell-2j)!}{(\ell-2j-m)!} z^{\ell-2j-m} r^{2j} \qquad \text{(B-24)}$$

Thus by combining the expressions in Equations B-22 through B-24 and using the definition of the modified regular solid spherical harmonics given in Equation B-3, we find the following expansion:

$$\hat{y}_{\ell}^{m}(\underline{r}) = \frac{(-1)^m}{2^{\ell}\ell!(\ell+m)!} \sum_{j} \sum_{k} \binom{m}{k} \binom{\ell}{j} \frac{(2\ell-2j)!}{(\ell-2j-m)!} i^k (-1)^j$$

$$r^{2j} x^{m-k} y^{k} z^{\ell-2j-m} \qquad \text{(B-25)}$$

We may also expand r^{2j} into products of powers of the Cartesian coordinates x, y, and z:

$$r^{2j} = \sum_{p=0}^{j} \sum_{q=0}^{p} \binom{j}{p} \binom{p}{q} x^{2q} y^{2p-2q} z^{2j-2p} \qquad \text{(B-26)}$$

Thus we have an expansion of $\hat{y}_{\ell}^{m}(\underline{r})$ in products of powers of the Cartesian coordinates:

$$\hat{y}_{\ell}^{m}(\underline{r}) = \frac{(-1)^m}{2^{\ell}\ell!(\ell+m)!} \sum_{j} \sum_{p} \sum_{q} \sum_{k} \binom{m}{k} \binom{\ell}{j} \binom{j}{p} \binom{p}{q} i^k (-1)^j$$

$$\frac{(2\ell-2j)!}{(\ell-2j-m)!} x^{m-k+2q} y^{2p+k-2q} z^{\ell-2p-m} \qquad \text{(B-27)}$$

We may trivially evaluate the quantity:

$$\partial_{\underline{A}}^{\hat{n}} \hat{y}_{\ell}^{m}(\underline{A}) = \frac{(-1)^m}{2^{\ell}\ell!\,(\ell+m)!} \sum_{j} \sum_{p} \sum_{q} \sum_{k} i^k (-1)^j \binom{m}{k} \binom{\ell}{j} \binom{j}{p} \binom{p}{q}$$

$$\frac{(2\ell-2j)!}{(\ell-2j-m)!} \frac{(m-k+2q)!}{(m-k+2q-n_1)!} \frac{(2p+k-2q)!}{(2p+k-2q-n_2)!} \frac{(\ell-2p-m)!}{(\ell-2p-m-n_3)!}$$

$$x^{m-k+2q-n_1}\, y^{2p+k-2q-n_2}\, z^{\ell-2p-m-n_3} \tag{B-28}$$

where the summation indices have the following ranges:

$$0 \le 2j \le \ell - m \tag{B-29}$$

$$\ell - m - n_3 \le 2p \le n_1 + n_2 - m \tag{B-30}$$

$$2p - n_2 + m \le 2q \le n_1 - m \tag{B-31}$$

$$2q + m - n_1 \le k \le 2q + n_2 - 2p \tag{B-32}$$

This set of equations completes the evaluation of all necessary quantities for the computation of the multipole moments of Hermite-Gaussian functions and of nuclear centers.

APPENDIX C
RECIPROCAL LATTICE EXPANSIONS

C-1. General Properties

Many of the quantities evaluated in this work may be expressed as an expansion in the lattice vectors $\underline{R}$ generated from the primitive lattice vectors $\underline{R}_1$ and $\underline{R}_2$ defined in Section 2-1:

$$f(\underline{r}) = \sum_{\underline{R}} \exp[i\underline{k}_{//}\cdot\underline{R}]\, U(\underline{r} + \underline{R}) \tag{C-1}$$

where $\underline{r}$ is a vector in a three-dimensional Cartesian coordinate system. Let us define $\underline{r}$ then by the Cartesian coordinates $\underline{r} = (x, y, z)$ and furthermore define $\underline{s}$ to be a vector in a two-dimensional Cartesian coordinate system such that $\underline{s} = (x, y)$. Since the Bloch function $f(\underline{r})$ has the property:

$$f(\underline{r} + \underline{R}) = \exp[-i\underline{k}_{//}\cdot\underline{R}]\, f(\underline{r}) \tag{C-2}$$

we may express $f(\underline{r})$ as the product of a phase factor and a periodic function $f_p(\underline{s}, z)$ such that:

$$f(\underline{r}) = \exp[-i\underline{k}_{//}\cdot\underline{s}]\, f_p(\underline{s}, z) \tag{C-3}$$

where $f_p(\underline{s}, z)$ is periodic only in the coordinate $\underline{s}$:

$$f_p(\underline{s} + \underline{R}, z) = f_p(\underline{s}, z) \tag{C-4}$$

We may expand $f_p(\underline{s}, z)$ as an expansion in the reciprocal lattice vectors $\underline{K}$ described in Chapter 2 as:

$$f_p(\underline{s}, z) = \sum_{\underline{K}} \exp[i\underline{K}\cdot\underline{s}]\ \tilde{f}(\underline{K}, z) \tag{C-5}$$

where $\tilde{f}(\underline{K}, z)$ may be expressed as an integral over the entire plane defined by $\underline{s}$:

$$\tilde{f}(\underline{K}, z) = \Omega^{-1} \int d^2s \exp[-i(\underline{K}-\underline{k}_{//})\cdot\underline{s}]\ U(\underline{r}) \tag{C-6}$$

Thus we may expand our original function $f(\underline{r})$ in a reciprocal lattice expansion of the form:

$$f(\underline{r}) = \sum_{\underline{K}} \tilde{f}(\underline{K}, z) \exp[i(\underline{K}-\underline{k}_{//})\cdot\underline{s}] \tag{C-7}$$

As an example of this approach let us consider the reciprocal lattice expansion of a Bloch function constructed from the Hermite-Gaussian functions $f(\hat{n}, a, \underline{A}; \underline{r})$ defined in Appendix A:

$$\phi(\underline{r}; \underline{k}_{//}) = \sum_{\underline{R}} \exp[i\underline{k}_{//}\cdot\underline{R}]\ f(\hat{n}, a, \underline{A}; \underline{r} + \underline{R}) \tag{C-8}$$

The expansion coefficient $\tilde{f}(\underline{K}, z)$ will then equal:

$$f(\underline{K}, z) = \Omega^{-1}\int d^2s \exp(-i(\underline{K}-\underline{k}_{//})\cdot\underline{s}]\ f(\hat{n}, a, \underline{A}; \underline{r}) \tag{C-9}$$

$$= \frac{\pi}{a\Omega}\ \partial^{\hat{n}}_{\underline{A}} \exp[-i(\underline{K}-\underline{k}_{//})\cdot\underline{A}]\ \exp[-a(z-A_z)^2]$$

$$= \frac{\pi}{a\Omega}\ i^{-(n_1+n_2)} (K_x-k_{//x})^{n_1} (K_y-k_{//y})^{n_2} a^{n_3/2}$$

$$H_{n_3}[a^{1/2}(z-A_z)]\ \exp[-a(z-A_z)^2]\ \exp[-i(\underline{K}-\underline{k}_{//})\cdot\underline{A}]$$

Thus we see that

$$\phi(\underline{r};\ \underline{k}_{//}) = \frac{\pi}{a\Omega}\, i^{-(n_1+n_2)}\ a^{n_3/2}\ H_{n_3}[a^{1/2}(z-A_z)]\ \exp[-a(z-A_z)^2]$$

$$\sum_{\underline{K}} (K_x-k_{//x})^{n_1}(K_y-k_{//y})^{n_2}\ \exp[-i(\underline{K}-\underline{k}_{//})\cdot\underline{A}] \qquad \text{(C-10)}$$

Overlap matrix elements may be calculated using Equation C-10 if we use the identity (where the integration over $\underline{r}$ is over the entire three-dimensional space):

$$\sum_{R} \exp[i\underline{k}_{//}\cdot\underline{R}] \int d^3r\ f(\hat{n},\ a,\ \underline{A};\ \underline{r})\ f(\hat{n};\ b,\ \underline{B};\ \underline{r}+\underline{R})$$

$$= \left[\frac{\pi}{a+b}\right]^{3/2}(-1)^n \sum_{\underline{R}} \exp[i\underline{k}_{//}\cdot\underline{R}]\ f(\hat{n}+\hat{n}';\ \frac{ab}{a+b},\ \underline{B}-\underline{A};\ \underline{R}) \qquad \text{(C-11)}$$

since this expression is equivalent to a Bloch function $\phi(\underline{r};\ \underline{k}_{//})$ as defined in Equation C-8 evaluated at $\underline{r} = \underline{0}$, multiplied by a constant.

C-2. Coulomb Integrals

Much of the work using reciprocal lattice expansions to expand Coulomb integrals relies upon the expansion of the Coulomb potential in a reciprocal lattice expansion. One difficulty with this approach is that the long range behavior of the Coulomb potential leads to many problems with the $\underline{K} = \underline{0}$ term in the reciprocal lattice expansion, although Schwalm and Monkhorst (1980) have pointed out how one may treat the difficulties in this approach. A more useful approach for the purposes of this work is first to create a direct lattice expansion of the desired integral and integrate each term analytically. We now proceed

to construct such an expansion and derive an equivalent expansion in reciprocal lattice vectors.

First let us consider a Coulomb integral of the form:

$$V(\underline{s}) = \sum_{\underline{R}} \{\int d^3r \int d^3r' \exp[-a|\underline{r}-\underline{s}-\underline{A}-\underline{R}|^2] \exp[-b|\underline{r}'-\underline{B}|^2] \frac{1}{|\underline{r}-\underline{r}'|}$$

$$-[\frac{\pi}{b}]^{3/2} \frac{1}{Z_{tot}} \sum_{m=1}^{N} Z_m \int d^3r \exp[-a|\underline{r}-\underline{s}-\underline{A}-\underline{R}|^2] \frac{1}{|\underline{r}-\underline{C}_m|} \} \quad (C-12)$$

where

$$Z_{tot} = \sum_{m=1}^{N} Z_m \quad (C-13)$$

It has been demonstrated in Appendix B that this lattice sum will be convergent if we sum in order of increasing $|\underline{R}|$. We may reduce Equation C-12 to the form:

$$V(\underline{s}) = \sum_{\underline{R}} \{ \sum_{m=0}^{N} \alpha_m \int_0^1 \exp[-\beta_m|\underline{s}+\underline{r}_m+\underline{R}|^2 u^2] du\} \quad (C-14)$$

where terms for which the index m is zero correspond to electronic terms such that:

$$\alpha_0 = 2\pi^{5/2}/\{ab[a+b]^{1/2}\} \quad (C-15)$$

$$\beta_0 = ab/[a+b] \quad (C-16)$$

$$\underline{r}_0 = \underline{A} - \underline{B} \quad (C-17)$$

Terms for which the index m is greater than zero correspond to nuclear terms such that:

$$\alpha_m = -2\pi^{5/2} Z_m / \{Z_{tot}\, a\, b^{3/2}\} \tag{C-18}$$

$$\beta_m = a \tag{C-19}$$

$$\underline{r}_m = \underline{A} - \underline{C}_m \tag{C-20}$$

We may expand $V(\underline{s})$ in a reciprocal lattice expansion of the form:

$$V(\underline{s}) = \sum_{\underline{K}} \exp[i\underline{K}\cdot\underline{s}]\, \tilde{V}(\underline{K}) \tag{C-21}$$

where each coefficient $\tilde{V}(\underline{K})$ is given by:

$$\tilde{V}(\underline{K}) = \Omega^{-1} \int d^2s \exp[-i\underline{K}\cdot\underline{s}]\, V(\underline{s}) \tag{C-22}$$

$$= \Omega^{-1} \int d^2s\, e^{-i\underline{K}\cdot\underline{s}} \int_0^1 du \sum_{m=0}^{N} \alpha_i \exp[-\beta_m |\underline{s}+\underline{r}_m|^2 u^2]$$

For lattice vectors such that $|\underline{K}|$ is greater than zero, we may interchange the order of integration in Equation C-22 without difficulty. Bearing in mind that restriction, we interchange the order of integration to yield:

$$\tilde{V}(\underline{K}) = \pi\Omega^{-1} \sum_{m=0}^{N} \frac{\alpha_m}{\beta_m} \exp[i\underline{K}\cdot\underline{r}_m] \int_0^1 u^{-2} \exp[-\beta_m z_m^2 u^2 - K^2/4\beta_m u^2]\, du \tag{C-23}$$

A proper treatment of $\tilde{V}(\underline{K})$ requires a more complicated analysis for the case of $\underline{K} = \underline{0}$. The reason that the order of integration may not immediately be interchanged is the singularity of the integral over $\underline{s}$ for values of the integrand near u = 0. By use of the expression:

$$\int_0^1 \exp[-\beta_m |\underline{s}+\underline{r}_m|^2 u^2]\, du = \frac{1}{2s}\left[\frac{\pi}{\beta_m}\right]^{1/2} + \frac{1}{2}\left[\frac{\pi}{\beta_m}\right]^{1/2}\left\{\frac{1}{|\underline{s}+\underline{r}_m|} - \frac{1}{s}\right\}$$

$$- \int_1^\infty \exp[-\beta_m |\underline{s}+\underline{r}_m|^2\, u^2]\, du \qquad \text{(C-24)}$$

let us examine the integral

$$\tilde{V}(\underline{0}) = \Omega^{-1} \int d^2s \left\{\left(\frac{1}{2s} \sum_{m=0}^{N} \frac{\alpha_m}{\beta_m^{1/2}} \pi^{1/2}\right) + \left(\sum_{m=0}^{N} \frac{\alpha_m}{2} \left(\frac{\pi}{\beta_m}\right)^{1/2}\left[\frac{1}{|\underline{s}+\underline{r}_m|} - \frac{1}{s}\right]\right)\right.$$

$$\left. - \left(\sum_{m=0}^{N} \alpha_m \int_1^\infty du\, \exp[-\beta_m |\underline{s}+\underline{r}_m|^2\, u^2]\right)\right\} \qquad \text{(C-25)}$$

term by term. We see that the values of the quantities $\alpha_m \beta_m^{-1/2}$ for the case of m = 0 yield

$$\alpha_0 \beta_0^{-1/2} = 2\pi^{5/2}\, [ab]^{-3/2} \qquad \text{(C-26)}$$

and for the case of m greater than zero

$$\alpha_m \beta_m^{-1/2} = -\frac{2\pi^{5/2} Z_m}{Z_{tot}[ab]^{3/2}} \qquad \text{(C-27)}$$

lead to the result:

$$\sum_{m=0}^{N} \alpha_m \beta_m^{-1/2} = 0 \qquad \text{(C-28)}$$

In order to evaluate the contribution of the second term of Equation C-25 let us consider the integral:

$$\int d^2s \left\{\frac{1}{|\underline{s}+\underline{r}_m|} - \frac{1}{|s|}\right\} = \int d^2s \left\{\frac{1}{|\underline{s}+z_m\hat{k}|} - \frac{1}{|s|}\right\} \qquad \text{(C-29)}$$

$$= 2\pi \int_0^\infty \left(\frac{s}{[s^2+z_m^2]^{1/2}} - 1\right) ds$$

We may transform this integral to the form:

$$2\pi \int_0^{\infty} \left(\frac{s}{[s^2+z_m^2]^{1/2}} - 1 \right) ds = - 2\pi z_m \int_0^{\pi/2} \frac{d\theta}{1 + \sin\theta} \qquad \text{(C-30)}$$

By use of the indefinite integral

$$\int \frac{d\theta}{1 + \sin\theta} = - \tan\left(\frac{\pi}{4} - \frac{\theta}{2}\right) \qquad \text{(C-31)}$$

Equation C-29 reduces to

$$\int d^2s \left(\frac{1}{|\underline{s}+\underline{r}_m|} - \frac{1}{|s|} \right) = - 2\pi z_m \qquad \text{(C-32)}$$

Interchanging the order of integration of the last term of Equation C-25 leads to

$$\int d^2s \int_1^{\infty} du \sum_{m=0}^{N} \alpha_m \exp[-\beta_m |\underline{s}+\underline{r}_m|^2 u^2]$$

$$= \pi \sum_{m=0}^{N} \frac{\alpha_m}{\beta_m} \int_1^{\infty} \exp[-\beta_m z_m^2 u^2] \frac{du}{u^2} \qquad \text{(C-33)}$$

Integration by parts yields

$$\int_1^{\infty} \exp[-\beta_m z_m^2 u^2] \frac{du}{u^2} = \exp[-\beta_m z_m^2] - 2\beta_m z_m^2 \int_1^{\infty} \exp[-\beta_m z_m^2 u^2] du \qquad \text{(C-34)}$$

By use of the relationship

$$\int_1^{\infty} \exp[-\beta_m z_m^2 u^2] du = \frac{1}{2}\left(\frac{\pi}{\beta_m z_m^2}\right)^{1/2} - \int_0^1 \exp[-\beta_m z_m^2 u^2] du \qquad \text{(C-35)}$$

$$= \frac{1}{2}\left(\frac{\pi}{\beta_m z_m^2}\right)^{1/2} - F_0(\beta_m z_m^2)$$

where F_0 is the incomplete gamma function defined in Appendix A, we may reduce Equation C-33 to the form

$$\int d^2s \int_1^\infty du \sum_{m=0}^{N} \alpha_m \exp[-\beta_m |\underline{s}+\underline{r}_m|^2 u^2] = \pi \sum_{m=0}^{N} \alpha_m \{\frac{1}{\beta_m} \exp[-\beta_m z_m^2]$$

$$- (\frac{\pi}{\beta_m})^{1/2} z_m + 2z_m^2 F_0(\beta_m z_m^2)\} \qquad \text{(C-36)}$$

Notice that while the integral in Equation C-35 will be undefined for $z_m = 0$, an analysis of Equation C-33 indicates that Equation C-36 will remain valid. Inserting the results of Equations C-29, C-32, and C-36 into Equation C-25 yields

$$\tilde{V}(\underline{0}) = - \pi\Omega^{-1} \sum_{m=0}^{N} \alpha_m \{+ \frac{1}{\beta_m} \exp[-\beta_m z_m^2] + 2z_m^2 F_0(\beta_m z_m^2)\} \qquad \text{(C-37)}$$

Let us consider the evaluation of the following expression:

$$\partial_{\underline{A}}^{\hat{n}} \partial_{\underline{B}}^{\hat{n}'} V(\underline{s}) = \sum_{\underline{K}} e^{i\underline{K}\cdot\underline{s}} \partial_{\underline{A}}^{\hat{n}} \partial_{\underline{B}}^{\hat{n}'} \tilde{V}(\underline{K}) \qquad \text{(C-38)}$$

The partial derivatives with respect to the vector components B_i do not apply by construction to nuclear terms. Since $V(\underline{0})$ depends only upon A_x, A_y, B_x, or B_y we see that

$$\partial_{\underline{A}}^{\hat{n}} \partial_{\underline{B}}^{\hat{n}'} \tilde{V}(\underline{0}) = - \frac{\pi}{\Omega} \delta_{n_1,0} \delta_{n_2,0} \delta_{n_1',0} \delta_{n_2',0}$$

$$[(-1)^{n_3'} \alpha_0 \{\frac{1}{\beta_0} f(\hat{n}_z+\hat{n}_z', \beta_0, z_0; \underline{0}) + 2z_0^2 R(\hat{n}_z+\hat{n}_z', \beta_0, z_0)\}$$

$$+ \delta_{n_3,0} \sum_{m=1}^{N} \alpha_m \{\frac{1}{\beta_m} f(\hat{n}_z, \beta_m, z_m; \underline{0}) + 2z_m^2 R(\hat{n}_z, \beta_m, z_m)\}] \qquad \text{(C-39)}$$

where the notation $\hat{n}_z$ denotes the set $(0, 0, n_3)$. For vectors $\underline{K}$ not equal to the zero vector:

$$\delta_{\underline{A}}^{\hat{n}} \delta_{\underline{B}}^{\hat{n}'} \tilde{V}(\underline{K}) = \frac{\pi}{2} \{\frac{\alpha_0}{\beta_0} i^{n_1+n_2-n_1'-n_2'} K_x^{n_1-n_1'} K_y^{n_2-n_2'} \partial_{z_0}^{n_3+n_3'}$$

$$\{\int_0^1 \exp[-\beta_0 z_0^2 u^2 - K^2/4\beta_0 u^2] \frac{du}{u^2}\} + \delta_{n_1',0} \delta_{n_2',0} \delta_{n_3'},$$

$$\sum_{m=1}^{N} \frac{\alpha_m}{\beta_m} i^{n_1+n_2} K_x^{n_1} K_y^{n_2} \partial_{z_m}^{n_3} \int_0^1 \exp[-\beta_m z_m^2 u^2 - K^2/4\beta_m u^2] \frac{du}{u^2} \} \tag{C-40}$$

We may reduce the integrals in Equation C-40 to known form if we consider the following construction.

First let us define the quantity $f_0(a,b)$:

$$f_0(a,b) = \int_0^1 \exp[-a^2u^2 + b^2/u^2] \frac{du}{u^2} \tag{C-41}$$

$$= \frac{1}{2b} \{e^{-2ab} \int_0^1 (a + \frac{b}{u^2}) \exp[-(au-b/u)^2] \, du$$

$$- e^{2ab} \int_0^1 (a - \frac{b}{u^2}) \exp[-(au+b/u)^2] \, du \}$$

$$= \frac{1}{2b} \{e^{-2ab} \int_{b-a}^{\infty} e^{-v^2} dv + e^{2ab} \int_{b+a}^{\infty} e^{-v^2} dv \}$$

Since

$$\int_{\gamma}^{\infty} e^{-v^2} dv = \frac{\pi^{1/2}}{2} - \int_0^{\gamma} e^{-v^2} dv \tag{C-42}$$

$$= \frac{\pi^{1/2}}{2} - \gamma F_0(\gamma^2)$$

we see that

$$f_0(a,b) = \frac{1}{2b}\{\pi^{1/2}\cosh 2ab - e^{2ab}(b+a)\ F_0([b+a]^2)$$

$$- e^{-2ab}(b-a)\ F_0([b-a]^2)\} \qquad (C\text{-}43)$$

Consider the relationship:

$$\frac{\partial}{\partial a}\{e^{\pm 2ab}(b\pm a)\int_0^1 \exp[-(b\pm a)^2u^2]du\} = \pm\{2b\ e^{\pm 2ab}(b\pm a)F_0([b\pm a]^2)$$

$$+ e^{\pm 2ab}\ F_0([b\pm a]^2) - 2e^{\pm 2ab}(b\pm a)^2\int_0^1 u^2e^{-(b\pm a)^2u^2}du\} \qquad (C\text{-}44)$$

Utilization of the identity

$$\int_0^1 u^2e^{-\gamma^2u^2}du = \frac{1}{2\gamma^2}[\int_0^1 e^{-\gamma^2u^2}du - e^{-\gamma^2}] \qquad (C\text{-}45)$$

results in

$$\frac{\partial}{\partial a}\{e^{\pm 2ab}(b\pm a)\int_0^1 \exp[-(b\pm a)^2u^2]du\}$$

$$= \pm\ 2b\{e^{\pm 2ab}(b\pm a)\ F_0([b\pm a]^2)\} \pm e^{-(a^2+b^2)} \qquad (C\text{-}46)$$

Thus we see that

$$f_1(a,b) = \frac{\partial}{\partial a}f_0(a,b) = \pi^{1/2}\sinh 2ab - e^{2ab}(b+a)\ F_0([b+a]^2)$$

$$+ e^{-2ab}(b-a)\ F_0([b-a]^2) \qquad (C\text{-}47)$$

and

$$f_2(a,b) = 4b^2\ f_0(a,b) - 2e^{-(a^2+b^2)} \qquad (C\text{-}48)$$

The above results then lead to the recursion relations

$$f_n(a,b) = \partial_a^n f_0(a,b) \tag{C-49}$$

$$= \partial_a^{n-2} f_2(a,b)$$

$$= 4b^2 \partial_a^{n-2} f_0(a,b) - 2\partial_a^{n-2} e^{-(a^2+b^2)}$$

$$= 4b^2 f_{n-2}(a,b) - 2(-1)^n H_{n-2}(a) e^{-(a^2+b^2)}$$

where $H_n(x)$ refers to the Hermite polynomials. This reduces the factors in Equation C-40 to the form:

$$\partial_{z_m}^n \int_0^1 \exp[-\beta_m z_m^2 u^2 - K^2/4\beta_m u^2] \frac{du}{u^2}$$

$$= \beta_m^{n/2} f_n(\beta_m^{1/2} z_m, |\underline{K}|/2\beta_m^{1/2}) \tag{C-50}$$

APPENDIX D
NUMERICAL INTEGRATION GRID

We wish to describe briefly the scheme for selecting the numerical integration grid points and weights used in the exchange fitting procedures discussed in Chapter III. A general review of numerical integration techniques is contained in Davis and Rabinowitz (1975). Several different calculations have been performed testing various schemes for numerical integration over the three-dimensional unit cell defined in Chapter II, with results indicating that the details of the selection scheme are not as important as the total number of points chosen. Two basic guidelines have been followed in all schemes tested:

1) The arrangement of grid points near each nuclear center should remain the same with respect to changes in the lattice constant. This condition minimizes the potential problems arising from changes in the grid in regions of high density near the nuclei, which would tend to mask the effect of actual changes of the density on the desired integrals.
2) The coordinates for the three-dimensional grid should be chosen so as to take advantage of the property that Hermite-Gaussian functions may be factored into the product of independent functions of each of the Cartesian coordinates. This property results in being able to factor the Bloch functions which we must calculate at each grid point into the product of a function of the coordinates parallel to the surface (x and y) and a

function of the coordinate normal to the surface (z). Choosing a grid where several points share the same value of the coordinate normal to the surface for each choice of the normal coordinate can lead to a substantial savings in computation time in evaluating the Bloch functions.

The scheme used for the calculations presented in this dissertation begins by constructing a grid using the cylindrical coordinates (ρ,ϕ,z) about each nucleus located in the primitive unit cell under consideration. Each grid point lies at the center of a representative volume, with the weight assigned to that sampling point equal to approximately that part of the representative volume contained in the region of space nearer to the central nucleus than to any other nucleus (including nuclei in adjacent unit cells). The values of the normal coordinate (z) were chosen using the radial distance of every fifth point of the Herman-Skillman mesh (Herman and Skillman, 1963). This Herman-Skillman mesh contains 441 radial points where the interval between adjacent points doubles at every 40-th point. The initial interval between the origin (the first point) and the second point of this Herman-Skillman mesh equals $0.0025(9\pi^2/128z)^{1/3}$, where z is the atomic number of the central nucleus. The values of the radial coordinate ρ were also chosen using every fifth point of the Herman-Skillman mesh for values of the normal coordinate (z) sufficiently small in magnitude. At progressively larger values of the magnitude of the normal coordinate (z) every tenth, fifteenth, twentieth, etc. point of the Herman-Skillman mesh was used for the value of the radial coordinate (ρ). For each choice of the normal coordinate and the radial coordinate, four, eight, or twelve values of the angular coordinate ϕ were used. All points having a representative volume lying

completely outside the region nearer the central nucleus than any other nucleus were excluded from the integration grid since the volume assigned to that grid point either lies outside the primitive unit cell integration region or will be treated with points centered about another nucleus in the primitive unit cell. A set of FORTRAN subroutines capable of calculating the sampling points and weights generated by the above mentioned procedure is given in Table D-1.

Table D-1. IBM System/370 FORTRAN IV code for generating sampling points and weights used in numerical integration procedures.

```
      SUBROUTINE INTNUM(RNUC, ZCHG, VECT, NNUC)
      IMPLICIT REAL*8(A-H,O-Z)
      LOGICAL OUT, TRUE, FALSE
C
C     THIS SUBROUTINE CALCULATES THE NUMERICAL GRID POINTS
C     AND WEIGHTS USED IN THE EXCHANGE FITTING PROCEDURE.
C     THE SUBROUTINE INTGRD IS REQUIRED FOR USE OF THIS
C     SUBROUTINE.
C
C     INPUT VARIABLES:
C
C     RNUC(3,NNUC):    CARTESIAN COORDINATES OF NUCLEI
C
C     ZCHG(NNUC): ATOMIC NUMBER OF NUCLEI
C
C     NNUC:         NUMBER OF NUCLEI IN PRIMITIVE UNIT CELL
C
C     VECT(2,2):  X AND Y CARTESIAN COORDINATES OF PRIMITIVE
C                      LATTICE TRANSLATIONS
C
      DIMENSION RNUC(3,NNUC), VECT(2,2), ZCHG(NNUC)
      DIMENSION INUC(10), R(32), RX(32), WTZ(32)
      DATA PI/3.14159265358979D+00/
      DATA TRUE,FALSE/ .TRUE., .FALSE./
      DATA RTOL/1.D-5/
      DATA NSKIP/5/
      WRITE (6,3000)
      IPT = 0
C
C     SORT NUCLEI IN ORDER
C
      DO 20 I=1,NNUC
20    INUC(I) = I
      IF (NNUC.EQ.1) GO TO 40
      DO 30 I=1,NNUC
      DO 30 J=I,NNUC
      IF (RNUC(3,INUC(J))-RNUC(3,INUC(I))) 25, 30, 30
25    IN = INUC(I)
      INUC(I) = INUC(J)
      INUC(J) = IN
30    CONTINUE
C
C     LOOP OVER NUCLEAR SITES IN ORDER
C
40    DO 960 IN=1,NNUC
      IZN = INUC(IN)
      CALL INTGRD(ZCHG(IZN), NSKIP, R, RX, WTZ, NPNT, SCALE)
      UNIT = 1.D0 - R(2)
C
C     LOOP OVER RADIAL POINTS
C
      DO 950 IR=1,NPNT
      OUT = TRUE
      DEL = R(IR) - R(IR+1)
      NP = 4 * IDINT(DEL/UNIT)
      IF (NP.GT.12) NP = 12
      IF (NP.LT.4) NP = 4
      IF (IR.EQ.1) NP = 1
      ARC = PI / DFLOAT(NP)
C
```

Table D-1. (Continued)

```
C       LOOP AROUND CIRCUMFERENCE OF CIRCLE
C
70      DO 900 IP=1,NP
        ANGLE = ARC * DFLOAT(2*IP) + PI / 4.D0
        X0 = RX(IR) * DCOS(ANGLE)
        Y0 = RX(IR) * DSIN(ANGLE)
        X1 = X0 + RNUC(1,IZN)
        Y1 = Y0 + RNUC(2,IZN)
        WT0 = 1.D0
C
C       LOOP OVER Z (NORMAL) DIRECTION
C
        NZ = -NPNT
        N2 = 2*NPNT - 1
        DO 800 N=1,N2
        NZ = NZ + 1
        ICHK = NSKIP * IABS(NZ) / 40 + 1
        ICHK = MIN0(ICHK, NPNT)
        IF (MOD(IR-1, ICHK).NE.0) GO TO 800
        Z0 = DFLOAT(ISIGN(1,NZ)) * RX(IABS(NZ)+1)
        Z1 = Z0 + RNUC(3,IZN)
        RMX = 0.D0
        IF (IR+ICHK.LT.NPNT) RMX = R(IR + ICHK)
        RMX = -DLOG( (R(IR) + RMX)/2.D0) / SCALE
        IF (IP-1) 130, 130, 140
130     VOL= PI * RMX**2
        GO TO 150
140     RMN = -DLOG( (R(IR) + R(IR-ICHK))/2.D0)/SCALE
        VOL = PI * (RMX + RMN) * (RMX - RMN)
150     WT = WT0 * WTZ(IABS(NZ)+1)
        VOL = VOL / DFLOAT(NP)
        VOL2 = VOL
        RMX2 = DSQRT(Z0**2 + RMX**2)
C
C       LOOP OVER ADJACENT UNIT CELLS
C
        DO 200 IXX=1,3
        DO 200 IYY=1,3
        XX = VECT(1,1)*DFLOAT(IXX-2) + VECT(1,2)*DFLOAT(IYY-2)
        YY = VECT(2,1)*DFLOAT(IXX-2) + VECT(2,2)*DFLOAT(IYY-2)
C
C       LOOP OVER NUCLEAR CENTERS IN UNIT CELL
C
        DO 200 IN2=1,NNUC
        IF (((IXX.EQ.2).AND.(IYY.EQ.2)).AND.(IN2.EQ.IZN))
     X      GO TO 200
        XI = RNUC(1,IN2) + XX - RNUC(1,IZN)
        YI = RNUC(2,IN2) + YY - RNUC(2,IZN)
        ZI = RNUC(3,IN2) - RNUC(3,IZN)
        R2 = XI**2 + YI**2
        R12 = DSQRT(R2 + ZI**2) / 2.D0
        IF (RMX2.LT.R12) GO TO 200
        IF (R2.GT.RTOL) GO TO 165
C
C       NUCLEAR CENTER LIES IN SURFACE NORMAL DIRECTION
C
        IF (DABS(Z0).GT.DABS(ZI-Z0)) GO TO 800
        GO TO 200
165     FACTOR = (1.D0 - ZI*(ZI-2.D0*Z0)/R2) / 2.D0
        R2 = DSQRT(R2)
```

Table D-1. (Continued)

```
      D = DABS(FACTOR * R2)
      AOUT = 0.D0
      IF (D.GT.RMX) GO TO 200
      THETA = DARCOS(D / RMX)
      THETP = 0.D0
      IF (D.LT.RMN) THETP =DARCOS(D / RMN)
      COSA = (XI*XO + YI*YO) / (R2 * RX(IP))
      PSI = DARCOS(COSA)
      IF (FACTOR.LT.0.D0) PSI = PI - PSI
C
C     COMPUTE LEFT-HAND AREA LOSS
C
      THET1 = DMAX1(-THETA, PSI-ARC)
      THET2 = DMAX1(-THETP, THET1)
      IF ((THET2-THET1).LT.RTOL) GO TO 171
      AOUT = ((THET2 - THET1)* RMX**2 - D**2 * (DTAN(THET2)
     X  - DTAN(THET1))) / 2.D0
C
C     COMPUTE CENTRAL AREA LOSS
C
171   THET1 = THET2
      THET2 = DMAX1(THET1, THETP)
      THET2 = DMIN1(THET2, PSI+ARC)
      AOUT = AOUT+(THET2-THET1)*(RMX+RMN)*(RMX-RMN)/2.D0
C
C     COMPUTE RIGHT-HAND LOSS
C
      THET1 = THET2
      THET2 = DMAX1(THET1, THETA)
      THET2 = DMIN1(THET2, PSI+ARC)
      IF ((THET2-THET1).LT.RTOL) GO TO 175
      AOUT=AOUT+((THET2-THET1)*(RMX**2)-(D**2)*(DTAN(THET2)
     X   - DTAN(THET1))) / 2.D0
175   CONTINUE
      IF (FACTOR) 176, 178, 178
176   VOL2 = VOL2 - (VOL - AOUT)
      GO TO 200
178   VOL2 = VOL2 - AOUT
200   CONTINUE
      IF (VOL2.LT.RTOL) GO TO 800
C
C     END OF CHECK FOR BOUNDARY POSITION
C
      OUT = FALSE
      WT = WT * VOL2
      IPT = IPT + 1
      WRITE (6,20000) IPT, X1, Y1, Z1, WT
C
800   CONTINUE
900   CONTINUE
      IF (OUT) GO TO 960
950   CONTINUE
960   CONTINUE
      WRITE (6,10000) IPT
      RETURN
10000 FORMAT(1H-,'TOTAL NUMBER OF INTEGRATION POINTS:',I3)
20000 FORMAT(1H ,I5,1P4D2).6)
30000 FORMAT(1H1,' PNT ',10X,'X',19X,'Y',19X,'Z',19X,'WT'/)
      END
      SUBROUTINE INTGRT(Z, NSKIP, R, RX, WTZ, NPT, SCALE)
```

Table D-1. (Continued)

```
      IMPLICIT REAL*8(A-H,O-Z)
C
C     THIS SUBROUTINE GENERATES A TABULAR GRID OF POINTS
C     USED FOR THE NUMERICAL INTEGRATION PROCEDURE WITH
C     EVERY NSKIP POINTS OF THE HERMAN-SKILLMAN MESH.
C
      DIMENSION R(1), RX(1), WTZ(I)
      DATA PI2/9.8696 04401 08936 D00/
      RTRAN(XXX,SSS) = -DLOG(XXX)/SSS
      SCALE = (9.00*PI2/(1.2802*Z))**(3.3333333333333D-01)
      NPT = 1
      RX(NPT) = 0.D0
      R(NPT) = 1.D0
      X = 0.D0
      DX = 2.5D-3 * SCALE
      SCALE = 1.D0 / (DX * DFLOAT(441))
      IJ = 0
C
C     GENERATE EVERY NSKIP POINT OF HERMAN-SKILLMAN GRID
C
      DO 200 I=1,10
      DO 100 J=1,40
      X = X + DX
      IJ = IJ + 1
      IF (MOD(IJ,NSKIP).NE.0) GO TO 100
      NPT = NPT + 1
      RX(NPT) = X
      R(NPT) =  DEXP(-SCALE*X)
100   CONTINUE
200   DX = 2.D0 * DX
      RX(NPT+1) = X
      R(NPT+1) = 0.D0
      RDWN = -RTRAN((1.D0 + R(2))/2.D0, SCALE)
      DO 400 I=1,NPT
      RUP = RTRAN((R(I) + R(I+1))/2.D0, SCALE)
      WTZ(I) = RUP - RDWN
400   RDWN = RUP
      RETURN
      END
```

BIBLIOGRAPHY

Alldredge, G. P., and Kleinman, L. (1972). Phys. Rev. Lett. 28, 1264.

Alldredge, G. P., and Kleinman, L. (1974). Phys. Rev. B 10, 559.

Appelbaum, J. A., Baraff, G. A., and Hamann, D. R. (1975a). Phys. Rev. B 11, 3822.

Appelbaum, J. A., Baraff, G. A., and Hamann, D. R. (1975b). Phys. Rev. B 12, 5749.

Appelbaum, J. A., and Hamann, D. R. (1972). Phys. Rev. B 6, 2166.

Appelbaum, J. A., and Hamann, D. R. (1973). Phys. Rev. Lett. 31, 106.

Appelbaum, J. A., and Hamann, D. R. (1978). Solid State Commun. 27, 881.

Arlinghaus, F. J., Gay, J. G., and Smith, J. R. (1980). Phys. Rev. B 21, 2055.

Bauschlicher, C. W. (1976). Ph. D. dissertation.

Bauschlicher, C. W., Liskow, D. H., Bender, C. F., and Schaefer, H. F. (1975). J. Chem. Phys. 62, 4815.

Bender, C. F., and Davidson, E. R. (1967). J. Chem. Phys. 47, 4972.

Blakemore, J. S. (1974). "Solid State Physics" W. B. Saunders, Philadelphia.

Born, M., and Oppenheimer, J. R. (1927). Ann. Physik 84, 457.

Born, M., and von Karman, Th. (1912). Phys. Zeit. 13, 292.

Boys, S. F. (1950). Proc. Roy. Soc. A200, 542.

Brewington, R. B., Bender, C. F., and Schaefer, H. F. (1976). J. Chem. Phys. 64, 905.

Clementi, E., and Mehl, J. (1971) "IBM System/360 IBMOL-5 Program Users Guide", IBM Report 889, and "IBM System/360 IBMOL-5 Quantum Mechanical Concepts and Algorithms", IBM Report 883.

Connolly, J. W. D. (1976). in "Modern Theoretical Chemistry" Vol. 7 (G. A. Segal, ed.), Plenum Press, New York.

Cooper, B. R. (1973). J. Vac. Sci. Technol. 10, 713.

Cooper, B. R. (1977). Phys. Rev. B 16, 5595.

Davis, P. J., and Rabinowitz, P. (1975) "Methods of Numerical Integration" Academic Press, New York.

Dunlap, B. I., Connolly, J. W. D., and Sabin, J. R. (1977). Int. J. Quantum Chem. S11, 81.

Dunlap, B. I., Connolly, J. W. D., and Sabin, J. R. (1979a). J. Chem. Phys. 71, 3396.

Dunlap, B. I., Connolly, J. W. D., and Sabin, J. R. (1979b). J. Chem. Phys. 71, 4993.

Dykstra, C. E., Schaefer, H. F., and Meyer, W. (1977). J. Chem. Phys. 65, 5141.

Ellis, D. E., and Painter, G. S. (1971). Phys. Rev. B 2, 7887.

Feibelman, P. J., Appelbaum, J. A., and Hamann, D. R. (1979). Phys. Rev. B 20, 1433.

Feibelman, P. J., and Hamann, D. R. (1980). Phys. Rev. B 21, 1385.

Feibelman, P. J., Hamann, D. R., and Himpsel, F. J. (1980). to be published.

Feibelman, P. J., and Himpsel, F. J. (1980). Phys. Rev. B 21, 1394.

Fomenko, V. S. (1966). "Handbook of Thermionic Properties" Plenum Press, New York.

Gaspar, R. (1954). Acta Physica 3, 263.

Gay, J. G., Smith, J. R., and Arlinghaus, F. J. (1977). Phys. Rev. Lett. 38, 561.

Gaydon, A. G. (1968). "Dissociation Energies and Spectra of Diatomic Molecules" Chapman and Hall, London.

Golebiewski, A., and Mrozek, J. (1973). Int. J. Quantum Chem. 7, 623; Int. J. Quantum Chem. 7, 1021.

Green, A. K., and Bauer, E. (1978). Surf. Sci. 74, 676.

Hattox, T. M., Conklin, J. B., Slater, J. C., and Trickey, S. B. (1973). J. Phys. Chem. Solids 34, 1627.

Herman, F., and Skillman, S. (1963). "Atomic Structure Calculations" Prentice-Hall, Englewood Cliffs.

Hohenberg, P., and Kohn W. (1964). Phys. Rev. 136, B864.

Johnson, K. H. (1973). Adv. Quantum Chem. 7, 143.

Jordan, K. D., and Simons, J. (1977). J. Chem. Phys. 67, 4027.

Kar, N., and Soven, P. (1975). Phys. Rev. B 11, 3761.

Kittel, C. (1976). "Introduction to Solid State Physics" (Fifth Ed.) John Wiley, New York.

Kohn, W. (1975). Phys. Rev. B 11, 3756.

Kohn W., and Sham, L. J. (1965). Phys. Rev. 140, A1133.

Koster, G. F. (1957). Solid State Phys. 5, 173.

Krakauer, H., and Cooper, B. R. (1977). Phys. Rev. B 16, 605.

Lang, N. D. (1973). Solid State Phys. 28, 225.

Lee, L. H. (1977). in "Characterization of Metal and Polymer Surfaces" Vol. 1 (L. H. Lee, ed.), Academic Press, New York.

Loucks, T. L., and Cutler, P. H. (1964). Phys. Rev. 133, A819.

Löwdin, P. O. (1956). Adv. Phys. 5, 1.

McMurchie, L. E., and Davidson, E. R. (1978). J. Comp. Phys. 26, 218.

Mintmire, J. W. (1979). Int. J. Quantum Chem. S13, 163.

Mintmire, J. W., and Sabin, J. R. (1980a). Chem. Phys. 50, 91.

Mintmire, J. W., and Sabin, J. R. (1980b). to be published.

Monkhorst, H. J., and J. D. Pack (1976). Phys. Rev. B 13, 5188.

Musket, R. G., and Fortner, R. J. (1971). Phys. Rev. Lett. 26, 80.

Piela, L., and Delhalle, J. (1978). Int. J. Quantum Chem. 13, 605.

Sambe, H., and Felton, R. (1975). J. Chem. Phys. 62, 1122.

Schaefer, H. F. (1972). "The Electronic Structure of Atoms and Molecules" Addison-Wesley, Reading, Massachusetts.

Schwalm, W. A., and Monkhorst, H. J. (1980). to be published.

Schwarz, K. (1972). Phys. Rev. B 5, 2466.

Siegbahn, K., Nordling, C., Fahlman, A., Nordberg, R., Hamrin, K., Hedman, J., Johansson, G., Bergmark, T., Karlsson, S. E., Lindgren, I., and Lindberg, B. (1967). "ESCA: Atomic, Molecular and Solid State Structure Studied by Means of Electron Spectroscopy" Almqvist and Wiksells, Uppsala.

Slater, J. C. (1951). Phys. Rev. 81, 385.

Slater, J. C. (1963). "Quantum Theory of Molecules and Solids" Vol. 1 McGraw-Hill, New York.

Slater, J. C. (1972a). "Symmetry and Energy Bands in Crystals" Dover Publications, New York.

Slater, J. C. (1972b). J. Chem. Phys. 57, 2389.

Slater, J. C. (1974). "The Self-Consistent Field for Molecules and Solids: Quantum Theory of Molecules and Solids" Vol. 4 McGraw-Hill, New York.

Slater, J. C., and Wood, J. H. (1971). Int. J. Quantum Chem. S4, 3.

Smith, J. R., Gay, J. G., and Arlinghaus, F. J. (1980). Phys. Rev. B 21, 2201.

Steinborn, E. O., and Reudenberg, K. (1973). Adv. Quantum Chem. 7, 1.

Stolarczyk, L. E., and Piela, L. (1979). Int. J. Quantum Chem. 15, 701.

Suleman, M., and Pattinson, E. B. (1971). J. Phys. F 1, L24.

Tinkham, M. (1964). "Group Theory and Quantum Mechanics" McGraw-Hill, New York.

Trickey, S. B., and Worth, J. P. (1977). Int. J. Quantum Chem. S11, 529.

van Duijneveldt, F. B. (1971). "Gaussian Basis Sets for the Atoms H - Ne for Use in Molecular Calculations" IBM Report RJ 945.

von Laue, M. (1931). Phys. Rev. 37, 53.

Wang, C. S., and Freeman, A. J. (1978). Phys. Rev. B 18, 1714.

Wang, C. S., and Freeman, A. J. (1979). Phys. Rev. B 19, 793.

Wang, C. S., and Freeman, A. J. (1980). Phys. Rev. B 21, 4585.

Zivkovic, T., and Maksic, Z. B. (1968). J. Chem. Phys. 49, 3083.

BIOGRAPHICAL SKETCH

John Wallace Mintmire was born on September 16, 1955, in Somerset, Kentucky. After attending public schools in Russell Springs, Kentucky, for several years, he and his family moved to Port Charlotte, Florida, in 1969. He graduated from Charlotte County High School in Punta Gorda, Florida, in June, 1972. After enrolling at the University of Florida as an undergraduate in September, 1972, he received the Bachelor of Science in physics in March, 1976. He then began graduate study for the Doctor of Philosophy degree at the University of Florida and has been working in the Quantum Theory Project since that time.

I certify that I have read this study and that in my opinion it conforms to acceptable standards of scholarly presentation and is fully adequate, in scope and quality, as a dissertation for the degree of Doctor of Philosophy.

John R. Sabin, Chairman
Professor of Physics and Chemistry

I certify that I have read this study and that in my opinion it conforms to acceptable standards of scholarly presentation and is fully adequate, in scope and quality, as a dissertation for the degree of Doctor of Philosophy.

Samuel B. Trickey
Professor of Physics

I certify that I have read this study and that in my opinion it conforms to acceptable standards of scholarly presentation and is fully adequate, in scope and quality, as a dissertation for the degree of Doctor of Philosophy.

N. Yngve Ohrn
Professor of Chemistry and Physics

I certify that I have read this study and that in my opinion it conforms to acceptable standards of scholarly presentation and is fully adequate, in scope and quality, as a dissertation for the degree of Doctor of Philosophy.

Thomas L. Bailey
Professor of Physics

I certify that I have read this study and that in my opinion it conforms to acceptable standards of scholarly presentation and is fully adequate, in scope and quality, as a dissertation for the degree of Doctor of Philosophy.

Robert C. Stouffer
Associate Professor of Chemistry

This dissertation was submitted to the Graduate Faculty of the Department of Physics in the College of Liberal Arts and Sciences and to the Graduate Council, and was accepted as partial fulfillment of the requirements for the degree of Doctor of Philosophy.

December, 1980

Francis Stehli
Dean for Graduate Studies and Research